BUBBLE GROWTH IN SUPERSATURATED SOLUTION

A Thesis submitted for the Degree of

DOCTOR OF PHILOSOPHY

in the

FACULTY OF ENGINEERING

of the

UNIVERSITY OF LONDON

by

JOHN EDMUN BURMAN, B.E.

Department of Chemical Engineering and Chemical Technology,

Imperial College of Science and Technology,

London, S.W.7

July, 1974.

ABSTRACT

In this work, diffusive bubble growth in newtonian liquids and non-newtonian liquids of the power law type is studied. Three regions are considered, the first where growth is limited entirely by the arrival of diffusant at the bubble surface, the second where growth is limited entirely by hydrodynamic forces and the third, a general case, where both diffusion and hydrodynamics play a part. Previously defined parameters used to define regions where viscosity, inertia, surface tension and diffusion are important are shown to hold good for power law liquids. It is found that, all else being equal, bubbles in power law liquids grow more slowly the smaller the characteristic exponent. In general, bubbles in power law liquids grow more slowly but eventually approach the growth curve for a newtonian liquid of the same characteristic parameters; together they eventually approach the growth curve for an inviscid liquid and the whole group eventually approach the growth curve calculated for diffusive limitation alone.

Experiments are carried out to test the diffusion limited asymptotic bubble growth theory of Scriven. In the three systems used, supersaturated solutions of carbon dioxide in water and in glycerol and oxygen in water, excellent agreement with the theory is obtained. This previously inadequately tested theory is thus concluded to be accurate, and suitable for use in calculations in some industrial applications which are briefly described.

To Kay

ACKNOWLEDGEMENTS

I would like to express my thanks to Dr G.J. Jameson for his assistance during the course of this project.

CSR Limited of Sydney, Australia, have provided me with generous financial support and leave, for which I am sincerely thankful.

My wife and our families have encouraged and helped me in every possible way.

LIST OF CONTENTS

		PAGE
Abstract		2
Acknowledgements		4
List of contents		5
List of figures		8
List of tables		9
Chapter 1	Introduction	10
Chapter 2	Theoretical and experimental background	17
Chapter 3	Theoretical analysis	36
3.1	Derivation of the governing equations	37
3.1.1	Basic assumptions	37
3.1.2	Continuity equation	39
3.1.3	Momentum equation	39
3.1.4	Diffusion equation	40
3.1.5	Diffusional mass balance	40
3.2	Scriven's solution for diffusional bubble growth	41
3.2.1	Derivation of the asymptotic solution	41
3.2.2	Approximations for small and large β	44
3.2.3	Comparison with earlier solutions	44
3.3	Expansion of the momentum equation for a newtonian liquid	45
3.4	Expansion of the momentum equation for a non-newtonian (power law) liquid	47
3.5	Intermediate liquid - the Sisko model	53
3.6	Expansion of the diffusion equation	54
3.7	Expansion of the boundary conditions	54
3.8	"Film Theory" approach to Scriven's analysis	56
3.9	Summary	60

Chapter 4	Numerical solution of the bubble growth equations	62
4.1	Growth limited by hydrodynamic forces	63
4.1.1	Forming the appropriate equations for numerical solution	63
4.1.2	Method of solution	65
4.1.3	Computational procedure	66
4.1.4	Results for newtonian liquids	67
4.1.5	Results for power law liquids	71
4.1.6	Discussion of results	77
4.2	Growth limited by both hydrodynamics and diffusion	80
4.2.1	Forming the appropriate equations for numerical solution	80
4.2.2	Method of solution	85
4.2.3	Computational procedure	89
4.2.4	Selection of parameters for the numerical solution	95
4.2.5	Results of the numerical solution	97
4.2.6	Discussion of results	102
Chapter 5	Experimental - Apparatus and Techniques	104
5.1	Introduction	105
5.2	Pressure vessel	105
5.3	Initiation of bubbles	107
5.4	Photography	110
5.4.1	Camera	110
5.4.2	Optics	111
5.4.3	Illumination	112
5.4.4	Films and development	112
5.5	Film analysis	112
5.6	Chemicals used	113
5.7	Other apparatus used	113
5.8	Experimental procedure	114

Chapter 6 Experimental results 118
6.1 Data sources 119
6.2 Experimental conditions 121
6.3 Analysis of experimental results 126
6.4 Discussion of results 147

Chapter 7 Conclusions 151

Appendices 154
A.1 Table showing the relationship between the dimensionless growth coefficient, the Jakob number and the Sherwood number for an expanding bubble 155
A.2 Mass diffusivity in highly viscous newtonian liquids and in non-newtonian liquids 156
A.3 Testing the computer programme DP01A 158
A.4 Solubility of carbon dioxide in glycerol solutions 161
A.5 Statistical analysis of data 163
A.6 Table of experimental results 171

Computer Programmes 183
P 1 Solution of the hydrodynamically limited bubble growth equations 184
P 2 Solution of the general case of bubble growth 187
P 3 Non-linear least squares regression 190

References 193

List of symbols 200

LIST OF FIGURES PAGE

2.1 Theoretical and experimental results of Plesset and Zwïck and Dergarabedian for growth of vapour bubbles in superheated water 24

2.2 Buehl and Westwater's experimental results 29

2.3 Driving force versus growth coefficient 29

3.1 Coordinate system and nomenclature 38

3.2 Jakob number versus Sherwood number for a growing bubble 59

4.1 Hydrodynamically controlled bubble growth Effect of viscous forces 68

4.2 Hydrodynamically controlled bubble growth Effect of surface tension 68

4.3 Hydrodynamically controlled bubble growth 69

-4.5 in newtonian liquids (Various parameters) -70

4.6 Hydrodynamically controlled bubble growth 72

-4.14 in power law liquids (Various parameters) -76

4.15 Coordinate transformation nomenclature 84

4.16 Flow diagram for the solution of the complete bubble growth equations 91

4.17 Variation of interface concentration with spacing parameter, Set 4 93

4.18 Optimum spacing parameter versus initial time steps, Sets 1 - 10 94

4.19 Bubble growth curves for the general case 98

-4.22 (Various parameters) -101

5.1 Half-sectional view of pressure vessel 106

5.2 Bubble initiating tips 109

5.3 Diagram of experimental setup 115

5.4 Typical bubble growth sequence 117

6.1 Experimental results, Radius versus Time 131

-6.16 Sets 1 - 16 -146

6.17 Calculated and experimental values of the dimensionless growth coefficient 150

A.4.1 Solubility of carbon dioxide in glycerol 162

A.5.1 Flow diagram for the non-linear regression technique (Law and Bailey (1963)) 168

LIST OF TABLES

		PAGE
4.1	Parameters used in the numerical solutions	96
6.1	Experimental conditions	123
6.2	Experimental conditions for the carbon dioxide and glycerol system	125
6.3	Experimental values of the bubble growth exponent	128
6.4	Calculated and experimental values of the dimensionless growth coefficient for consecutive bubbles	149

CHAPTER 1

INTRODUCTION

In this chapter, the reasons for the present study will be discussed. Details of the organisation of the thesis will be given.

In the last two decades there have been substantial and significant advances made in the study of bubble dynamics and phase growth. Much of the work has been directed towards a better understanding of the nucleate boiling process, prompted by the development of high flux heat exchange devices such as nuclear reactors and high pressure steam generating systems. In the design of these devices and others it is important to know the rate of bubble evolution and the limits and checks to evolution provided by the surroundings. A better understanding of cavitation, of the evolution of gas bubbles from a super-saturated solution and of the dissolution of gas bubbles in an undersaturated one has also been gained.

The study is an important one. Apart from the many aspects of the boiling and cavitation investigation, it is necessary to be able to understand the behaviour of gaseous impurities dissolving in or evolving from liquids such as water or molten glass, the evolution of bubbles in vacuum degassing processes (such as that of degassing a steel melt), the growth of bubbles in the dissolved air flotation process, the determination of coefficients of diffusivity by observation of evolving or dissolving gas bubbles, the foaming of liquid plastics by gaseous evolution and the rate of solution of dispersed air bubbles in processes for BOD (biological oxygen demand) reduction in pollution control.

An increasingly important application which initially gave the impetus to this work was that of dissolved air

flotation. Froth flotation has been used as a mineral separation technique for several decades. Since its earliest times a controversy has raged over whether the flotation was due to injected bubbles striking mineral particles and attaching to them, or whether bubbles of gas grew on the particles from the solution, made suddenly supersaturated by the reduced pressure in the wake of impellers in the flotation cell. Much of the controversy was pursued in an unscientific fashion by designers of "novel" devices and their patent lawyers. It is apparent that both mechanisms can and do operate but that in mineral flotation, where relatively large particles are usually floated, the former is dominant. (The literature of flotation is enormous but for a discussion of this point see Sutherland and Wark (1955) and Klassen and Mokrousov (1963)). That the mechanism of dissolved air flotation can also be a dominant one is proved conclusively and discussed at length by Packham and Richards (1972a, 1972b) who have designed dissolved air units to remove flocculate scum as a water treatment process. The number of applications for which the process is already used is shown by Packham and Richards to range from sewerage sludge flotation to flotation of multitudinous industrial wastes, to oil dispersions and algae. It is likely that this method will be increasingly used in waste disposal processes. Conditions of super-saturation will lie in the region described by the inadequately tested theory of Scriven (1959) ; it was decided that some conclusive experimental examination of the theory was required. This is done in the present work.

Investigation of the growth of gas bubbles in non-newtonian liquids of the power law type was undertaken because of the industrial importance of this class of material. Indeed plastics are often foamed by the nucleation and growth of bubbles of a diffusive substance. All the following remarks thus apply to both newtonian and non-newtonian liquids, perhaps more so to the latter since the former have been extensively investigated already.

This study, then, is of the evolution of gas bubbles from supersaturated solution. In a real process, the total rate of dissolution is a function of the rate of nucleation and the rate of growth from the nucleus. The nucleation problem has been much studied and it seems that homogeneous nucleation is a relatively rare occurrence. Calculations show that extremely large superheats or supersaturations are needed, by which time heterogeneous nucleation has almost inevitably taken place at sites which probably consist of stabilised gas or vapour. A study of the mechanisms of nucleation is not a part of this work. (See Himmelblau (1972) and many others). In most experimental work on bubble growth, as in this instance, an artificial nucleation site is used and only the bubble growth from that site is studied.

When nucleation has taken place, a bubble of gas or vapour begins to grow. The growth must self evidently be checked by some factor and it is possible that depletion of the diffusing species at the bubble wall and liquid inertia, viscosity and surface tension all have a rôle to play. The extent to which all these factors check the growth will be

examined.

It should be plain that, no matter what limits the rate of bubble growth initially, the limitation of insufficient material is eventually arrived at. In the case of boiling, vapourisation of the material on the bubble wall will lead to a drop in the temperature of the wall which in turn reduces the vapour pressure driving force. The wall temperature is maintained by a flow of heat from the bulk. When an evolving gas bubble is considered, diffusion of the evolving species to the bubble wall from the liquid bulk is not instantaneous so a concentration profile will eventually develop which will limit the rate of bubble growth. The development of this limitation and its characterisation will be examined.

When simple diffusive limitation develops so rapidly that all other limitations can be neglected, a useful asymptotic solution can be found. This was best done by Scriven (1959) whose asymptotic theory predicts that bubble radius should be proportional to the square root of time. Scriven gave expressions to calculate the constant of proportionality from the properties of the liquid and gas. Surprisingly, the theory of Scriven for the evolving bubble in supersaturated solution seems not to have been adequately tested, even for common systems, despite its simplicity and possible applications. For example, Buehl and Westwater (1966) report the only known results for the carbon dioxide-water system and the results are not particularly good. A thorough test of the asymptotic theory was felt to be necessary and this will be done with the carbon dioxide-

water, oxygen - water and carbon dioxide - glycerol systems.

The mathematical problem, apart from the few asymptotic solutions which may be extracted by similarity and other methods, demands numerical solution. The equations of motion and diffusion may be linked and the problem is further complicated by the existence of a free boundary. This means that the location of the boundary is itself dependent on the amount of diffusant which has been brought up to it in the past. In the present work, suitable transformations of the spatial co-ordinates will be made, leaving linear, parabolic partial differential equations. These can be solved numerically by standard methods without too much difficulty.

The problem of the rising bubble, dissolving or evolving as it goes, has not received much attention no doubt because of the extreme mathematical complexity of a translating free boundary. However, it is possible to examine it from the point of view of existing correlations for rising or sinking and dissolving solid spheres and this will be done briefly.

Turning to the present work, Chapter 2 deals with the background to the problem and surveys some of the previously reported results of significance, both theoretical and experimental. Chapters 3 and 4 then examine the growth of diffusive bubbles in liquids, particularly non-newtonian liquids. In Chapter 3 the governing equations are set up; in Chapter 4 they are solved numerically and the solutions reported and discussed. In Chapter 5 the experimental part

of the work will be discussed and the details of the apparatus and techniques will be given. In Chapter 6 the experimental results will be presented and discussed. Chapter 7 is a chapter of discussion and conclusion.

CHAPTER 2

THEORETICAL AND EXPERIMENTAL BACKGROUND

In this chapter, the background to the work will be presented. Some major articles which provide comprehensive treatments will be referred to but in addition, several of the more significant publications will be discussed individually. Particular attention will be paid to publications not included in, or published since, the last major review of 1966.

A review article by Bankoff (1964) surveyed the fields of heat conduction and diffusion with a change of phase. This review was mainly concerned with cases where the motion of the phase boundary was induced solely by the phase change and where the diffusion and momentum equations could be considered to be uncoupled. These cases include phenomena such as the freezing of a liquid surface, where the density change is negligible, the penetration of a reactant into an ion-exchange particle and the oxidation of a surface. Uncoupling implies that the momentum equation need not be considered in formulating the differential equation or the initial and boundary conditions for the diffusion equation. However, in such problems as diffusive vapour or gas bubble growth, particularly in the early periods of the growth, there is a large change in density between the phases which will induce a radial convective motion, which itself will modify the concentration and temperature fields surrounding the bubble and hence the radial motion of the front. In addition, inertial, viscous and surface tension effects may not be negligible. All these conditions may then appear linked to the diffusion equation or to its boundary conditions.

It is to this more complex problem that Bankoff (1966) directs his second major review. In this article, Bankoff provides an excellent summary of the formulation of the general problem and of the simplifications made possible by the assumptions of spherical symmetry and uniform initial conditions, for the growth of both vapour bubbles

(the major part) and of gas bubbles. He then surveys growth with non-uniform initial conditions and in multicomponent liquids as well as giving a brief examination of other pertinent areas such as nucleation. The growth of bubbles in non-newtonian liquids, a major part of the present work, attracts no attention from Bankoff.

Bankoff (1966) also provides a summary of much of the experimental work which has been reported and so provides a comprehensive summary of both the theoretical and experimental work in the field, up to 1965 .

Several papers, including many published since Bankoff's 1966 review have been of particular relevance to this work and will be discussed in more detail below. Both theoretical and experimental developments will be discussed.

Lord Rayleigh (1917), in a classic formulation dealing with the collapse of a spherical cavitation bubble, derived an equation which has since borne his name. By assuming that the pressure within the cavity and in the liquid at a distance were constant, he deduced the radius - time relationship from an energy balance. Two cases were considered, one when the bubble contained only vapour and another when the bubble contained a gas obeying Boyle's law. Whereas Rayleigh had assumed a constant pressure in the liquid, Plesset (1949) considered the case of a bubble moving through a region in which the pressure varied rapidly, as would be found in, say, cavitation at a propeller tip. He derived, for an inviscid liquid, the following equation:

$$R\ddot{R} + \frac{3}{2}\dot{R}^2 = \frac{P(R) - P(t)}{\rho_g} \qquad (2.1)$$

where $P(t)$ is the varying external pressure and $P(R)$ the pressure at the bubble boundary. The original Rayleigh formulation is a special case where:

$$P(t) - P(R) = P_o = \text{a constant} \qquad (2.2)$$

Plesset defined three regimes of cavitating liquid flow and used his formulation to investigate the second regime, cavitation at a number of sites in the field of flow. His experimental results in the regime were in fair agreement with the numerical solution of the formulation and this paper gave an impetus to the study of the collapse and growth of vapour bubbles and of gas bubbles.

The first significant paper dealing with gas bubble growth was that of Epstein and Plesset (1950). By neglecting any effects due to the translational motion of the bubble front, they found approximate solutions for the rate of solution by diffusion of a gas bubble in an undersaturated solution and for the growth of a gas bubble in a super-saturated solution. They also considered the effect of surface tension on the diffusion process.

By assuming that the transport term in the diffusion equation could be neglected i.e. the velocity of the liquid and convection caused by the growth or shrinkage could be neglected, and then applying Fick's second law of diffusion, Epstein and Plesset showed that, when surface tension is

neglected (and writing in the present nomenclature):

for a bubble dissolving in an undersaturated solution:

$$\frac{R}{R_o} = \sqrt{1 - \frac{2(C_{sat} - C_o)}{\rho_g} \frac{D\,t}{R_o^2}} \qquad (2.3)$$

for a bubble growing in a supersaturated solution:

$$\frac{R}{R_o} = \sqrt{1 + \frac{2(C_o - C_{sat})}{\rho_g} \frac{D\,t}{R_o^2}} \qquad (2.4)$$

This was the first time that the radius and time had been linked through known properties of the gas solution. In discussing surface tension, Epstein and Plesset showed that the effect is a transient one. For a growing bubble, only a little longer is required before the surface tension forces are overcome and then growth is resumed at a rate which would obtain if the forces were absent; for the dissolving bubble, the surface tension forces ensured that the bubble dissolves somewhat more rapidly. A solution, similar in form to equations 2.3 and 2.4 was given for the case when surface tension is not neglected.

During the 1950's, a number of significant papers appeared concerning the growth of vapour bubbles in boiling. An early review by Westwater (1956) was an important summary of the experimental and theoretical developments in boiling theory. Authors were now taking into account the combined effects of heat and mass transfer. As the bubble grows, vapour passes from the superheated liquid into the bubble. Latent heat of vapourisation is removed from the surrounding

liquid, which cools and thus reduces the vapour pressure driving force between liquid and bubble. This temperature drop strongly affects the bubble's rate of growth and causes it to approach asymptotically a condition whereby the radius increases with the square root of time. A solution for heat diffusion across a spherical boundary with radial motion was presented by Plesset and Zwick (1952). By a procedure of successive approximations, they were able to predict the temperature field in the liquid provided it could be assumed that the thermal boundary layer was thin and that translational motion of the bubble could be neglected.

Two progressive papers concerning the growth of vapour bubbles in superheated liquids were published simultaneously by Forster and Zuber (1954) and Plesset and Zwick (1954), the latter extending the work of their 1952 paper. Forster and Zuber, starting with Rayleigh's equation and assuming that there is thermodynamic equilibrium at the boundary so that the Clausius-Clapeyron equation can be used to relate the vapour pressure within the bubble to the surface temperature, derived an expression which includes inertial effects. When the bubble has reached its asymptotic stage and inertial effects have died away, the full expressions derived may be considerably simpified to:

$$R = k(\alpha t)^{\frac{1}{2}} = \pi^{\frac{1}{2}} \frac{\rho_l \, c_p \, (T_\infty - T_s)}{L \, \rho_v} (\alpha t)^{\frac{1}{2}} \qquad (2.5)$$

where c_p is the heat capacity of the liquid, ρ_l and ρ_v are the densities of the liquid and vapour, L the latent

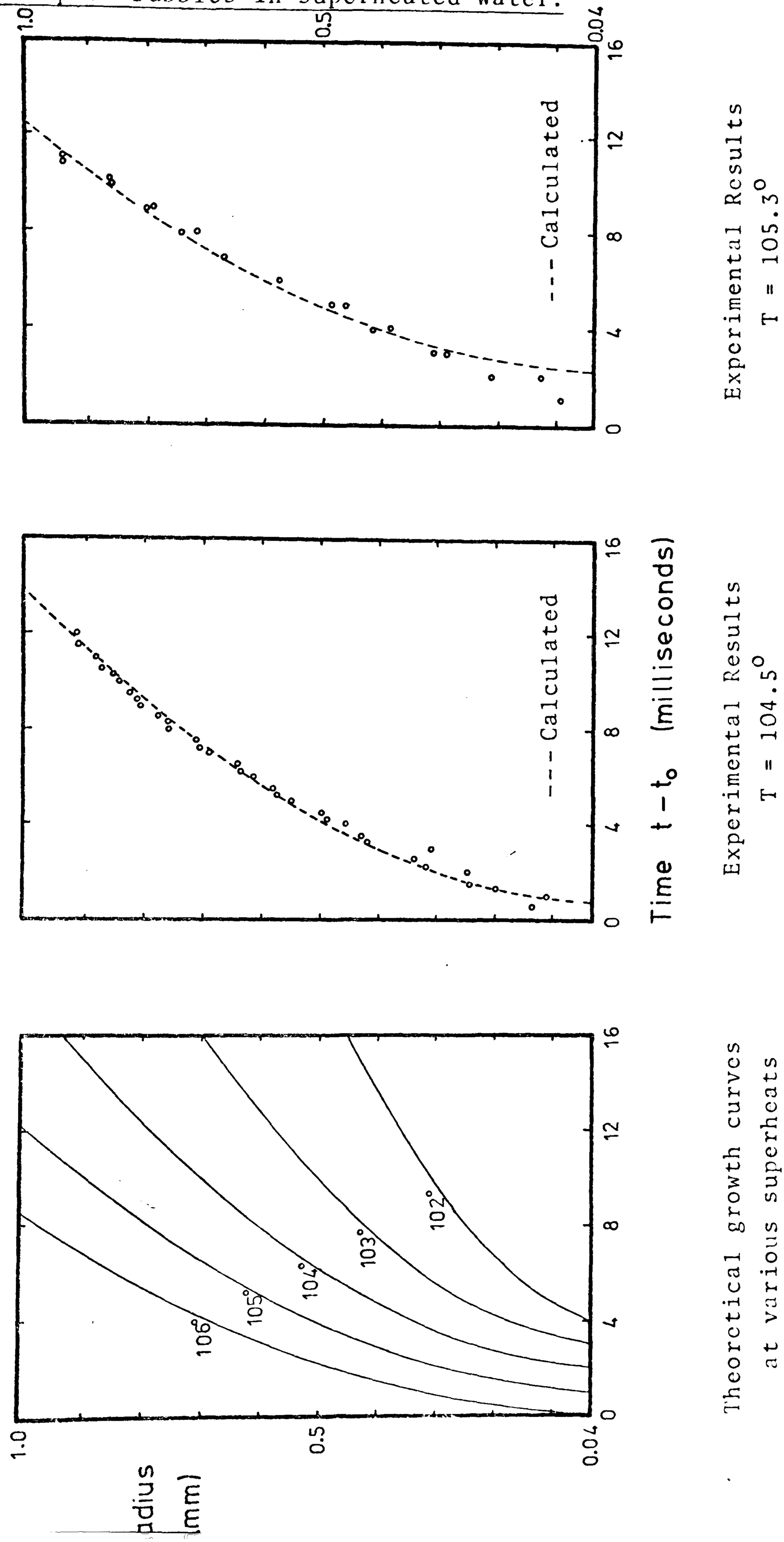
heat of vapourisation, T_∞ and T_s the superheated and saturation temperatures and α the thermal diffusivity.

In approaching the same problem but using the "thin boundary layer approach", Plesset and Zwick (1954) derived ~~an equation of the same form~~ different to (2.5) another asymptotic solution only in that the constant $\pi^{\frac{1}{2}}$ is now $(12/\pi)^{\frac{1}{2}}$. These two constants are only 9% apart so both solutions may be taken as adequate.

The classic experiments of the period were those of Dergarabedian (1953). His work (and later work of 1960) has been much quoted and his experimental techniques used by other investigators. Dergarabedian used liquid uniformly superheated by infrared lamps. As a matter of interest, some results of Dergarabedian are shown along with the theoretical results of Plesset and Zwick (1954) in Figure 2.1. Agreement is seen to be very good indeed. In later experiments Dergarabedian (1960) used other liquids, carbon tetrachloride, benzene, ethyl alcohol and methyl alcohol and once again found good agreement with Plesset and Zwick.

On the gas bubble side there was little comparable development. Liebermann (1957) concluded that the departure from the radius squared versus time relationship that he had observed in dissolving bubbles was due to surface contamination; certainly he was able to detect residues after the bubble had dissolved. Manley (1960) also observed the same departure and again concluded that impurities were the significant cause due to their increasing effect on the diffusivity as they concentrated near the shrinking bubble.

Figure 2.1 Theoretical and experimental results of Plesset and Zwick and Dergarabedian for growth of vapour bubbles in superheated water.



The definitive formulation of the whole problem was given by Scriven (1959). (Some minor corrections were made to some of the expressions by Scriven (1962) and Pignet and Scriven (1972). These do not affect the final conclusions as the incorrect terms eventually disappear in the asymptotic solution). Firstly, Scriven presented all the equations governing spherically symmetric phase growth in an infinite medium and then simplified them, listing precisely all assumptions and restrictions, to describe growth controlled by transport of heat or matter. He obtained analytical solutions for the size of a vapour bubble in boiling pure liquids and binary mixtures in the asymptotic phase and also for the growth of gas bubbles from supersaturated solutions. He then went on to establish the ranges of pressure and superheat over which the approximate solutions of Plesset and Zwick (1954) and Forster and Zuber (1954) are accurate. Scriven concluded that, whilst the similar results of the authors are in good agreement with the experimental results of Dergarabedian (1953) they would be in serious error if the vapour densities were large and/or the superheats were small.

Basically, Scriven's solutions can be summarised in the form:

$$R = 2\beta\sqrt{k\,t} \qquad (2.6)$$

where R, radius and t, time, are related through a dimensionless growth coefficient β and the thermal diffusivity ($k = \alpha$) or the mass diffusivity ($k = D$).

gives a table of β versus a quantity $\Phi\{\varepsilon,\beta\}$ a superheat or supersaturation parameter which can be calculated from the properties of the boiling liquid or the supersaturated solution. He also obtained two asymptotic regions within the general asymptotic solution, for large β and for small β.

Following Scriven, most authors have concentrated on situations where an analytical solution has become extremely difficult or, at present, impossible and have extended the work through analogue and digital computer studies. It is then possible to treat cases with initial and boundary conditions which, though more plausible from a physical point of view, lead to intractable analytical problems. Also it is easier to include effects due to surface tension, liquid viscosity and inertia, largely neglected in the asymptotic forms of solution.

Marique and Houghton's (1962) analogue computer investigation of the growth of cavitation bubbles looked at the effects of various initial conditions and of liquid properties. The initial conditions applied varied from an initial wall velocity to a step increase in the bubble radius, so that the initial radius was instantly greater that the metastable equilibrium radius. They found that, at low initial wall velocities, the growth began slowly and increased rapidly as the surface tension was overcome. However, as the initial wall velocity was increased, the wall velocity passed through a minimum since, during the early stages, most of the energy supplied was used to increase the radius against

surface tension until these forces became insignificant. As would be expected, they determined that a higher initial pressure or larger initial radius more rapidly overcame the surface tension forces; also that a step increase in radius led to a more rapid growth. Increasing the surface tension led to a longer delay period of very slow growth, until the forces were overcome. Their studies of the effects of kinematic viscosity showed that for light liquids such as water, the effect is negligible but as the kinematic viscosity is increased, the effect is to reduce the growth rate. This is somewhat ameliorated if there is a high surface tension to density ratio.

Buehl and Westwater (1966) noted that most of the theoretical studies of diffusional bubble growth had assumed conditions of spherical symmetry or hemispherical symmetry on a frictionless plane with an infinite or semi-infinite liquid surrounding the growing bubble. To take any account of the effect of contact angle was felt to be either too difficult or destructive to the simplicity of the results found by assuming symmetry. Possible contact angles range from 0^{o} (tangent sphere) to 90^{o} (sphere or frictionless hemisphere).

An estimate of the effect of at least one contact angle, the case of a tangent sphere, had been made by Liebermann (1957). The electrical capacitance of a conducting sphere tangent to an infinite, plane, ungrounded conductor is reduced by a factor of $\ln(2) = 0.693$ and by making an analogy to a

tangentially growing bubble, the growth rate should be reduced by some 30.7% . Because this result is for a static sphere one would expect that such a correction would apply only for the limiting case of bubble growth extrapolated to zero growth rate. Buehl and Westwater derived a set of equations which did not assume spherical symmetry and solved these equations numerically to show that at low growth rates, the growth coefficient for a tangent sphere is indeed 30.7% less than that for an isolated sphere. As the driving force increases, the effect of the contact angle diminishes rapidly, there being a difference of less than 5% at a growth coefficient $\beta = 1$. Since the two cases represent the extremes, calculations for other contact angles would show an intermediate effect. Thus an important conclusion was that contact angle was a weak variable and the neglect of the effect by almost all authors did not seriously weaken theoretical or experimental studies. A further implication was that the depletion of the diffusing solute is confined to a thin shell at larger growth rates. If the depletion was more general throughout the liquid, a tangent sphere would grow more slowly due to disturbance of the diffusion and flow fields by the plane. The smaller the shell, the less the effect of contact angle. Values of β versus the driving force parameter $\Phi\{\varepsilon,\beta\}$ are shown in Figure 2.3, reproduced from their Figure 2 for both tangent sphere and isolated sphere (Scriven's result).

Buehl and Westwater (1966) also published results of experiments of carbon dioxide bubbles growing from a super-

Figure 2.2 Buehl and Westwater's experimental results

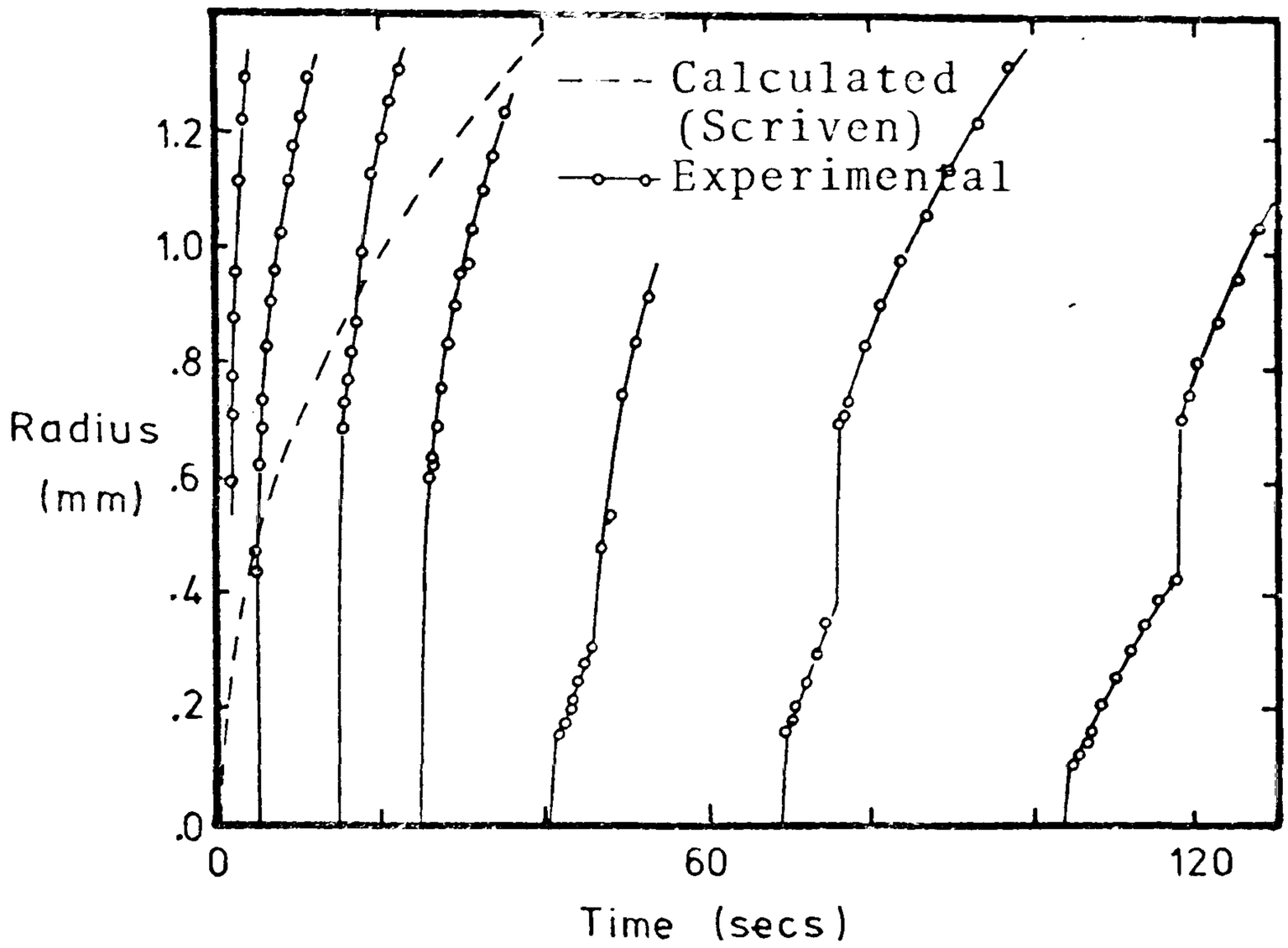
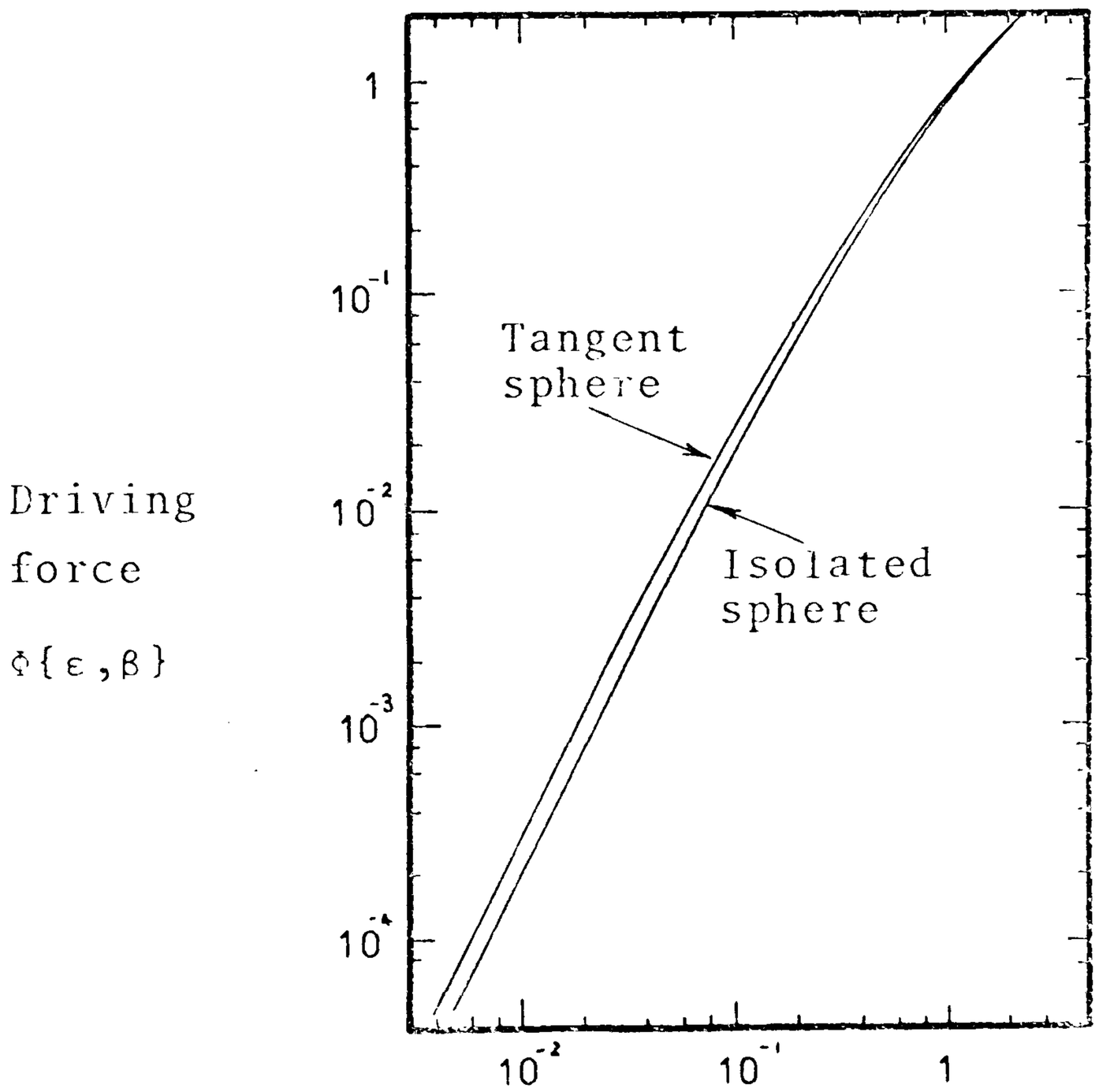


Figure 2.3 Driving force versus growth coefficient



saturated solution in water, obtained by releasing the pressure on a pressurised saturated solution. An artificial nucleation site on a plane surface was used. It was hoped to vary the contact angle by coating the surface with various non-wetting agents. The results did not prove or disprove the theory because the growth rates used were reasonably large and the expected differences small and it was found that the contact angle varied as the bubble grew. In addition, the growth curve showed strange discontinuities, perhaps due to "friction" at the wall/ gas/ liquid interface as it moved across the surface. The bubbles also exhibited a growth rate greatly in excess of that predicted by Scriven's (1959) theory. Consecutive bubbles exhibited markedly different growth rates; some were different by a factor of three. This is illustrated by the reproduction of Buehl and Westwater's Figure 4, given here as Figure 2.2 .

Buehl and Westwater's theoretical and experimental results have been given a fair amount of attention here because of concern about the effect of contact angle and the fact that, as far as is known, the experimental results are the only ones to have been published on this system, apart from the present work. This is extremely surprising as the system is a common one and known since antiquity through observation of natural waters and carbonated beverages.

Whereas Buehl and Westwater (1966) had investigated asymmetrical growth in an initially uniform concentration field, Cheh and Tobias (1968) reported theoretical calcul-

ations on hemispherical growth in a non-uniform concentration field where the initial concentration gradients at the infinite plane surface were either linear or exponential. They obtained numerical solutions for the case where the convective mass transport is negligible compared with the diffusive mass transport.

Another interesting variation was taken up by Ready and Cooper (1966) who considered the case of spheres growing or dissolving in a solution, the density of which was a function of the solvent concentration. Again, they set up the appropriate differential equations and solved them numerically.

The case of the dissolving bubble was taken up again in more detail by Cable (1967) and Cable and Evans (1967). Dissolving bubbles have often been used to estimate diffusivity coefficients of gases in liquids. The work was undertaken because only approximate analytical solutions (including that of Epstein and Plesset (1950), see equation 2.3) had been used for calculations involving dissolving bubbles. The asymptotic solution of Scriven (1959) for a growing bubble insists that the bubble has zero radius at zero time and so cannot be used for a dissolving bubble. Cable reports that many investigators (including Liebermann (1957) and Manley (1960)), when plotting their results for dissolving bubbles in the form square of radius versus time noticed, instead of linearity, a decrease in the slope of the curve. They had inferred that an organic skin was

gathering at the surface and reducing the diffusivity as the bubble dissolved. Cable set up the equations and solved them numerically for a dissolving bubble with an initial radius and showed that the decreasing slope and the shape of the radius squared versus time curve was in fact correct and in no way due to any change in liquid or surface properties. When data on dissolving spheres from many authors were examined the theoretical solutions were found to give a good fit. The error had been in assuming that the solution of Epstein and Plesset (1953) was valid over the whole lifetime of the bubble. In fact, the results of Cable (1967) showed that, for a dissolving sphere, the approximate solution and the numerical solution were not too different down to sizes of about 60% of the initial radius. Cable concluded that any calculation of diffusity coefficients could be based on the initial slope of the radius versus time curve without serious error.

Florschuetz and Chao (1965), working in the areas of boiling and cavitation collapse, made an important advance when they were able to define a parameter which can be used to characterise the regime in which a bubble finds itself. The parameter, which they call B, is defined as:

$$B = \frac{Ja^2}{G^{\frac{1}{2}}} \qquad (2.7)$$

where Ja is the Jakob number, a driving force parameter and G is a dimensionless parameter which characterises the inertial properties of the system. Both Ja and G can be defined for both the heat transfer and mass transfer systems. The parameter B is then a measure of the relative

significance of diffusion and inertia. Whilst these two regimes had long been recognised in a broad sense, the conditions under which one or the other predominated had not been established. Florschuetz and Chao proposed a classification whereby for $0 < B < 0.05$, diffusion limitation was the predominant mechanism, for $B > 10$, inertial limitation was the predominant mechanism and for $0.05 < B < 10$, an intermediate region, both mechanisms were important. This classification was decided by solving the appropriate differential equations numerically with different values of B and then looking at the deviations from the solutions which would be obtained for the limiting cases. In experiments on the collapse of a vapour bubble, they found significant justification for their choice of the parameter B to specify the regime.

In a paper published at about the same time, Cole and Shulman (1966) recognised that there was a discrepancy between expected and experimental results at high Jakob numbers, but did not use a regime characterisation parameter (such as the B of Florschuetz and Chao) to explain why.

Florschuetz and Chao's work was extended to the case of growth of gas bubbles by Szekely and Martins (1971) who thus corrected the imbalance of attention which had been paid to mass transfer in comparison with nucleate boiling or cavitation. Szekely and Martins were unable to locate any quantitative information on the range of validity of the asymptotic solutions for mass transfer and set out to examine

the problem from the same viewpoint as Florschuetz and Chao. They set up the equations of motion and diffusion, along with the appropriate boundary conditions and then solved the equations numerically to show that the same parameter B could be used to characterise the three regimes. In addition, they defined another parameter V, particularly useful in the inertia limited region, which characterises the importance of viscous effects:

$$V = \frac{Sc}{G^{\frac{1}{2}}} \qquad (2.8)$$

where Sc is the Schmidt number and G is as previously defined. Viscous effects were only found to be important for V greater than 0.1 ; the values of B which define the diffusional, inertial and mixed regions were as previously defined. Szekely and Martins then reported the results of experiments on the growth of n-pentane bubbles in n-tetradecane, under vacuum. Bubbles were photographed at a predetermined site. They were able to work in the region of $B >> 1$ (between 248 and 808) where inertia would be expected to be the dominant mechanism. The experimental results show a remarkable agreement with the numerical solutions. The Scriven solution would have been quite unacceptable, even as an approximation as it would have been in error by more than an order of magnitude. Similarly, an entirely inertial solution would have been in error; only the mixed solution was satisfactory. They were thus able to conclude that the paramaters V and B (and also ϕ , a surface tension parameter) were able to characterise the mass transfer system as well as the boiling/cavitation systems.

Szekely and Martins (1971) had made the usual assumption that a Henry's law equilibrium is obeyed at the bubble surface. Rosner and Epstein (1972) claimed that this is not always satisfactory and that there is often a departure from equilibrium at the gas-liquid interface owing to kinetic restrictions to dissolution. They looked at the effect of a kinetic law for dissolution of the type:

$$m = k (C_o^n - C_{sat}^n) \qquad (2.9)$$

where m is the mass transfer flux across the interface, k is a constant and n a kinetic order of the dissolution process. They derived a set of governing equations which include this rate process and treat the case where this limits the growth. They also considered the effects of surface tension and non-zero initial bubble size but did not treat the case where limitation to growth is a combination of non-equilibrium surface kinetics and hydrodynamics.

In a recent paper, Szekely and Fang (1973) corrected this shortcoming in Rosner and Epstein's (1972) analysis by defining a new parameter B_K, consistent with the old B parameter, to characterise the region of importance of surface kinetics and hydrodymamics. They presented a considerable number of numerical solutions.

CHAPTER 3

THEORETICAL ANALYSIS

In this chapter the governing equations for the growth of gas bubbles in newtonian and non-newtonian (power law) liquids will be set up. Spherical symmetry will be assumed and the equations will include terms taking account of the liquid inertia, viscosity and surface tension and the concentrations of the dissolved gas. Scriven's (1959) asymptotic solution for a diffusionally limited gas bubble will then be summarised and compared with earlier solutions. The governing equations will then be expanded and put into a dimensionless form suitable for numerical solution.

A simple relationship, appropriate to the case of a bubble rising in a supersaturated solution, will be derived.

The equations required for a numerical solution for the two limiting cases

(i) limitation by diffusion

(ii) limitation by the hydrodynamic properties of the liquid

and the intermediate case where both diffusion and hydrodynamics are important, are summarised in Section 3.9, together with the initial and boundary conditions.

3.1 Derivation of the governing equations

3.1.1 Basic assumptions

Consider a spherical gas bubble growing in a quiescent supersaturated liquid of infinite extent. The bubble is growing because of the transfer of dissolved gas from the liquid phase to the gas phase. The rate of growth is determined by the difference between the pressure within the bubble and the ambient pressure, liquid inertia, viscosity and surface tension, the diffusivity of the dissolved gas in the liquid and the concentration, or degree of supersaturation, of the dissolved gas.

Assume that the bubble maintains a spherical shape because of surface tension. Further, that the centre of the bubble remains fixed and is the centre of a spherically symmetric co-ordinate system. The nomenclature of the co-ordinate system is shown in Figure 3.1 .

The composition of the liquid phase is assumed to be initially homogeneous and the gas phase within the bubble is assumed to be at a uniform pressure, and homogeneous. The gas phase is at all times in thermodynamic equilibrium with the liquid phase, at the gas-liquid interface.

Since the system is assumed to be spherically symmetric, there is only a radial component of the liquid velocity; there is no angular dependence to be considered, i.e.:

$$\left.\begin{aligned} v_r &= v_r(r) \\ v_\theta &= 0 \\ v_\phi &= 0 \end{aligned}\right| \qquad (3.1)$$

where r is the radial co-ordinate.

Figure 3.1 Coordinate system and nomenclature

r = coordinate distance

R = bubble radius

R_o = initial bubble radius

a = r/R_o = dimensionless coordinate distance

A = R/R_o = dimensionless bubble radius

P_g = pressure inside the bubble

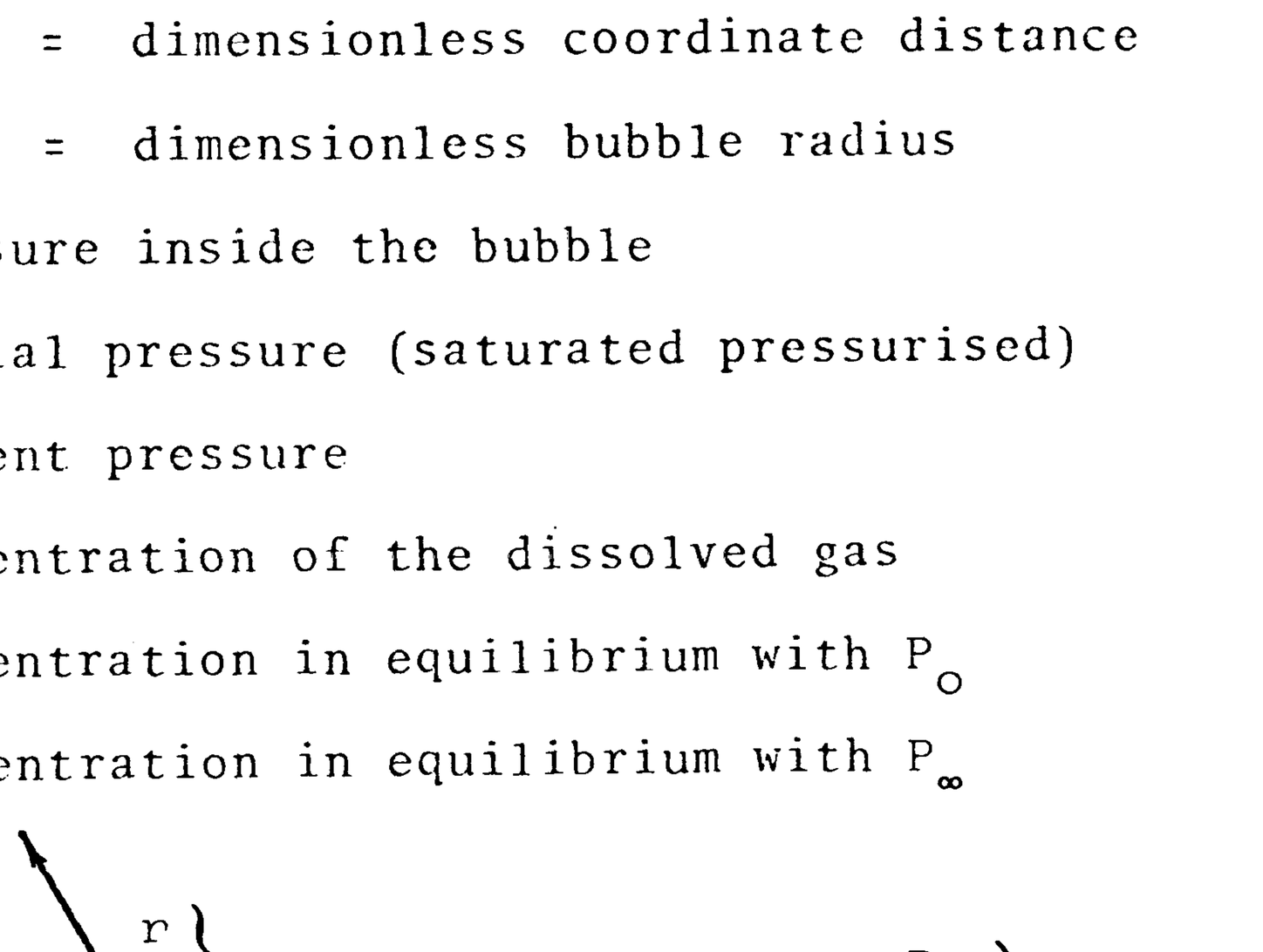
P_o = initial pressure (saturated pressurised)

P_∞ = ambient pressure

C = concentration of the dissolved gas

C_o = concentration in equilibrium with P_o

C_{sat} = concentration in equilibrium with P_∞



3.1.2 Continuity equation

The general equation of continuity in the liquid:

$$\frac{D\rho}{Dt} = -\rho (\nabla \cdot \underline{v})$$

becomes, for the case of spherical symmetry with no θ or ϕ dependence, and constant liquid density:

$$v_r r^2 = k(t) = k \qquad (3.2)$$

A mass balance readily yields $k(t)$. When the rate of change of the density of the gas within the bubble is much less rapid than the rate of change of the volume of the bubble, equation 3.2 becomes:

$$v_r r^2 = \varepsilon \dot{R} R^2 \qquad (3.3)$$

where:

R = radius of the bubble

$\dot{R}$ = velocity of the bubble surface

$$= \frac{dR}{dt}$$

$$\varepsilon = 1 - \frac{\rho_g}{\rho_\ell} = 1 \text{ for } \rho_g << \rho_\ell \qquad (3.4)$$

3.1.3 Momentum equation

The general momentum equation is:

$$\frac{D\,\underline{v}}{D\,t} = -\nabla P - (\nabla \cdot \tau) + \rho_\ell g$$

For spherical symmetry and no body forces, this reduces to:

$$\rho_\ell \left[\frac{\partial v_r}{\partial t} + v_r \frac{\partial v_r}{\partial r} \right] = - \frac{\partial P}{\partial r} - \left[\frac{1}{r^2} \frac{\partial}{\partial r}(r^2 \tau_{rr}) - \frac{\tau_{\theta\theta} + \tau_{\phi\phi}}{r} \right] \qquad (3.5)$$

When the pressure gradient term is replaced by a pressure

tensor with components:

$$P_{rr} = -P - \tau_{rr} \qquad \text{etc.} \tag{3.6}$$

equation 3.5 can be rewritten as:

$$\rho_\ell \left[\frac{\partial v_r}{\partial t} + v_r \frac{\partial v_r}{\partial r} \right] = \frac{\partial P_{rr}}{\partial r} + \frac{\tau_{\theta\theta} + \tau_{\phi\phi} - 2\tau_{rr}}{r} \tag{3.7}$$

3.1.4 Diffusion equation

The general diffusion equation for constant liquid density and constant gas diffusivity is:

$$\frac{DC}{Dt} = D\nabla^2 C + Q$$

When the rate of reaction term Q is zero, and with spherical symmetry this reduces to:

$$\frac{\partial C}{\partial t} = D \left[\frac{\partial^2 C}{\partial r^2} + \frac{2}{r} \frac{\partial C}{\partial r} \right] - v_r \frac{\partial C}{\partial r} \tag{3.8}$$

Substituting the continuity expression, equation 3.3, the equation 3.8 then becomes:

$$\frac{\partial C}{\partial t} = D \left[\frac{\partial^2 C}{\partial r^2} + \frac{2}{r} \frac{\partial C}{\partial r} \right] - \frac{\varepsilon \dot{R} R^2}{r^2} \frac{\partial C}{\partial r} \tag{3.9}$$

3.1.5 Diffusional mass balance

The rate of change of the bubble mass is:

$$\frac{\partial}{\partial t} \left(\frac{4}{3} \pi R^3 \rho_g \right) \tag{3.10}$$

If it is assumed again that the rate of change of the gas density is much less than that of the bubble volume then expression 3.10 becomes:

$$4 \pi R^2 \rho_g \dot{R} \tag{3.11}$$

The rate of mass flow of the dissolved gas to the bubble surface is:

$$C(R,t)\ (\dot{R} - v_r)\ 4 \pi R^2 \quad + \quad 4 \pi R^2 D \left.\frac{\partial C}{\partial r}\right|_R \tag{3.12}$$

Equating 3.11 and 3.12 and writing:

$$\varepsilon = 1 - \frac{\rho_g}{\rho_\ell} = \frac{v_r}{\dot{R}}$$

equation 3.12 becomes:

$$\rho_g \dot{R} = C(R,t)\ (1 - \varepsilon)\dot{R} + D \left.\frac{\partial C}{\partial r}\right|_R \tag{3.13}$$

Equations 3.3, 3.7, 3.9 and 3.13 are now the basic equations governing the system. Some initial and boundary conditions have still to be obtained.

3.2 Scriven's solution for diffusional bubble growth

3.2.1 Derivation of the asymptotic solution

Initially, the growth of the bubble depends very strongly on the inertia, viscosity and surface tension of the surrounding liquid. However, the growth soon becomes limited by the rate at which material can diffuse to the bubble surface. Thereafter, the growth is governed solely by the diffusion equation 3.9 and the diffusional mass balance equation 3.13 . Thus, solution of these two equations represents one asymptotic solution, an other being when the growth is limited solely by the momentum equation 3.7 . This former case was

solved analytically by Scriven (1959) but for the case of a vapour bubble, with a footnote giving the final result for a gas bubble. The derivation for a gas bubble is described below.

The diffusion equation 3.9 and the diffusional mass balance equation 3.13 are the basis for the solution. Initially the liquid is of uniform composition so:

$$C(r,0) = C_o \qquad \text{all } r > R: \; t = 0 \tag{3.14}$$

At large distances from the bubble, the concentration of dissolved gas remains unchanged so the boundary condition at infinity is:

$$C(\infty,t) = C_o \qquad r = \infty : \text{all } t \tag{3.15}$$

It is assumed that the gas inside the bubble is at the ambient pressure, P_∞ , and that the adjacent liquid is in thermodynamic equilibrium with it. Hence, the boundary condition at the bubble surface is:

$$C(R,t) = C_{sat} \qquad r = R : \text{all } t > 0 \tag{3.16}$$

Assume that it is possible to have a similarity solution of the form:

$$C(S) = C(r,t) \tag{3.17}$$

where:

$$S = \frac{r}{2\sqrt{Dt}} \tag{3.18}$$

Note that, at the bubble surface:

$$R = 2\beta\sqrt{Dt} \tag{3.19}$$

where β is the dimensionless growth coefficient.

Substituting equation 3.18 into equation 3.9 gives:

$$\frac{d^2C}{dS^2} = 2\frac{dC}{dS}\left(-S - \frac{1}{S} + \frac{\varepsilon\beta^3}{S^2}\right) \qquad (3.20)$$

Integrating equation 3.20 once gives:

$$\frac{dC}{dS} = \frac{A}{S^2}\exp\left(-S^2 - \frac{2\varepsilon\beta^3}{S}\right) \qquad (3.21)$$

where A is a constant of integration to be determined from the diffusional mass balance equation 3.13 . When this is done, equation 3.21 is integrated again and when the initial and boundary conditions 3.14, 3.15 and 3.16 are substituted, the final result is:

$$\Phi\{\varepsilon,\beta\} = \frac{\rho_\ell (C_o - C_{sat})}{\rho_g (\rho_\ell - C_{sat})} \qquad (3.22)$$

$$= 2\beta^3 \exp\left[\beta^2 + 2\varepsilon\beta^2\right] \int_\beta^\infty x^{-2} \exp\left[-x^2 - \frac{2\varepsilon\beta^3}{x}\right] dx$$

Equation 3.22 is that obtained by Scriven. The right hand side is easily integrated by numerical means and Scriven presents a table of values of β versus $\Phi\{\varepsilon,\beta\}$. Since Φ is readily calculated from the known densities and concentrations of the dissolved gas, the growth constant β may be quickly determined. Equation 3.19 then gives the relationship between bubble radius and time, for this diffusion limited asymptotic solution.

3.2.2 Approximations for small and large β

Scriven showed that:

(i) For small β

$$\Phi\{\varepsilon,\beta\} \rightarrow 2\beta^2 \qquad (3.23)$$

This is correct, within 5%, for $\beta < 0.025$, $\Phi < 0.00125$.

(ii) For large β

$$\Phi\{1,\beta\} \rightarrow \beta\sqrt{\frac{\pi}{3}} \qquad (3.24)$$

$$(\rightarrow \beta \text{ within } 2.3\%)$$

This is correct, within 5%, for $\beta > 8.0$, $\Phi > 8.0$.

3.2.3 Comparison with earlier solutions

For the case of small growth rates, when equation 3.23 applies, Scriven's solution may be written (for $C_{sat} << \rho_\ell$) as:

$$R = \sqrt{\frac{2(C_o - C_{sat})\ Dt}{\rho_g}} \qquad (3.25)$$

Epstein and Plesset (1950) gave an approximate solution for growth from an initial size R_o . When written in the present nomenclature, the solution is:

$$R = \sqrt{R_o^2 + \frac{2(C_o - C_{sat})\ Dt}{\rho_g}} \qquad (3.26)$$

This approaches the Scriven solution as R becomes increasingly greater than R_o , the initial radius.

3.3 Expansion of the momentum equation for a newtonian liquid

The momentum equation has already been presented in a form (equation 3.7) which applies equally to a newtonian or a non-newtonian liquid. It will now be expanded for a newtonian liquid.

The components of the stress tensor τ_{ij} of equation 3.7 may be written, for $v_r = v_r(r)$, $v_\theta = 0$, $v_\phi = 0$ as:

$$\left.\begin{aligned} \tau_{rr} &= -2\mu \frac{\partial v_r}{\partial r} \\ \tau_{\theta\theta} &= -2\mu \frac{v_r}{r} \\ \tau_{\phi\phi} &= -2\mu \frac{v_r}{r} \end{aligned}\right| \quad (3.27)$$

From the equation of continuity 3.3:

$$v_r r^2 = \varepsilon \dot{R} R^2 = k(t) = k \quad (3.3)$$

Substituting equation 3.3 into equation 3.27 gives the components as:

$$\left.\begin{aligned} \tau_{rr} &= \frac{4\mu k}{r^3} \\ \tau_{\theta\theta} &= \tau_{\phi\phi} = -\frac{2\mu k}{r^3} \end{aligned}\right| \quad (3.28)$$

and so the momentum equation 3.7 becomes:

$$\rho_\ell \left[\frac{\partial v_r}{\partial t} + v_r \frac{\partial v_r}{\partial r}\right] = \frac{\partial p_{rr}}{\partial r} - \frac{12\mu k}{r^4} \quad (3.29)$$

Equation 3.29 can be arranged and integrated from the bubble

surface to infinity to yield:

$$\frac{1}{\varepsilon \rho_\ell}\left[P_{rr}(\infty) - P_{rr}(R)\right] = R\ddot{R} + (2 - \frac{\varepsilon}{2})\dot{R}^2 + \frac{4\nu\dot{R}}{R} \qquad (3.30)$$

The radial component of the radial stress at infinity $P_{rr}(\infty)$ is simply the negative of the ambient pressure, P_∞ . The normal stress at the bubble surface is given by:

$$-P_{rr}(R) = P_g - \frac{2\sigma}{R} + \rho_\ell (\dot{R} - v_r(R)) v_r(R) \qquad (3.31)$$

The first term on the right hand side is the pressure inside the bubble, the second term is due to the surface tension and the third is due to the velocity difference across the moving surface at which there is a density discontinuity. This third term may be neglected when $\rho_g << \rho_\ell$. When equation 3.31 is substituted into equation 3.30, the final result is:

$$\frac{P_g - P_\infty}{\varepsilon \rho_\ell} = R\ddot{R} + (1 + \frac{\varepsilon}{2})\dot{R}^2 + 4\nu\frac{\dot{R}}{R} + \frac{2\sigma}{\varepsilon\rho_\ell R} \qquad (3.32)$$

It is convenient to put equation 3.32 into dimensionless form. The following substitutions are made:

$$\left.\begin{aligned} A &= \frac{R}{R_o} && \text{a} \\ \tau &= \frac{Dt}{R_o^2} && \text{b} \\ \Pi &= \frac{P_g - P_\infty}{P_o - P_\infty} && \text{c} \\ \Delta P &= P_o - P_\infty && \text{d} \end{aligned}\right| \qquad (3.33)$$

$$G = \frac{R_o^2 \, \Delta P}{D^2 \, \rho_\ell} \qquad (3.33)$$

where:

R_o = the initial radius

τ = the dimensionless time

P_o = the equilibrium pressure of the supersaturated solution

Π = the dimensionless pressure within the bubble

G = a dimensionless parameter containing a measure of the liquid inertia and the pressure driving force.

The final version of the momentum equation, for the case when $\varepsilon = 1$, can then be written as:

$$A \frac{d^2A}{d\tau^2} + \frac{3}{2}\left(\frac{dA}{d\tau}\right)^2 + 4\,Sc\,\frac{1}{A}\frac{dA}{d\tau} = G\left[\Pi - \frac{\phi}{A}\right] \qquad (3.34)$$

where:

Sc = Schmidt number = $\frac{\nu}{D}$

ϕ = surface tension parameter = $\frac{2\,\sigma}{\Delta P\, R_o}$

ϕ indicates the degree of displacement of the initial radius from the equilibrium radius. If ϕ is less than unity the bubble will grow; if greater than unity it will dissolve. When $\phi = 1$, the bubble will be in equilibrium with the surrounding liquid.

3.4 Expansion of the momentum equation for a non-newtonian (power law) liquid

In this section, the case of a bubble growing in a non-newtonian liquid of the Oswald-de Waele (power law) type will be investigated.

The power law is a two parameter model of the form:

$$\tau_{yx} = -m' \left| \frac{dv_x}{dy} \right|^{n-1} \frac{dv_x}{dy} \qquad (3.35)$$

For the case of $n = 1$, it reduces to Newton's law of viscosity with $m' = \mu$. The deviation of n from unity indicates the degree of departure from newtonian behaviour. For n less than unity, the behaviour is termed pseudoplastic; for n greater than unity, dilatant. Many fluids, especially solutions of polymers and many plastics, have their flow properties well described by the power law model. (See Reiner (1960) and Skelland (1967)). It was felt that some recognition should be given to this class of material in terms of the current problem of diffusional bubble growth.

Bird, Stewart and Lightfoot (1960) discuss how the general form of Newton's law of viscosity may be extended approximately to non-newtonian, incompressible liquids.

Newton's law of viscosity for an incompressible liquid is:

$$\tau = -\mu \Delta \qquad (3.36)$$

where τ is the shear stress tensor and Δ the rate of deformation tensor. The "viscosity coefficient" μ does not depend on either τ or Δ . For non-newtonian fluids the expression 3.36 is not correct but it is possible to write:

$$\tau = -\eta \Delta \qquad (3.37)$$

where η is a non-newtonian "viscosity", a scalar and a function of τ or Δ . In order for η to be a scalar of the tensor Δ , it must depend only on the invariants of Δ , those components of Δ that transform as scalars when the co-ordinate system is rotated. The three invariants are:

$$\left.\begin{aligned} I_1 &= (\Delta:\delta) = 2(\nabla \cdot \underline{v}) \\ I_2 &= (\Delta:\Delta) \\ I_3 &= \det|\Delta| \end{aligned}\right| \qquad (3.38)$$

For the incompressible fluid, the first invariant vanishes and so:

$$\eta = \eta(I_2, I_3)$$

For many flows, the third invariant is also equal to zero and even when it is not zero (as will be shown to be the case for an expanding bubble) its effect is usually assumed to be not very important. Certainly authors studying the flow of non-newtonian fluids around a sphere neglect it. (See, for example Adachi, Yoshioka and Yamamoto (1973)).

So, it will be assumed that equation 3.37 can be used in this case with the result that:

$$\eta = \eta(I_2) = \eta(\Delta:\Delta) \qquad (3.39)$$

The power law model will thus be used in the form given by Bird, Stewart and Lightfoot (1960) (their equation 3.6-9) viz:

$$\tau = -\left\{ m' \left| \sqrt{\tfrac{1}{2}(\Delta:\Delta)} \right|^{n-1} \right\} \Delta \qquad (3.40)$$

For the case of the expanding bubble with spherical symmetry, the components of the rate of deformation tensor Δ are:

$$\left.\begin{aligned} \Delta_{rr} &= 2\,\frac{\partial v_r}{\partial r} \\ \Delta_{\theta\theta} &= 2\,\frac{v_r}{r} \\ \Delta_{\phi\phi} &= 2\,\frac{v_r}{r} \\ \Delta_{r\theta} = \Delta_{\theta r} = \Delta_{\theta\phi} &= \Delta_{\phi\theta} = \Delta_{r\phi} = \Delta_{\phi r} = 0 \end{aligned}\right| \qquad (3.41)$$

and the third invariant of the tensor is:

$$I_3 = \det|\Delta| = 8\,\frac{v_r^2}{r^2}\,\frac{\partial v_r}{\partial r} \qquad (3.42)$$

As explained above, the dependence of Δ on the third invariant will not be considered further.

The second invariant $(\Delta:\Delta)$, with spherical symmetry is:

$$(\Delta:\Delta) = 4\left[\left(\frac{\partial v_r}{\partial r}\right)^2 + 2\left(\frac{v_r}{r}\right)^2\right] \qquad (3.43)$$

or,
$$\eta = m'\left[2\left\{\left(\frac{\partial v_r}{\partial r}\right)^2 + 2\left(\frac{v_r}{r}\right)^2\right\}\right]^{\frac{n-1}{2}} \qquad (3.44)$$

The diagonal components of the stress tensor τ can be written as:

$$\tau_{rr} = -2\eta\,\frac{\partial v_r}{\partial r} \qquad a| \quad (3.45)$$

$$\tau_{\theta\theta} = \tau_{\phi\phi} = -2\eta \frac{v_r}{r} \qquad \text{b} \quad (3.45)$$

Substituting the equation of continuity 3.2 (~~3.3~~), equations 3.45 become:

$$\tau_{rr} = \frac{4\eta k}{r^3} \qquad \text{a}$$

$$\tau_{\theta\theta} = \tau_{\phi\phi} = -\frac{2\eta k}{r^3} \qquad \text{b} \quad (3.46)$$

If equations 3.44 and 3.46 are substituted into the momentum equation 3.7 , it becomes, for a power law liquid:

$$\rho_\ell \left[\frac{\partial v_r}{\partial t} + v_r \frac{\partial v_r}{\partial r}\right] = \frac{\partial p_{rr}}{\partial r} - \frac{12\, m'\, k\, (2)^{\frac{n-1}{2}}}{r^4} \left[\left(\frac{\partial v_r}{\partial r}\right)^2 + 2\left(\frac{v_r}{r}\right)\right]^{\frac{n-1}{2}} \qquad (3.47)$$

Equation 3.47 can be rearranged and integrated from the bubble surface to infinity to yield:

$$\frac{1}{\varepsilon\, \rho_\ell}\left[P_{rr}(\infty) - P_{rr}(R)\right] = R\ddot{R} + (2 - \frac{\varepsilon}{2})\dot{R}^2 + \frac{12^{\frac{n+1}{2}}\, \varepsilon^{n-1}\, m}{3\, n}\left[\frac{\dot{R}}{R}\right]^n \qquad (3.48)$$

Note that $m = \frac{m'}{\rho_\ell}$ and is equivalent to the kinematic viscosity coefficient of a newtonian fluid .

The normal stress at the bubble surface and at infinity are given by equation 3.31 and when these are substituted into equation 3.48 the result is:

$$\frac{P_g - P_\infty}{\varepsilon\, \rho_\ell} = R\ddot{R} + (1 + \frac{\varepsilon}{2})\dot{R}^2 + \frac{12^{\frac{n+1}{2}}\, \varepsilon^{n-1}\, m}{3\, n}\left[\frac{\dot{R}}{R}\right]^n + \frac{2\sigma}{\varepsilon \rho_\ell R} \qquad (3.49)$$

Equation 3.49 can now be conveniently put into dimensionless form, using the substitutions of equation 3.33 . When $\varepsilon = 1$ the final version of the momentum equation can be written as:

$$A\frac{d^2A}{d\tau^2} + \frac{3}{2}\left(\frac{dA}{d\tau}\right)^2 + \frac{12^{\frac{n+1}{2}}}{3n} Sc^{*}\left(\frac{1}{A}\frac{dA}{d\tau}\right)^n = G\left[\Pi - \frac{\phi}{A}\right] \quad (3.50)$$

where Sc^{*} is a Schmidt number appropriate to this case:

$$Sc^{*} = \frac{m\, R_o^{2(1-n)}}{D^{(2-n)}} \quad (3.51)$$

and other groups are as previously defined. Equation 3.50 is equivalent to equation 3.34 for the newtonian liquid and they are identical, of course, when $n = 1$.

An implicit assumption in this section has been that the diffusivity remains constant. Now, it is known that diffusivity bears an inverse relationship with liquid viscosity, as shown by the well known Wilke and Chang (1955) equation (See Bird, Stewart and Lightfoot (1960)). But in a power law liquid, the apparent viscosity varies with the rate of shear and the question is whether this leads to a change in the diffusivity. Apparently this is not so, the diffusivity remaining approximately constant, at least for such power law liquids as solutions of polymers. This question is discussed further in Appendix A.2 where justification for the assumption of constant diffusivity is made.

3.5 Intermediate liquid - the Sisko model

Three parameter models would be expected to describe more accurately than two parameter models, the behaviour of a non-newtonian fluid. A common model is the Ellis model:

$$-\frac{dv_x}{dy} = \left(\psi_1 + \psi_2 \left|\tau_{yx}\right|^{\alpha-1}\right) \tau_{yx} \qquad (3.52)$$

which include Newton's law and the power law. For the purposes of analysis of the expanding bubble, it is more convenient to have τ directly in terms of $\frac{dv_x}{dy}$ and a suitable model of this kind is the Sisko model (Sisko (1958)). This model is:

$$\tau_{yx} = -\left(\lambda_1 + \lambda_2 \left|\frac{dv_x}{dy}\right|^{n-1}\right) \frac{dv_x}{dy} \qquad (3.53)$$

As in the Ellis model, it includes Newton's law (when $n = 1$) and the power law (when $\lambda_1 = 0$).

It is obvious that the expanded momentum equation for the Sisko liquid is just a combination of equations 3.34 and 3.50 thus:

$$A\frac{d^2A}{d\tau^2} + \frac{3}{2}\left(\frac{dA}{d\tau}\right)^2 + 4\,Sc\left(\frac{1}{A}\frac{dA}{d\tau}\right) + \frac{12^{\frac{n+1}{2}}}{3n} S\overset{*}{c}\left(\frac{1}{A}\frac{dA}{d\tau}\right)^n = G\left[\Pi - \frac{\phi}{A}\right] \qquad (3.54)$$

where:

Sc = Schmidt number for the newtonian part

$$= \frac{\lambda_1}{\rho_\ell D}$$

$S\overset{*}{c}$ = Schmidt number for the power law part

$$= \frac{\lambda_2 R_o^{2(1-n)}}{\rho_\ell D^{(2-n)}}$$

3.6 Expansion of the diffusion equation

The appropriate form of the diffusion equation is given by equation 3.9 viz:

$$\frac{\partial C}{\partial t} = D\left[\frac{\partial^2 C}{\partial r^2} + \frac{2}{r}\frac{\partial C}{\partial r}\right] - \frac{\varepsilon \dot{R} R^2}{r^2}\frac{\partial C}{\partial r} \qquad (3.9)$$

It is convenient to have equation 3.9 in dimensionless form so make the following substitutions; in addition to those of equation 3.33 :

$$\left.\begin{aligned} a &= \frac{r}{R_o} \\ C^* &= \frac{C - C_{sat}}{C_o - C_{sat}} \end{aligned}\right| \begin{matrix} f \\ \\ g \end{matrix} \qquad (3.33)$$

where a is a dimensionless radial co-ordinate distance and C^* is a dimensionless concentration.

When put into equation 3.9 with $\varepsilon = 1$, the result is:

$$\frac{\partial C^*}{\partial \tau} = \frac{\partial^2 C^*}{\partial a^2} + \left\{\frac{2}{a} - \frac{A^2}{a^2}\frac{dA}{d\tau}\right\}\frac{\partial C^*}{\partial a} \qquad (3.55)$$

3.7 Expansion of the boundary conditions

Upon specifying an initial bubble size, zero initial growth rate and uniform solute distribution at zero time, the initial and boundary conditions may be written as:

$$\left.\begin{aligned} R &= R_o \quad \text{at} \quad t = 0 \\ \dot{R} &= 0 \quad \text{at} \quad t = 0 \\ C &= C_o \quad \text{at} \quad t = 0 : r \geq R_o \end{aligned}\right| \qquad (3.56)$$

The boundary condition assumes that the concentration remains unchanged at infinity:

$$C = C_o \quad \text{at} \quad r = \infty : \text{all } t \tag{3.57}$$

At the bubble wall, the diffusional mass balance equation 3.13 , for $\varepsilon = 1$, is:

$$\rho_g \dot{R} = D \left.\frac{\partial C}{\partial r}\right|_R \tag{3.58}$$

In addition, assume that the thermodynamic equilibrium at the bubble wall can be expressed by Henry's law:

$$P_g = H C\big|_R \tag{3.59}$$

When put into dimensionless form, equations 3.56 - 3.59 become:

$$\left.\begin{array}{llll} A = 1 & \tau = 0 & & a \\ \dot{A} = 0 & \tau = 0 & & b \\ C^* = 1 & \tau = 0 & : \quad a \geq 1 & c \\ C^* = 1 & a = \infty & : \quad \text{all } \tau & d \\ \left.\frac{\partial C^*}{\partial a}\right|_A = \frac{1}{Ja}\frac{dA}{d\tau} & a = A & : \quad \text{all } \tau & e \\ \Pi = C^*\big|_A & a = A & : \quad \text{all } \tau & f \end{array}\right| \tag{3.60}$$

where: $Ja = \dfrac{\Delta C}{\rho_g}$ = the Jakob number

$$\Delta C = C_o - C_{sat}$$

3.8 "Film theory" approach to Scriven's analysis

According to the Whitman two-film theory of absorption of gases (see Coulson and Richardson (1966)), a general expression for mass transfer across a phase boundary is:

$$N_g = k_g(P_g - P_i) = k_\ell(C_i - C_\ell) \qquad (3.61)$$

where N_g is the rate of mass transfer per unit area, k_g is the gas film mass transfer coefficient, k_ℓ is the liquid film mass transfer coefficient, P is the partial pressure of the soluble gas and C its concentration in the liquid. The subscripts g, ℓ and i refer to the gas phase, liquid phase and interface respectively. Since the concentrations of dissolved gas at the interface are not generally known, it is usual to write equation 3.61 in the following form, for the case where the mass transfer is controlled by diffusion through the liquid film:

$$N_g = K_\ell (C_o - C_{sat}) = K_\ell \Delta C \qquad (3.62)$$

where K_ℓ is the overall liquid film mass transfer coefficient and C_o and C_{sat} are as previously defined.

Now, in the asymptotic solution for bubble growth derived by Scriven (1959) and discussed in Section 3.2, it was assumed that the rate of bubble growth is limited by diffusion on the liquid side. No attempt has yet been made to apply an analysis similar to the film theory to the diffusional bubble growth problem, though in both instances this same assumption is made.

Suppose it is assumed that the instantaneous mass transfer rate can be represented by an equation of the form of equation 3.62 . The rate of change of the volume of the growing bubble is then:

$$\frac{dV}{dt} = \frac{a_b N_g}{\rho_g} \qquad (3.63)$$

where a_b is the instantaneous bubble area. Rewriting equation 3.63 as:

$$\frac{d}{dt}\left\{\frac{4}{3}\pi R^3\right\} = \frac{4\pi R^2 N_g}{\rho_g} \qquad \text{a}$$

$$\text{or,} \quad \frac{dR}{dt} = \frac{N_g}{\rho_g} = \frac{K_\ell \Delta C}{\rho_g} = K_\ell \, Ja \qquad \text{b} \qquad (3.64)$$

From the Scriven theory:

$$R = 2\beta\sqrt{Dt} \qquad (3.19)$$

Substitution of equation 3.19 into 3.64b yields, after some rearrangement:

$$Sh = \frac{2 R K_\ell}{D} = \frac{4\beta^2}{Ja} \qquad (3.65)$$

This gives a relationship between the instantaneous Sherwood number, Sh , the Jakob number, Ja , and the dimensionless growth coefficient β .

When Scriven's asymptotic approximations for β , for small and large values of $\Phi\{\varepsilon,\beta\}$ (equations 3.23 and 3.24) are substituted into equation 3.65, the result is:

(i) For small β

$$\Phi\{\varepsilon,\beta\} = Ja \rightarrow 2\beta^2 \tag{3.23}$$

$$Sh \rightarrow 2 \tag{3.66}$$

(ii) For large β

$$\Phi\{\varepsilon,\beta\} = Ja \rightarrow \beta\sqrt{\frac{\pi}{3}} \tag{3.24}$$

$$Sh \rightarrow \frac{12}{\pi}\ Ja \tag{3.67}$$

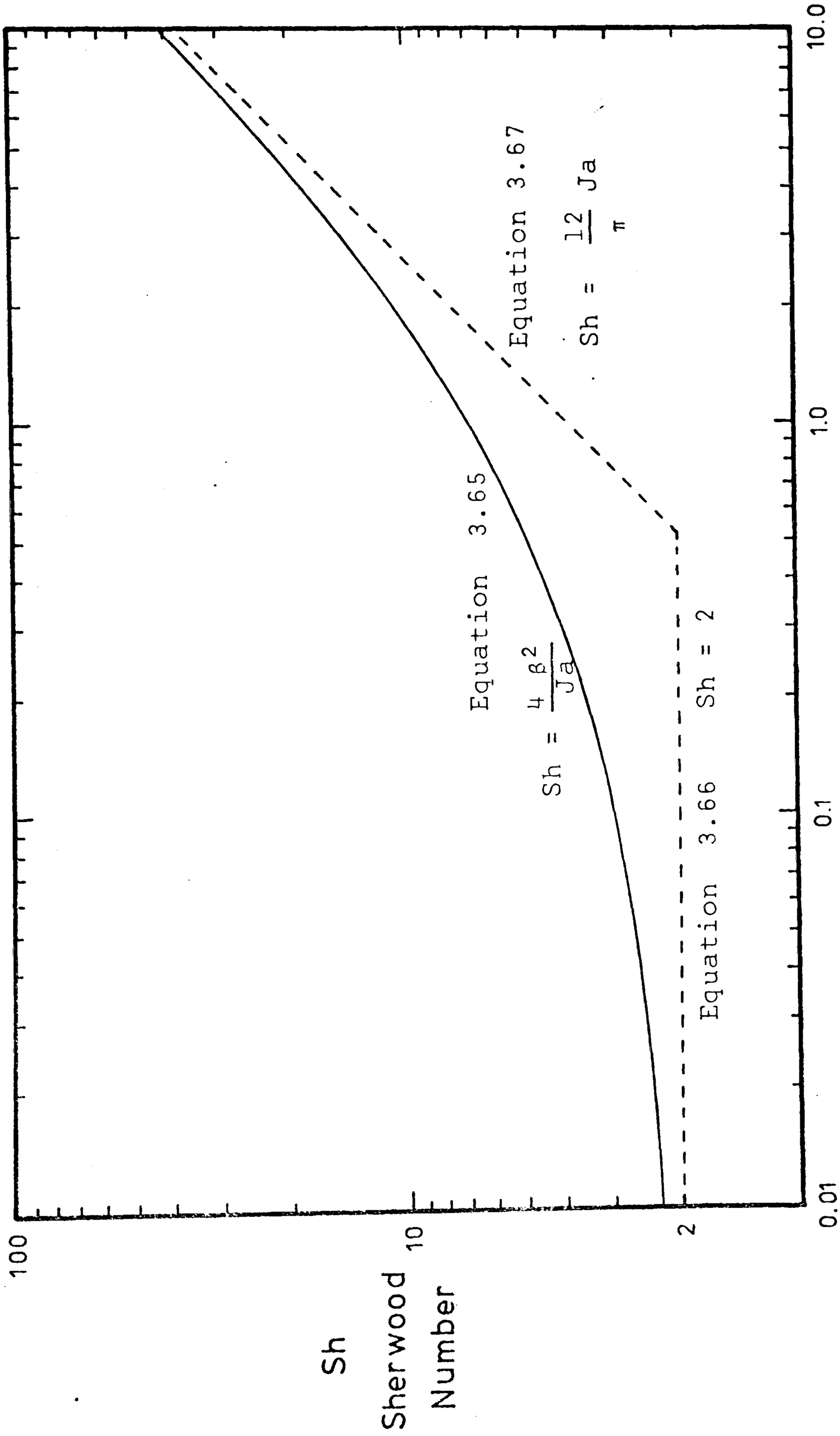
This is a particularly interesting result as equation 3.66 is identical to the classical Langmuir solution for diffusion from a stationary solid sphere into an infinite stagnant medium (see Valentin (1967)). The result suggests that the mass transfer to a bubble rising in a supersaturated solution might be able to be dealt with by existing correlations for moving solid spheres which involve the Reynolds and Schmidt numbers. Certainly, analytical or numerical solutions of the problem are extremely difficult and, to date, there does not appear to have been any successful attempts to investigate either. It is thus suggested that it is likely a correlation of the form:

$$Sh = \frac{4\ \beta^2}{Ja}\left[1 + f\{Re,Sc\}\right] \tag{3.68}$$

will be found to satisfy the case of a bubble rising in supersaturated solution.

Equation 3.65 and the asymptotes, equations 3.66 and 3.67 are illustrated on Figure 3.2 . A tabulation of equation 3.65 is found in Appendix A.1 .

Figure 3.2 Jakob number versus Sherwood number for a growing bubble



3.9 Summary

In this chapter, the governing equations of continuity momentum and diffusion and the initial and boundary conditions have been derived and put into dimensionless form. To summarise, these equations are:

(i) Momentum, for a newtonian liquid:

$$A \frac{d^2A}{d\tau^2} + \frac{3}{2}\left(\frac{dA}{d\tau}\right)^2 + 4\,Sc\,\frac{1}{A}\frac{dA}{d\tau} = G\left\{\Pi - \frac{\phi}{A}\right\} \quad (3.34)$$

(ii) Momentum, for a power law liquid:

$$A \frac{d^2A}{d\tau^2} + \frac{3}{2}\left(\frac{dA}{d\tau}\right)^2 + \frac{12^{\frac{n+1}{2}}}{3n} Sc^{*} \left(\frac{1}{A}\frac{dA}{d\tau}\right)^n = G\left\{\Pi - \frac{\phi}{A}\right\} \quad (3.50)$$

(iii) Diffusion:

$$\frac{\partial C^{*}}{\partial \tau} = \frac{\partial^2 C^{*}}{\partial a^2} + \left\{\frac{2}{a} - \frac{A^2}{a^2}\frac{dA}{d\tau}\right\}\frac{\partial C^{*}}{\partial a} \quad (3.55)$$

(iv) Initial and boundary conditions:

$$\left.\begin{array}{lll} A = 1 & \tau = 0 & a \\ \dot{A} = 0 & \tau = 0 & b \\ C^{*} = 1 & \tau = 0 : \quad a > 1 & c \\ C^{*} = 1 & a = \infty : \quad \text{all } \tau & d \\ \left.\frac{\partial C^{*}}{\partial a}\right|_A = \frac{1}{Ja}\frac{dA}{d\tau} & a = A : \quad \text{all } \tau & e \\ \Pi = \left.C^{*}\right|_A & a = A : \quad \text{all } \tau & f \end{array}\right| \quad (3.60)$$

There are three types of solution to be obtained from this set of equations. Firstly, if only diffusional mass transfer is limiting the bubble growth, equation 3.55 governs. The solution for this asymptotic case was obtained by Scriven and summarised in Section 3.2. When liquid properties dominate the growth, equations 3.34 or 3.50 govern. This asymptotic case has been solved numerically by Szekely and Martins (1971) for newtonian liquids and the solution for power law liquids will be investigated in Chapter 4 . When both liquid properties and diffusion govern the growth, equations 3.34 or 3.50 and 3.55 must be solved simultaneously. They are linked through the dimensionless pressure term Π in equation 3.34 and its equality to the the dimensionless interface concentration, found in boundary conditions 3.59e and f. This case also will be investigated in Chapter 4, for newtonian and power law liquids.

A relationship:

$$Sh = \frac{4\ \beta^2}{Ja}\left[1 + f\{Re,Sc\}\right]$$

has been suggested as a possible correlation for bubbles rising in a supersaturated solution.

CHAPTER 4

NUMERICAL SOLUTION OF THE BUBBLE GROWTH EQUATIONS

In this chapter, the equations derived in Chapter 3 (equations 3.34, 3.50, 3.55 and 3.60) will be put into a form suitable for numerical solution. The method of solution will then be described.

Firstly, the case where growth is limited by hydrodynamic forces will be considered, for both newtonian and power law liquids.

Secondly, the case where both hydrodynamic forces and diffusion are important will be considered, again for newtonian and power law liquids.

The case of diffusional limitation to growth will not be considered further but instead Scriven's (1959) solution will be taken for comparison with the other solutions.

Values of parameters which define the range of applicability of each of the solutions will be determined.

The results of the numerical solutions will be presented graphically.

4.1 Growth limited by hydrodynamic forces

4.1.1 Forming the appropriate equations for numerical solution

When growth is limited by hydrodynamic forces only, diffusion to the bubble surface is relatively so rapid that at all times the concentration of the diffusing species at the surface is equal to its initial value. Thus the dimensionless pressure within the bubble, Π , of equations 3.34 and 3.50 is equal to unity throughout the whole growth period.

So, in this instance the momentum equations 3.34 or 3.50 and the initial conditions 3.60a and b are appropriate.

In these momentum equations there are three parameters, the inertia parameter G , the Schmidt number Sc or Sc^* , the surface tension parameter ϕ as well as the two variables A and τ . The number of parameters and variables can be reduced from five to four by making the following change of variable:

$$T = \left[\frac{2}{3} G\right]^{\frac{1}{2}} \tau \qquad (4.1)$$

Actually, any transformation $T = (kG)^{\frac{1}{2}}\tau$ will be suitable but the factor $2/3$ is included for consistency with the work of Florschuetz and Chao (1965) and Szekely and Martins (1971). Also this transformation makes $\frac{dA}{dT}$ approach unity, as T increases, for the case of $Sc = 0$ and $\phi = 0$, which is a handy reference condition.

Making this substitution into equations 3.34 and 3.50 and noting that now $\Pi = 1$, the equations which result are:

for a newtonian liquid:

$$A\frac{d^2A}{dT^2} + \frac{3}{2}\left[\frac{dA}{dT}\right]^2 + 4\sqrt{\frac{3}{2}}\,V\,\frac{1}{A}\frac{dA}{dT} = \frac{3}{2}\left[1 - \frac{\phi}{A}\right] \qquad (4.2)$$

for a power law liquid:

$$A\frac{d^2A}{dT^2} + \frac{3}{2}\left[\frac{dA}{dT}\right]^2 + \frac{2^{\frac{3n}{2}}\,3^{\frac{1}{2}}}{n}\,V^*\left[\frac{1}{A}\frac{dA}{dT}\right]^n = \frac{3}{2}\left[1 - \frac{\phi}{A}\right] \qquad (4.3)$$

where:

$$V = \frac{Sc}{G^{\frac{1}{2}}} \qquad a \qquad (4.4)$$

$$V^* = \frac{Sc^*}{G^{(1-\frac{n}{2})}} \qquad b$$

V and V^* are measures of the relative importance of the viscous and inertial parameters.

The initial conditions for both equations 4.2 and 4.3 are:

$$A = 1 \qquad T = 0 \qquad a \qquad (4.5)$$

$$\frac{dA}{dT} = 0 \qquad T = 0 \qquad b$$

Equations 4.2 or 4.3 and 4.5 may now be solved numerically with different values of V and ϕ.

4.1.2 Method of solution

Equations 4.2 and 4.3 are non-linear, second order ordinary differential equations with initial conditions. Such equations may be solved readily by using the Runge-Kutta-Nyström method (see Kreyszig (1967)).

The problem to be solved is of the form:

$$\begin{aligned} y'' &= f(x,y,y') \\ \text{with:}\quad y(x_o) &= y_o \\ y'(x_o) &= y'_o \end{aligned} \qquad (4.6)$$

The method involves the computation of the following auxiliary quantities, for the (n+1)th step:

$$\begin{aligned} A_n &= \frac{h}{2} f(x_n, y_n, y'_n) \\ B_n &= \frac{h}{2} f(x_n + \frac{h}{2}, y_n + B_e, y'_n + A_n) \\ C_n &= \frac{h}{2} f(x_n + \frac{h}{2}, y_n + B_e, y'_n + B_n) \\ D_n &= \frac{h}{2} f(x_n + \frac{h}{2}, y_n + D_e, y'_n + 2C_n) \end{aligned} \qquad (4.7)$$

where:

$$\begin{aligned} h &= \text{step length} \\ B_e &= \frac{h}{2}(y'_n + \frac{A_n}{2}) \\ D_e &= \frac{h}{2}(y'_n + C_n) \end{aligned}$$

Having calculated these quantities, the new values of x, y and y' at the end of the step are approximated by:

$$\begin{aligned} x_{n+1} &= x_n + h \\ y_{n+1} &= y_n + h\left(y'_n + \frac{1}{3}(A_n + B_n + C_n) \right) \end{aligned} \qquad (4.8)$$

$$y'_{n+1} = y'_n + \frac{1}{3}(A_n + 2B_n + 2C_n + D_n) \quad (4.8)$$

These values are then used in the next step.

A computer programme (Program P1) was written to enable this calculation to be performed. It uses exactly the nomenclature of equations 4.6, 4.7 and 4.8 except y' is referred to as z in the programme.

4.1.3 Computational procedure

As mentioned above, it was found that the rate of increase of bubble radius $\frac{dA}{dT}$ approaches a constant value as T increases. In fact, for an inviscid liquid with no surface tension, the result is $A \doteqdot T$ when $T > 2$. This result suggests that a suitable range of integration might be from $T = 0$ to $T = 100$, when A , for this limiting case, will vary from 1 to about 100 . All other cases were thus integrated for T varying between 0 and 100 .

A suitable step length ΔT had to be determined for the numerical solution. It was necessary to examine the stability and convergence of the solution for each set of parameters and chose an appropriate ΔT . In this examination, the steplengths were successively halved until, at $T = 10$, A did not vary by more than ± 0.001 . This was an absolute error of between 0.1% and 0.01% according to the rate of growth in the early stages. This step length was again halved before the full integration was finally proceeded with, using Program P1. A variation of Program P1 was used to search for this step length.

The step lengths needed to give a stable solution and to satisfy the convergence criterion varied from $T = 0.01$ (resulting finally in 1000 iterations) for the case of the inviscid liquid with no surface tension ($V = 0$, $\phi = 0$), to $T = 0.01$ (10,000 iterations) for a power law liquid of exponent 0.5 with $V = 2$ and $\phi = 0.5$. The slower the initial growth rate, the smaller the time step required.

4.1.4 Results for newtonian liquids

The results calculated for diffusional bubble growth limited by newtonian hydrodynamic forces only are shown, for various parameters, in Figures 4.1 to 4.5 . The values of the parameters are given on each figure.

There are two limiting cases of special interest. Figure 4.1 shows bubble radius versus time T for the case where surface tension forces are absent ($\phi = 0$). The viscous/inertia parameter V is varied between 0 and 10 . It is seen that the viscous forces start to become significant only when V exceeds about 0.1 . Figure 4.2 shows radius versus time T when only surface tension forces are significant ($V = 0$). It is seen that there is only a short time during which the force is significant, after which bubble growth is resumed at the same rate as if the forces were absent. Even for the case of $\phi = 0.999$ (i.e. the initial bubble size is only 0.1% larger than the equilibrium radius), the overall growth is not significantly retarded.

Figure 4.1 Hydrodynamically controlled bubble growth

Effect of viscous forces

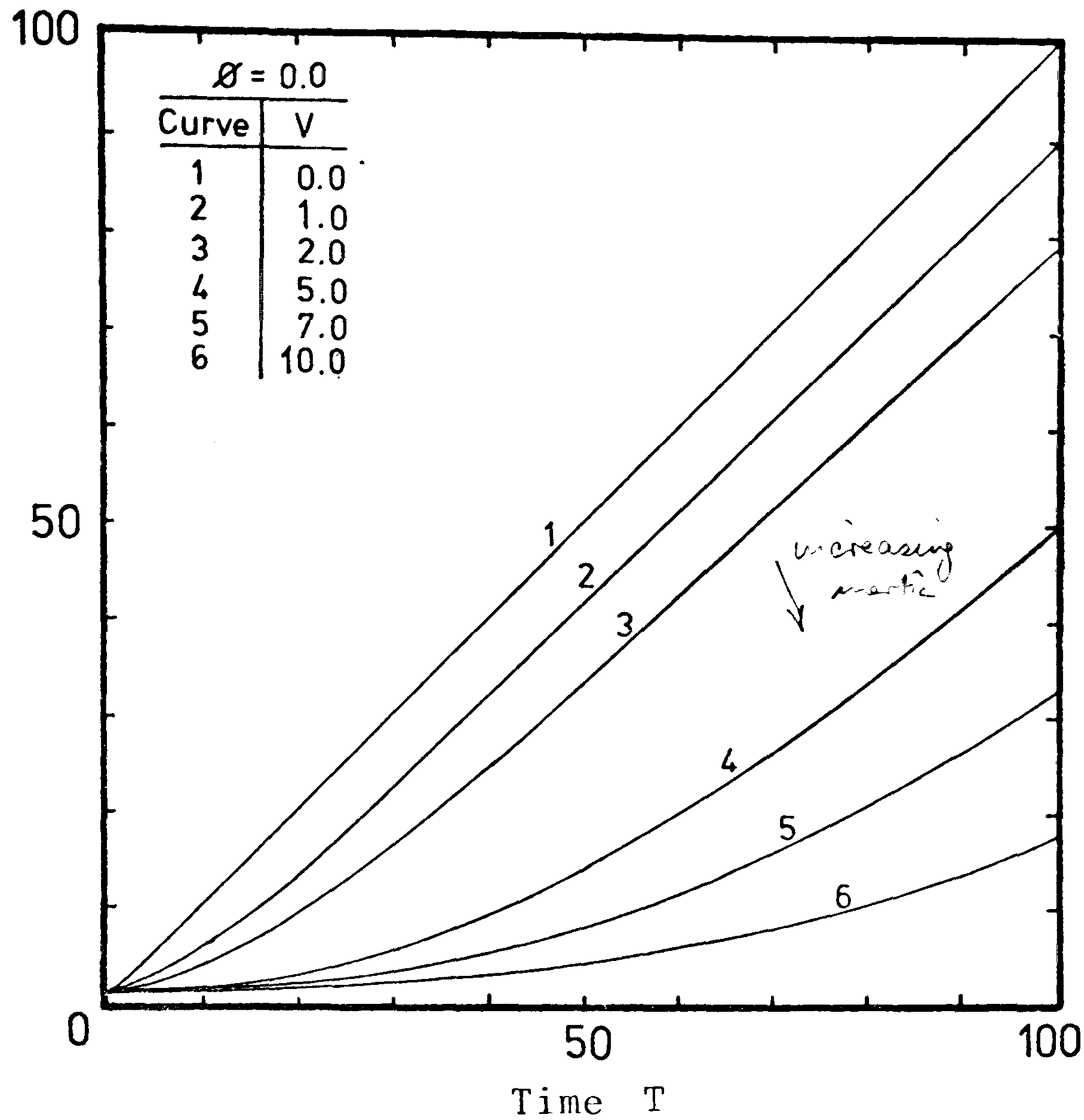


Figure 4.2 Hydrodynamically controlled bubble growth

Effect of surface tension

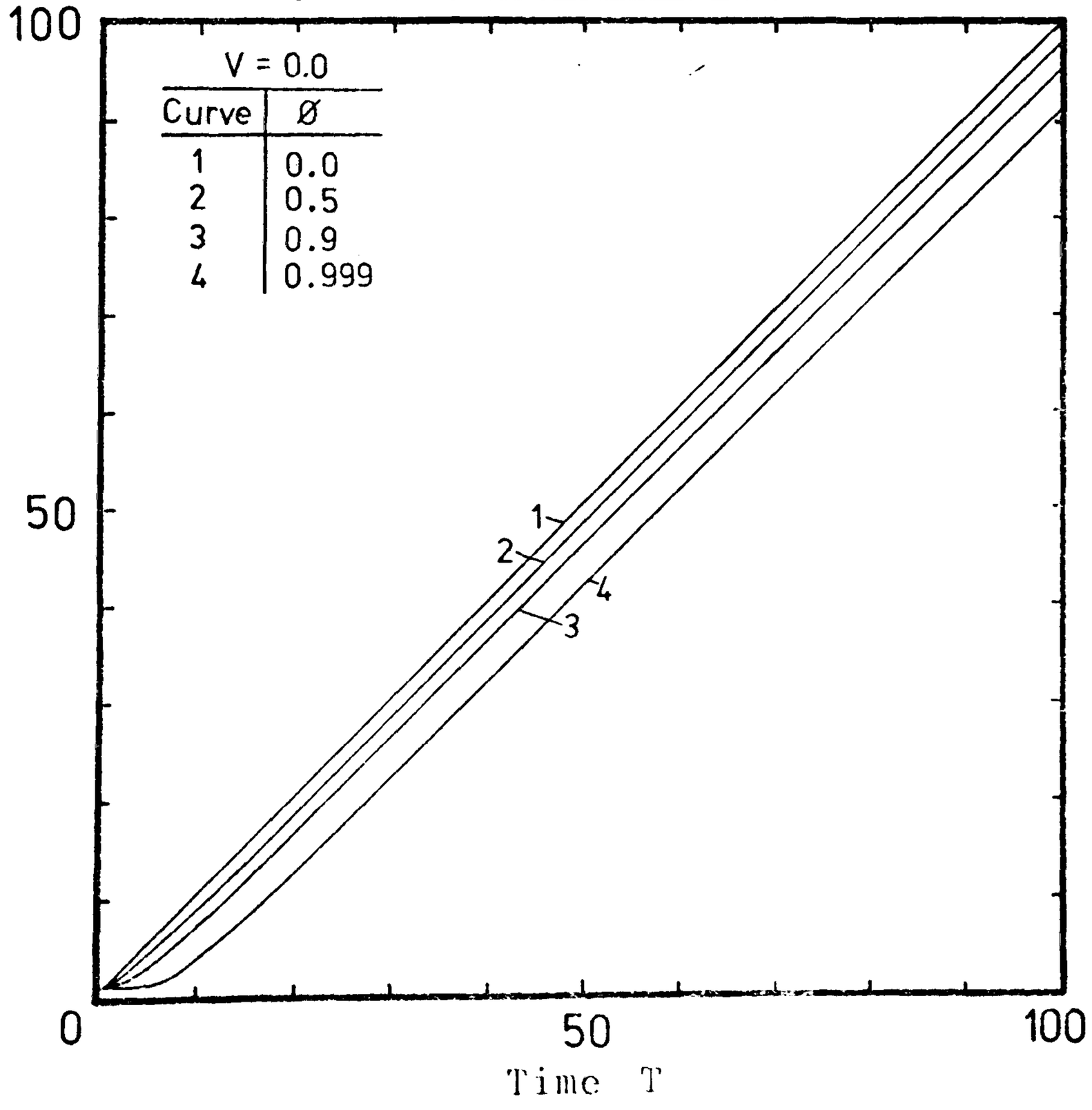


Figure 4.3 Hydrodynamically controlled bubble growth

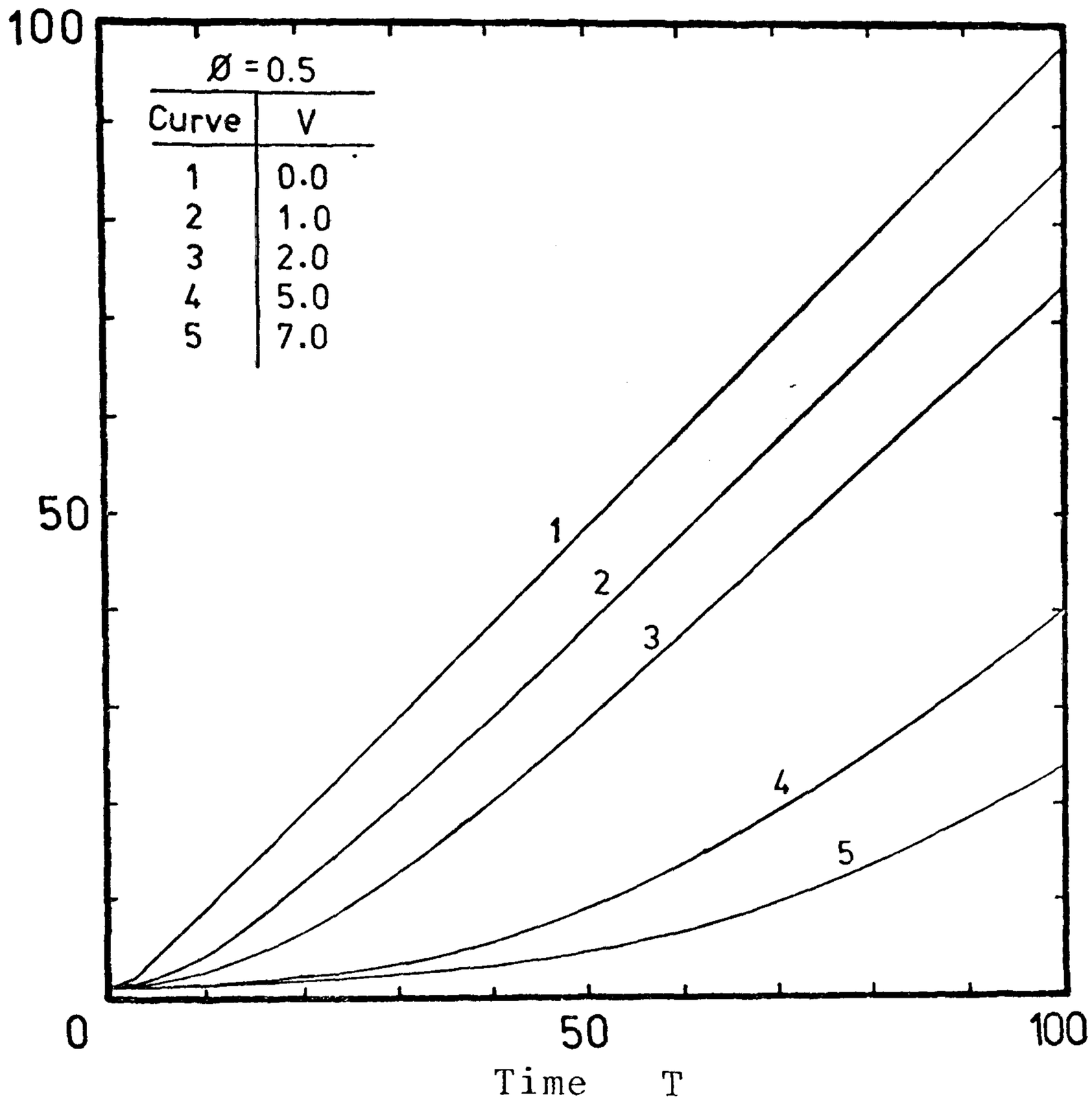


Figure 4.4 Hydrodynamically controlled bubble growth

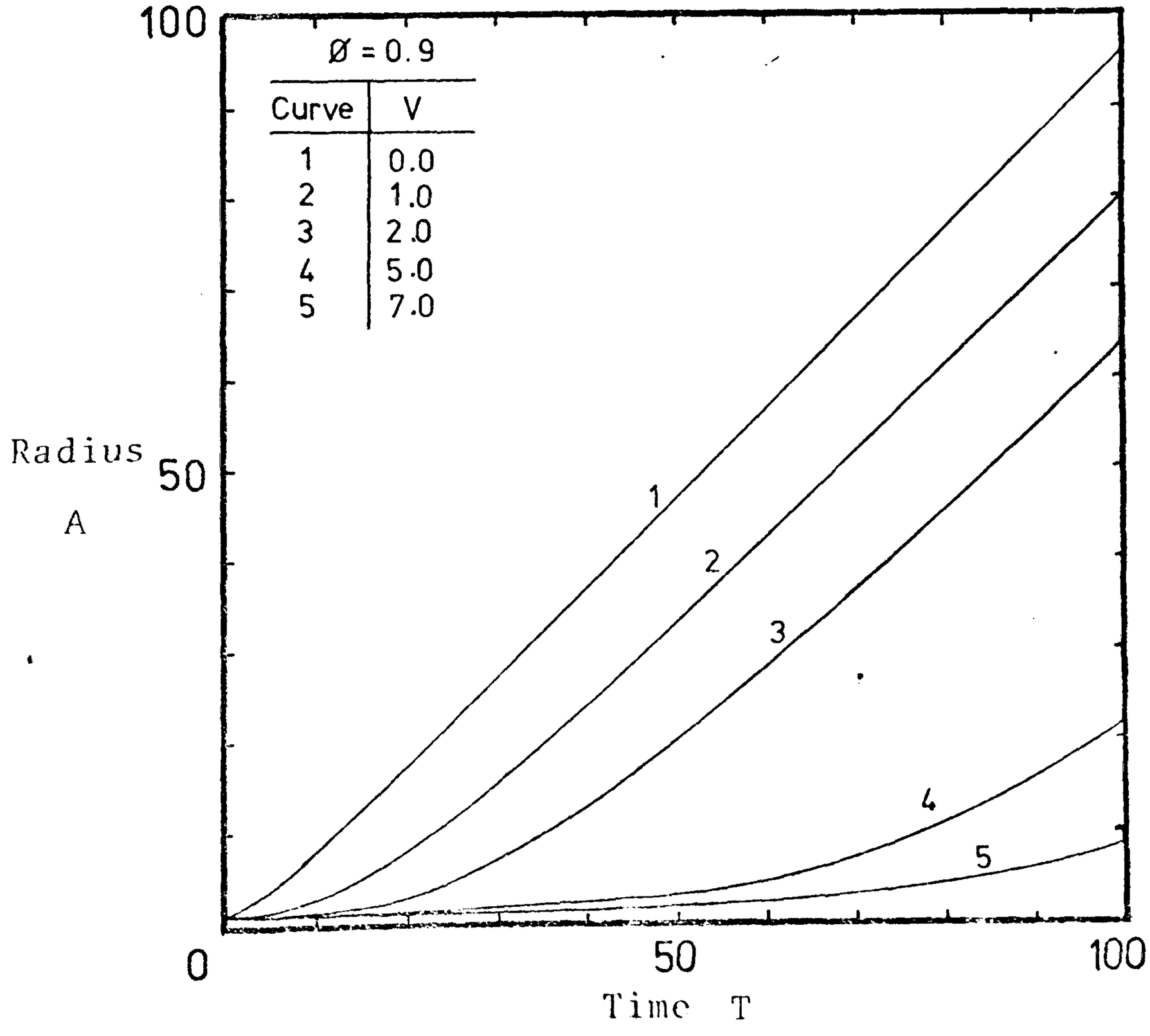
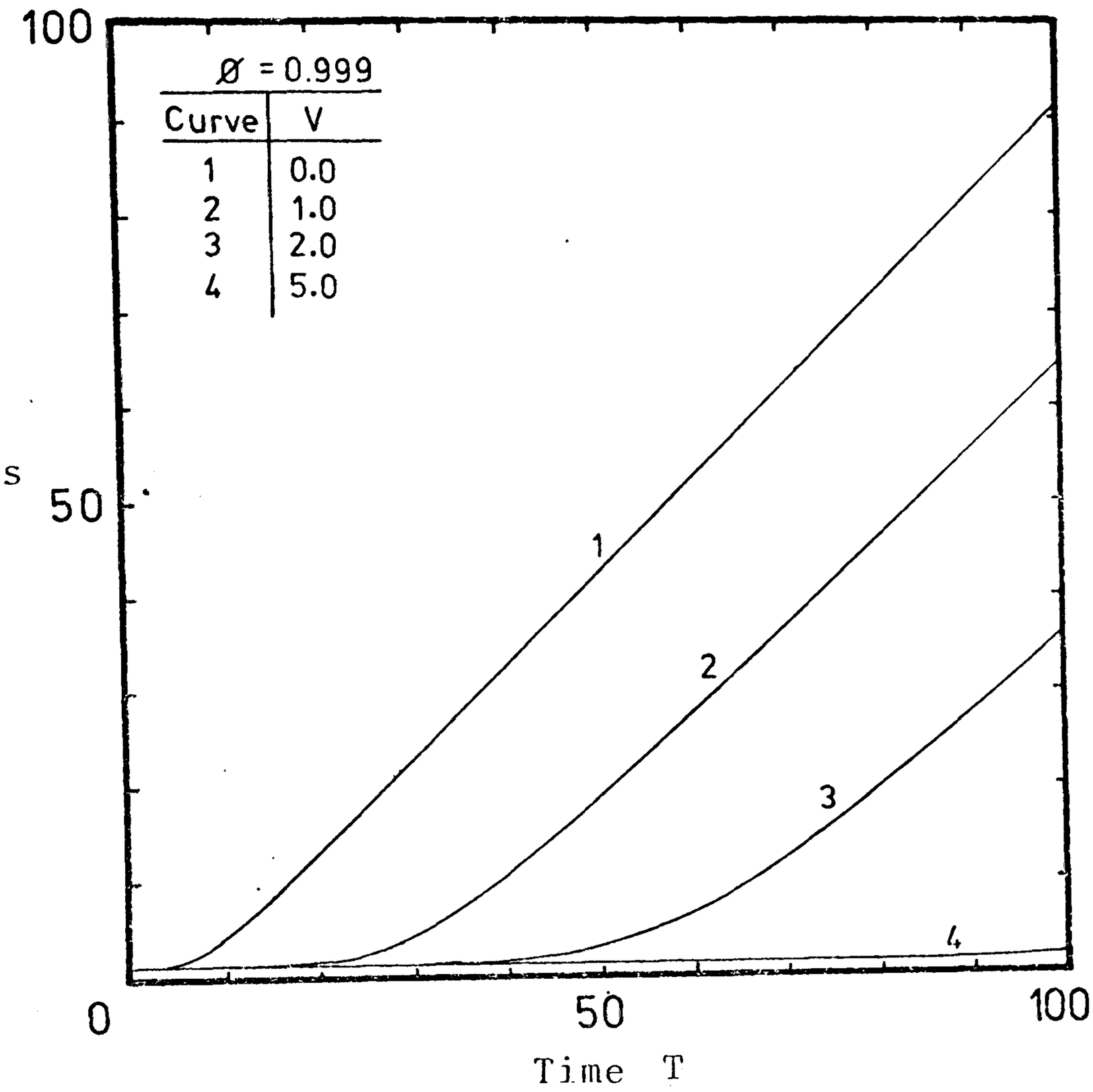


Figure 4.5 Hydrodynamically controlled bubble growth



4.1.5 Results for power law liquids

The results calculated for diffusional bubble growth in power law liquids, when limited by hydrodynamic forces, are shown in Figures 4.6 to 4.14 . The remarks made above concerning the effect of the surface tension parameter apply equally to the power law case. Figures 4.7 to 4.14 show that the most significant parameter is the power law exponent; the smaller the exponent, the slower the initial bubble growth rate.

Figure 4.6 Hydrodynamically controlled bubble growth

Power law liquid

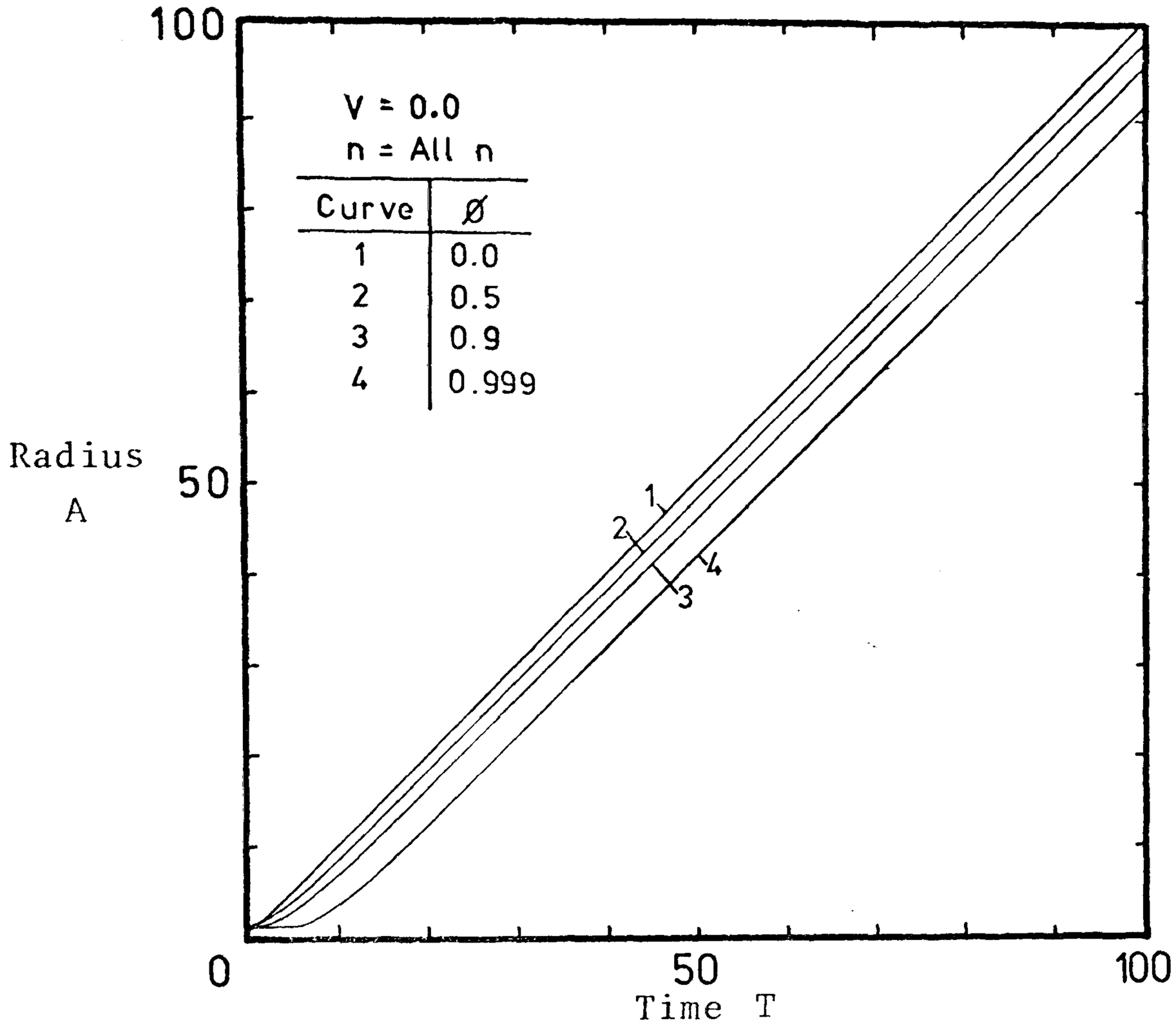


Figure 4.7 Hydrodynamically controlled bubble growth

Power law liquid

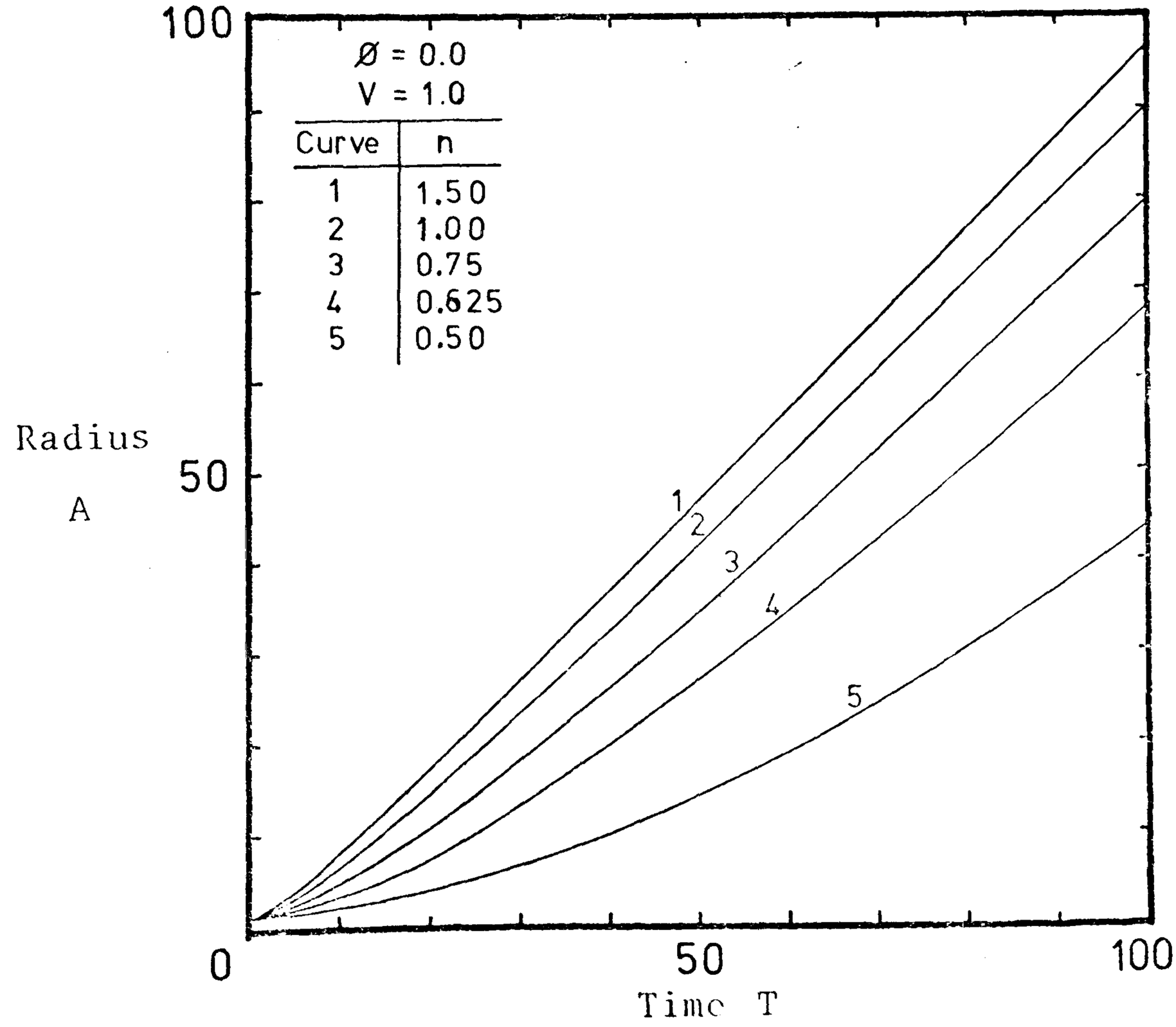


Figure 4.8 Hydrodynamically controlled bubble growth

Power law liquid

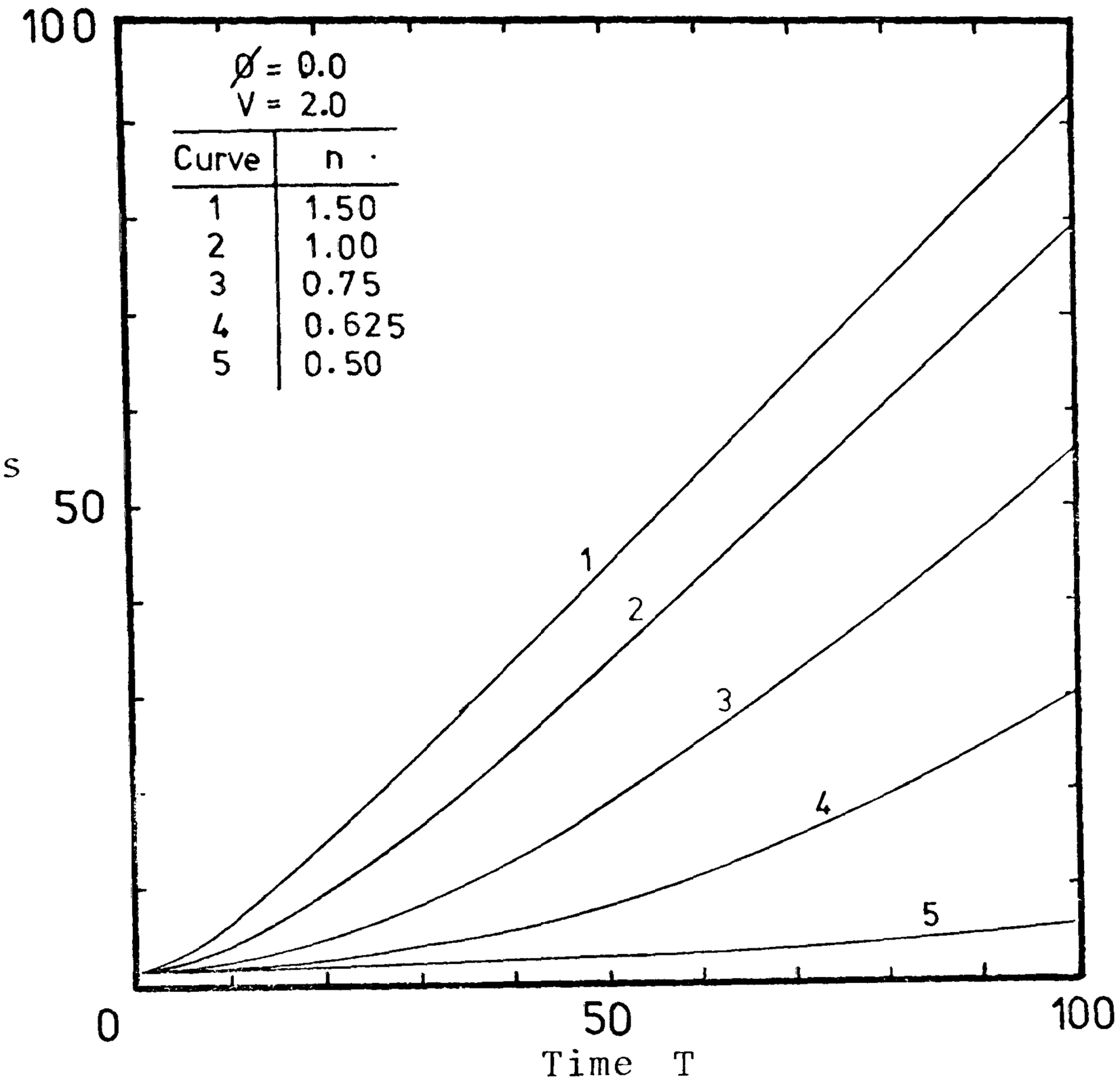


Figure 4.9 Hydrodynamically controlled bubble growth

Power law liquid

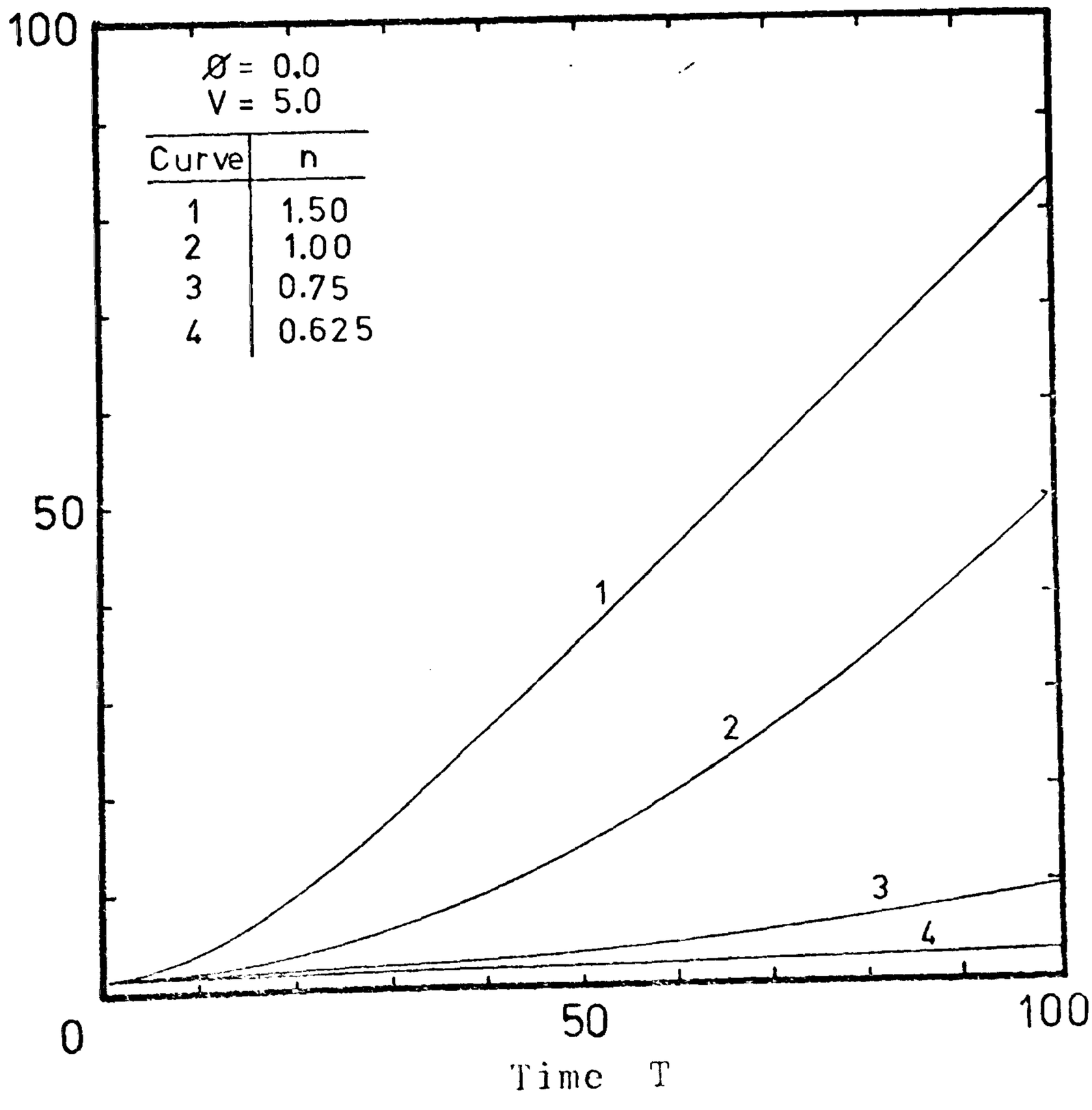


Figure 4.10 Hydrodynamically controlled bubble growth

Power law liquid

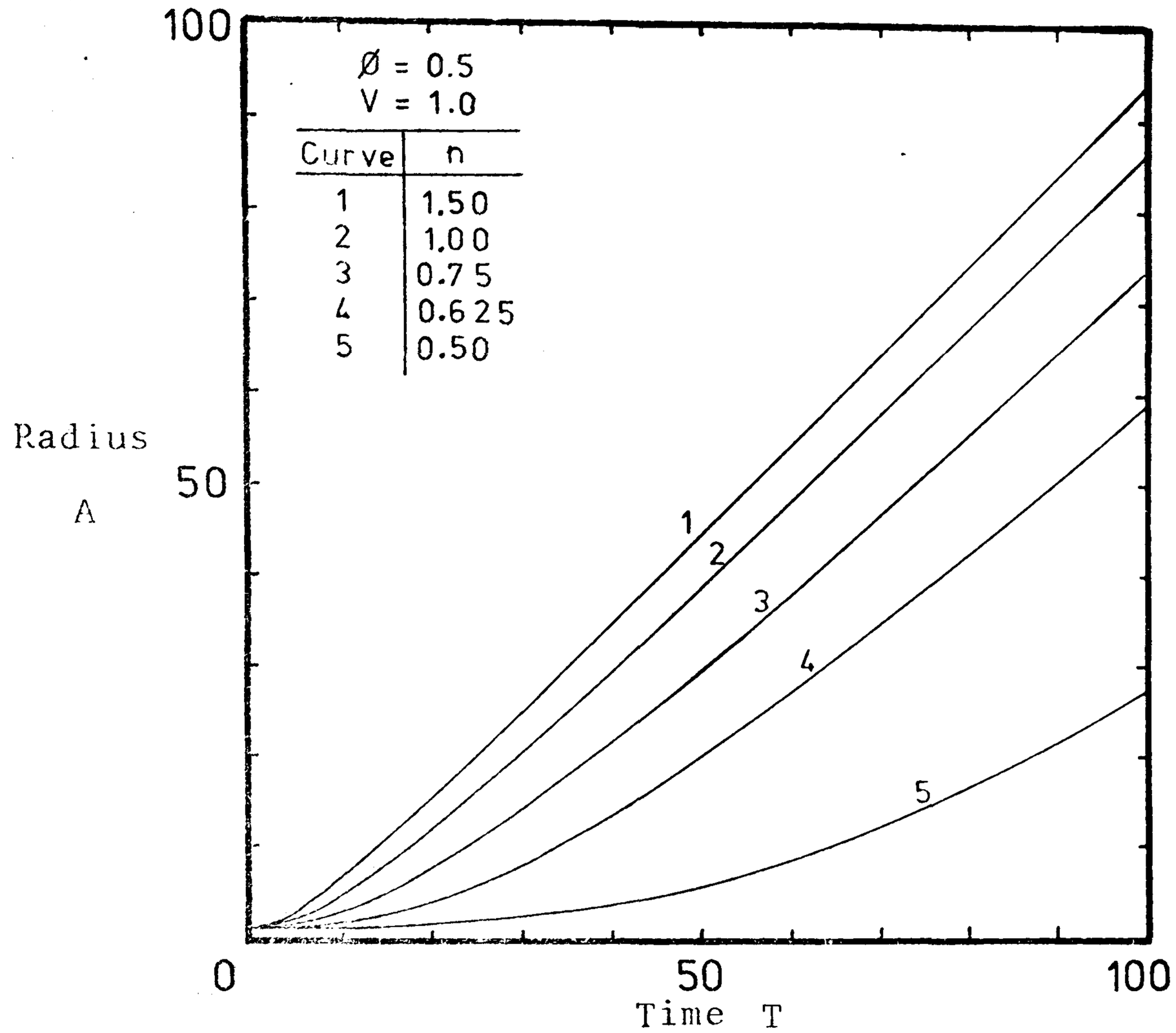


Figure 4.11 Hydrodynamically controlled bubble growth

Power law liquid

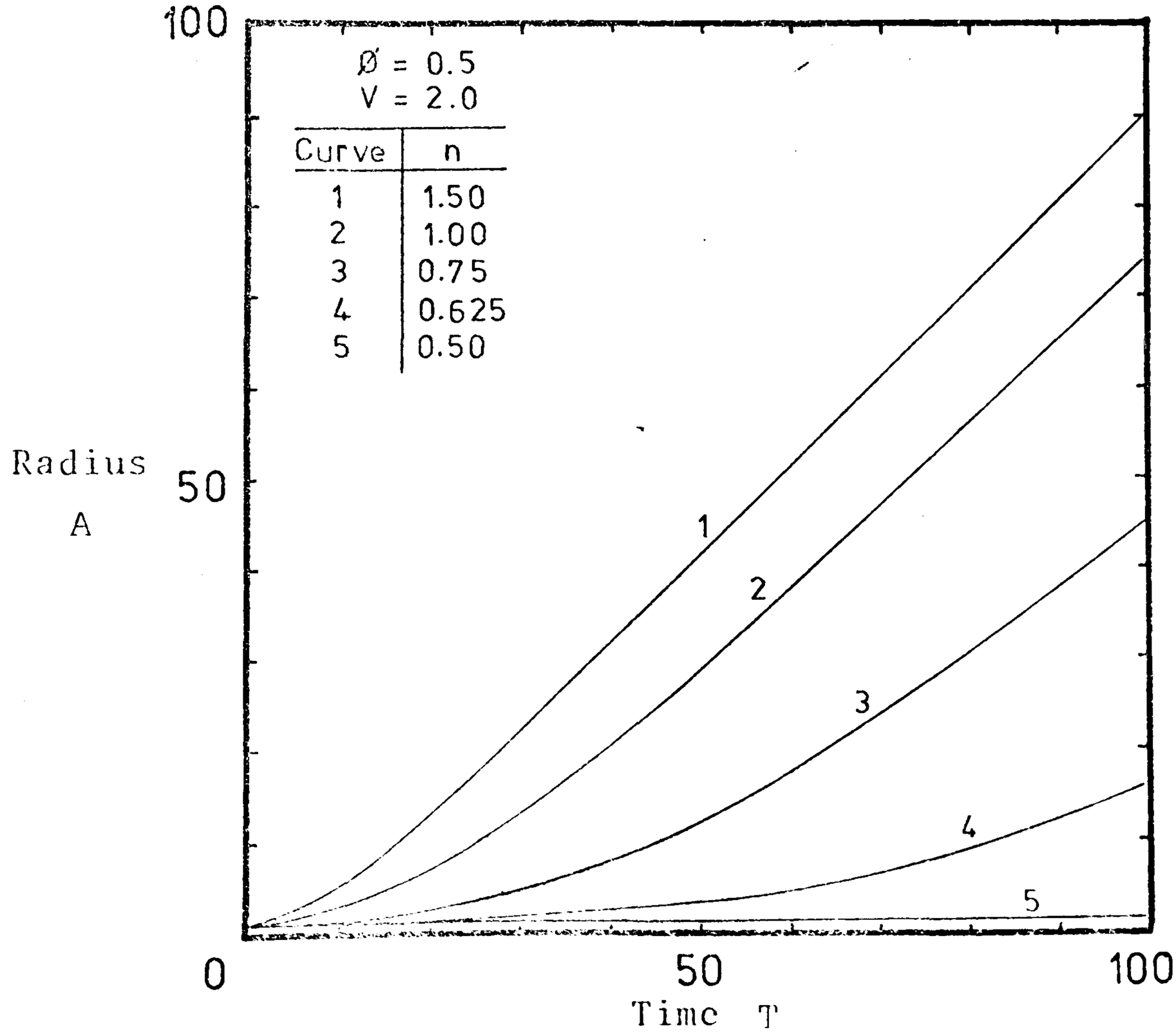


Figure 4.12 Hydrodynamically controlled bubble growth

Power law liquid

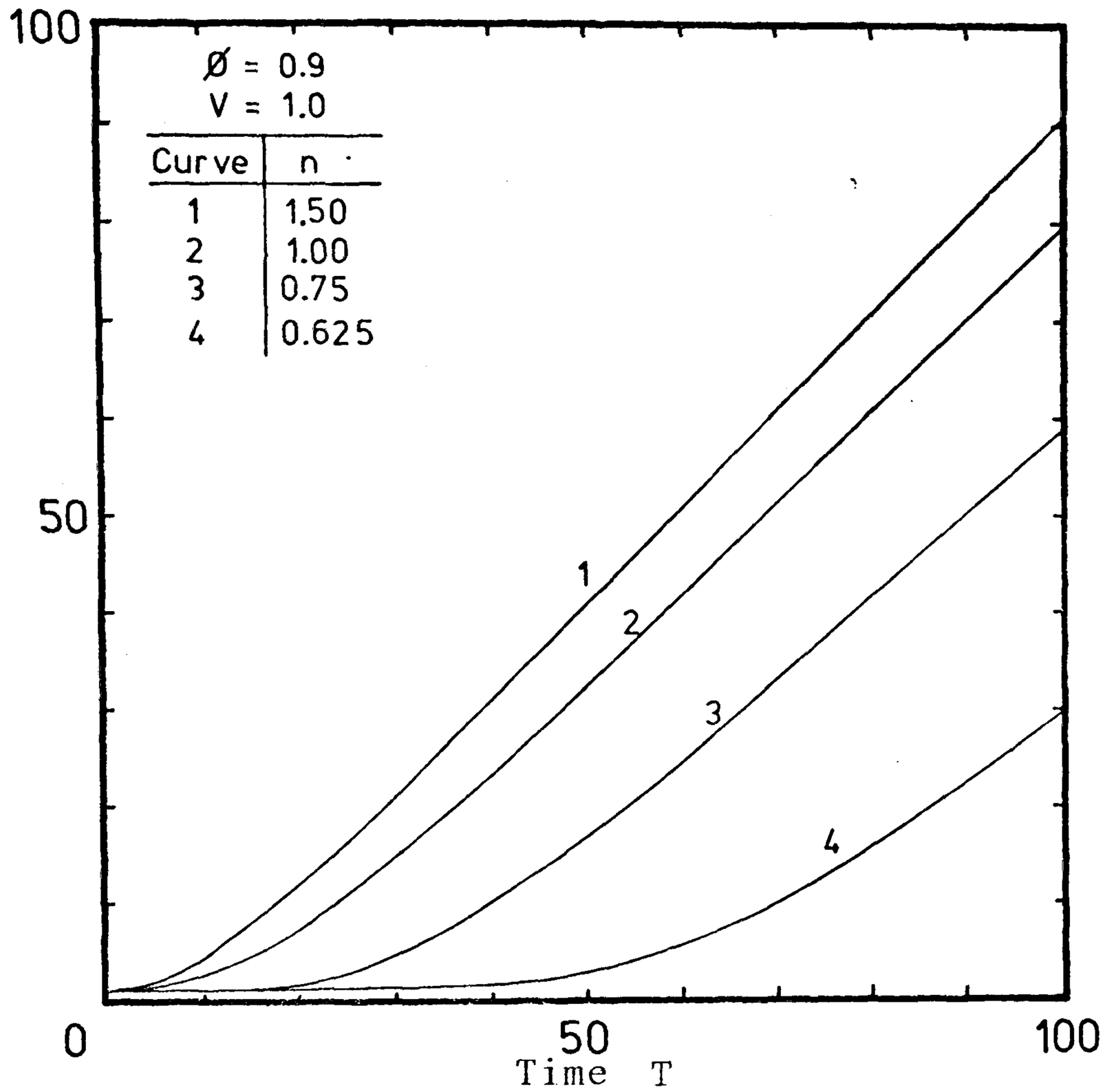


Figure 4.13 Hydrodynamically controlled bubble growth

Power law liquid

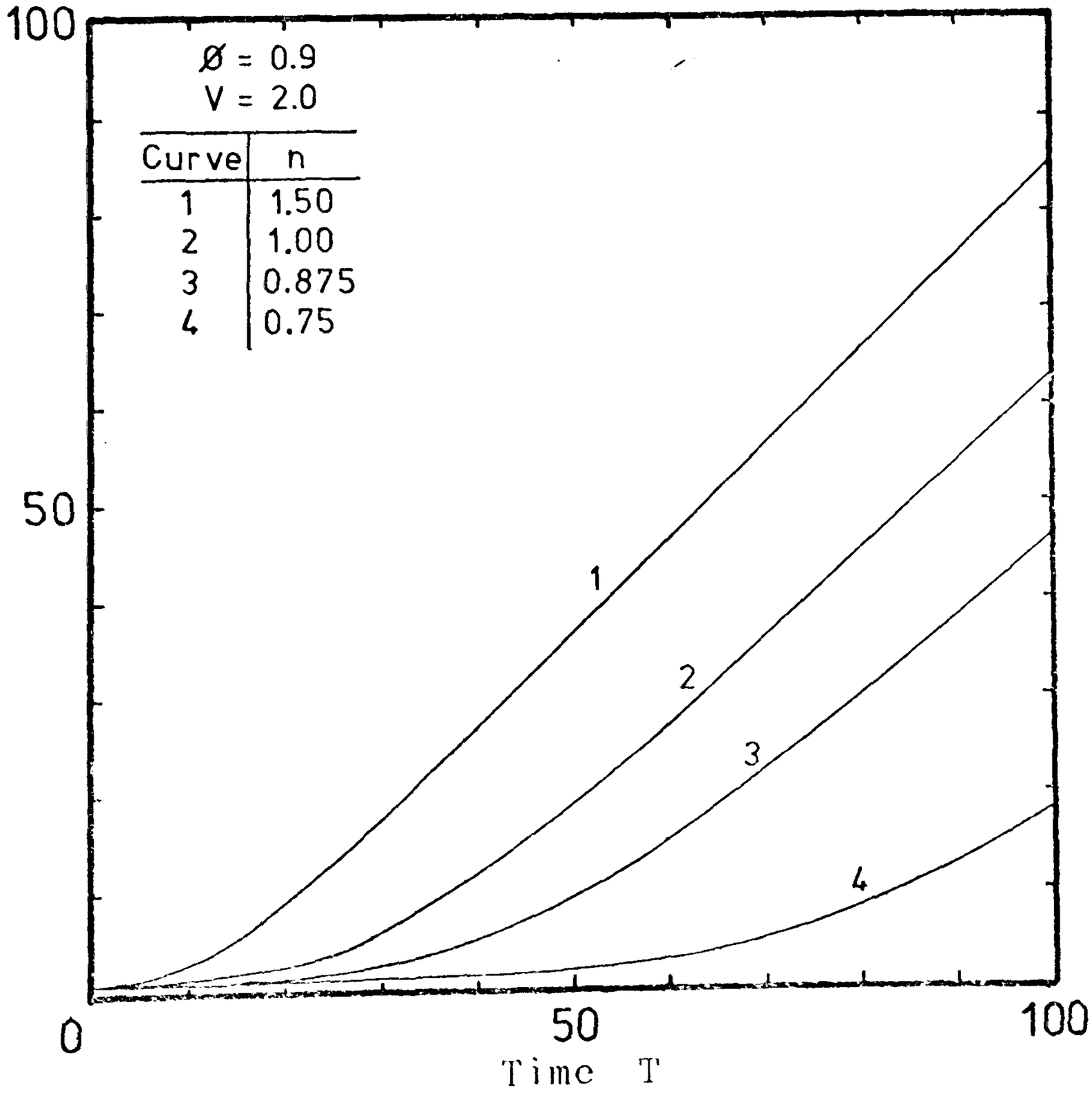
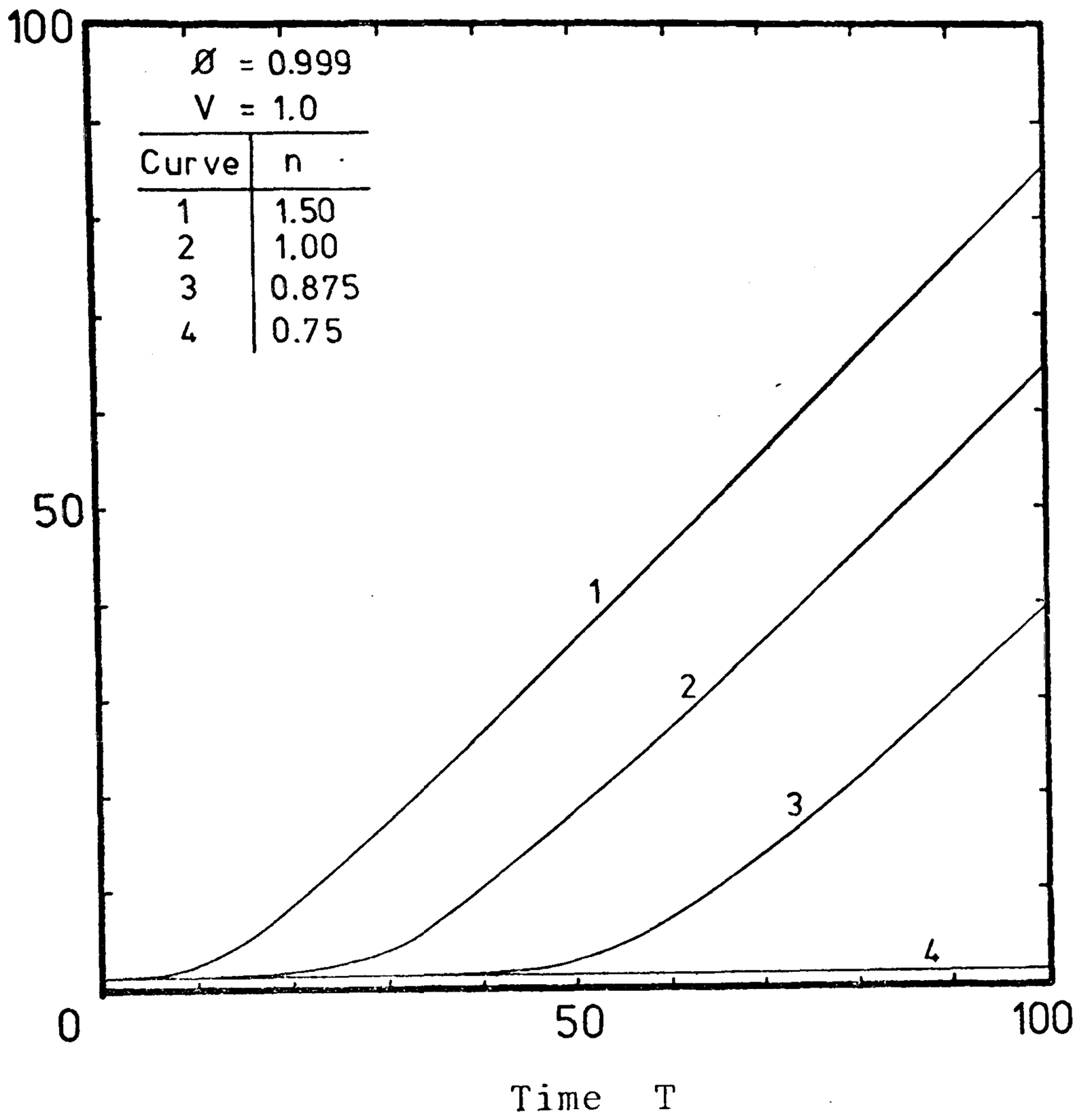


Figure 4.14 Hydrodynamically controlled bubble growth

Power law liquid



4.1.6 Discussion of results

The implications of the results for hydrodynamic limitation to growth in newtonian liquids have already been discussed by Szekely and Martins (1971). To summarise their conclusions, which are not altered by any of the results calculated here:

(i) Viscous forces become significant only when $V > 0.1$ or so. As time T increases, the growth rate $\frac{dA}{dT}$ approaches a constant value, which becomes less for smaller values of V .

(ii) The effect of increasing the surface tension parameter ϕ is to displace the whole growth curve along the time axis. When the surface tension is eventually rendered insignificant, growth is resumed at a rate which would have been achieved had these forces been absent.

The general remarks above apply equally well to the power law liquid with the addition:

(iii) All else being equal, the bubble radius and growth rate at a given time T decrease with decreasing power law exponent.

It is interesting to examine this behaviour of the power law liquid. Its trend is due to the rheological properties of a power law liquid; its magnitude is due partly to the physical properties and partly to the way in which the parameters are defined. When the bubble is just beyond its initial size and growing at a very slow rate, the viscosity of the liquid looks very large to the bubble.

Its expansion will thus be substantially retarded.

Restating the definitions of the parameters:

$$G = \frac{R_o^2 \, \Delta P}{\rho_\ell \, D^2} \qquad a$$

$$S_c^* = \frac{m \, R_o^{2(1-n)}}{D^{(2-n)}} \qquad b$$

$$V^* = \frac{S_c^*}{G^{(1-\frac{n}{2})}} \qquad c$$

$$= m \left[\frac{\rho_\ell}{\Delta P}\right]^{\frac{2-n}{2}} \cdot \frac{1}{R_o^n} \qquad d \qquad (4.9)$$

Considering the density of the liquid to be an unimportant variable and often close to unity for water-like liquids equation 4.9d can be written as:

$$V^* \propto \left[\frac{\rho_\ell}{\Delta P}\right]^{\frac{2-n}{2}} \cdot \frac{1}{R_o^n} \qquad (4.10)$$

Now, if the initial radius is that which can exist in ~~unstable~~ equilibrium with the supersaturated solution then, through the surface tension relationship:

$$R_o \propto \frac{1}{\Delta P} \qquad (4.11)$$

Substituting in equation 4.10 gives:

$$V^* \propto \left(R_o\right)^{1-\frac{3n}{2}} \qquad (4.12)$$

The expression illustrates the strong dependence of V^*

on the exponent n, for a given R_o, assuming that R_o and ΔP are inversely proportional. This is a weakness in the suitability of the parameter but nevertheless the conclusion still holds that, for equal G, V and ϕ, bubble radius and growth rate at a given time decrease with decreasing power law exponent. It is not possible to say more than that in a general way, and it is a valid result.

Note that the dimensionless time T and the dimensionless radius A also include the value of R_o viz:

$$T \propto R_o^{-\frac{3}{2}} t$$

$$A = R_o^{-1} R \qquad (4.13)$$

So all the parameters V^*, G, ϕ, T and A depend on the value of R_o and V^* on n as well. That this is not as serious a weakness as it might seem is shown by Szekely and Martins (1971). In calculations based on experimental results in a newtonian liquid, they used $R_o = 10^{-2}$, 10^{-3} and 10^{-4} centimetres and showed that the actual value chosen for R_o did not materially affect the actual radius versus real time curve.

4.2 Growth limited by both hydrodymanics and diffusion

4.2.1 Forming the appropriate equations for numerical solution

When growth is limited by diffusion as well as by hydrodynamic forces, the concentration of the diffusing species at the bubble surface, and hence the pressure within the bubble, decreases as the bubble expands. It would be expected that, given long enough times, this mixed case would always approach the solution given for diffusional limitation alone.

So, in this instance, all the equations 3.34 or 3.50, 3.55 and 3.60a to f will be significant. Now there are a large number of parameters and variables involved in these equations and it is not possible to reduce their total number. Thus, the equations will be left in terms of the first dimensionless time τ . Some alterations will be made to the equations to put parameters in terms of their reference or initial values only, and to transform the radial coordinate to a more suitable quantity (see Figure 4.15). The momentum equations 3.34 and 3.50 remain unchanged.

Make the following change of spatial variable:

$$x = a - A(\tau) \qquad (4.1)$$

x is the dimensionless distance beyond the bubble surface and changes as the bubble grows. Hence the chain rule must be used to transform the differentials of $C^*(a,\tau)$ to those of $C^*(x,\tau)$, thus:

$$\frac{\partial C^*(a,\tau)}{\partial \tau} = \frac{\partial C^*(x,\tau)}{\partial \tau} + \frac{\partial C^*(x,\tau)}{\partial x}\frac{\partial x}{\partial \tau}$$

obviously: $$\frac{\partial x}{\partial \tau} = -\frac{dA}{d\tau}$$

Also $$\frac{\partial C^*(a,\tau)}{\partial a} = \frac{\partial C^*(x,\tau)}{\partial x}$$

and $$\frac{\partial^2 C^*(a,\tau)}{\partial a^2} = \frac{\partial^2 C^*(x,\tau)}{\partial x^2}$$ (4.15)

Substituting the equations of 4.15 into 3.55 yields:

$$\frac{\partial C^*}{\partial \tau} = \frac{\partial^2 C^*}{\partial x^2} + \left[\frac{2}{x+A} + \left\{1 - \frac{A^2}{(x+A)^2}\right\}\frac{dA}{d\tau}\right]\frac{\partial C^*}{\partial x} \qquad (4.16)$$

The boundary condition 3.60e , which becomes:

$$\left.\frac{\partial C^*}{\partial x}\right|_{x=0} = \frac{1}{Ja}\frac{dA}{d\tau} \qquad (4.17)$$

may be put into a more convenient form by defining a reference value of the Jakob number:

$$\overline{Ja} = \frac{\Delta C}{\rho_g|_{P_\infty}} \qquad (4.18)$$

This is the Jakob number calculated at the ambient pressure.

Introduce a new quantity, the supersaturation driving force γ which, when Henry's law applies at the interface is:

$$\gamma = \frac{\Delta C}{C_{sat}} = \frac{\Delta P}{P_\infty} \qquad (4.19)$$

Combining equations 4.18 and 4.19 with previously defined

dimensionless quantities, it can be shown that equation 4.17 becomes:

$$\left.\frac{\partial C^*}{\partial x}\right|_{x=0} = \frac{1 + \Pi\ \gamma}{\overline{Ja}}\ \frac{dA}{d\tau} \qquad \text{at} \quad x = 0 \tag{4.20}$$

Three other boundary conditions have to be changed to the new variable. Equations 3.60c, d and f become respectively:

$$\left.\begin{array}{lllll} C^* = 1 & & \tau = 0 & : & x > 0 \\ C^* = 1 & & \text{all } \tau & : & x = \infty \\ C^* = \Pi & & & & x = 0 \end{array}\right| \tag{4.21}$$

It is proposed to solve the equations numerically. A suitable method will evaluate the solution at a fixed, finite number of points in the time and distance domains. That is, for a given time step, the concentration distribution in the x domain will be determined at a given number of points. However, the variable x is inconvenient for numerical solution as it ranges from zero to infinity and it is difficult to know where to terminate the grid of x-points (equivalent to altering the boundary conditions) to produce a finite range of integration. Also, the most interesting and significant events and the most rapid changes are occurring at the bubble surface and, to ensure accuracy, the spacing of the points at which the solution is evaluated should be closer near the surface. Such a dilemma may often be solved by transforming the spatial coordinate; a common transformation variable ζ is defined as:

$$\zeta = k\ \ln(\ f\{x\}\ )$$

Whilst this transformation will compress some points closer to the surface, it still leaves the problem of the infinite x domain. A more suitable transformation, applied to the present case, is to define a variable y :

$$y = \frac{x}{s + x} \tag{4.22}$$

The range is automatically restricted from $y = 0$ (when $x = 0$) to $y = 1$ (when $x = \infty$) and the spacing of the points near the bubble surface is determined by the spacing parameter s . This is well illustrated in Figure 4.15 .

So, this transformation enables the full range of integration to be handled and the spacing to be varied easily, to compress more points closer to the surface where needed, all with a finite number of points at which the solution is evaluated.

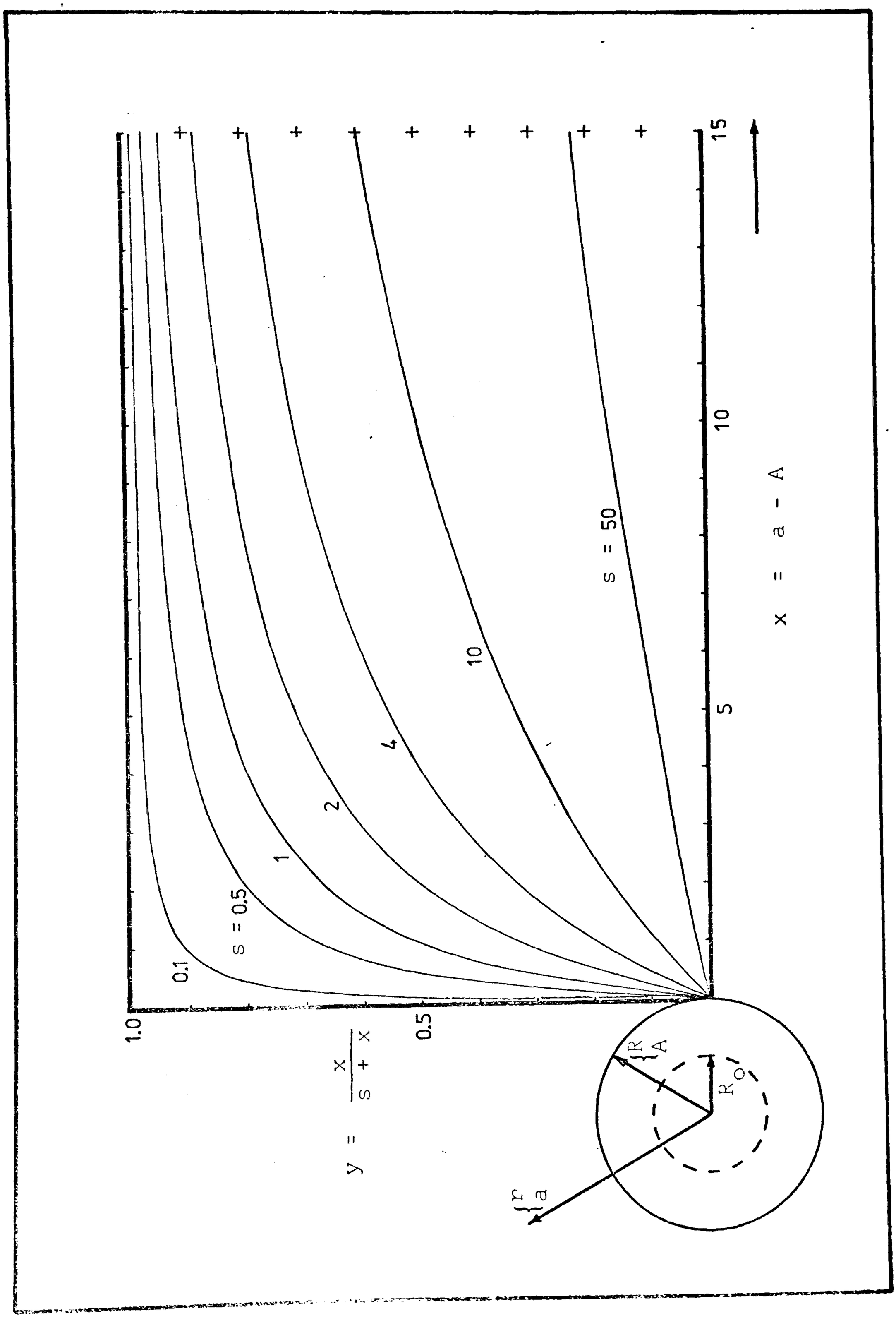
Substitution of equation 4.22 into equations 4.16 and 4.21 and recalling unchanged initial conditions 3.60a and b gives:

$$\frac{\partial C^*}{\partial \tau} = \frac{(1-y)^4}{s^2}\frac{\partial^2 C^*}{\partial y^2} + \left\{\frac{2(1-y)}{A(1-y)+sy} + \left[1-\left(\frac{A(1-y)}{A(1-y)+sy}\right)^2\right]\frac{dA}{d\tau}\right\}\frac{(1-y)^2}{s}\frac{\partial C^*}{\partial y} \tag{4.23}$$

with initial and boundary conditions:

$$\left.\begin{array}{lll} A = 1 & \tau = 0 & a \\ \dot{A} = 0 & \tau = 0 & b \\ C^* = 1 & \tau = 0 : y \geqslant 0 & c \\ C^* = 1 & \text{all } \tau : y = 1 & d \end{array}\right| \tag{4.24}$$

Figure 4.15 Coordinate transformation nomenclature



$$\frac{1}{s}\frac{\partial C^*}{\partial y}_{y=0} = \frac{1 + C^*\gamma}{\overline{Ja}}\frac{dA}{d\tau} \qquad y = 0 \qquad e \tag{4.24}$$

$$\Pi = C^* \qquad y = 0 \qquad f$$

The numerical solution will be performed on equations 4.23 and 4.24 (coupled with 3.34 or 3.50). Though these may appear more complicated than the initial equations, they are more suited to accurate handling by numerical methods.

The parameter $\overline{B}$ is also used:

$$\overline{B} = \frac{\overline{Ja}^2}{G^{\frac{1}{2}}} \tag{4.25}$$

First suggested by Florschuetz and Chao (1965), $\overline{B}$ defines whether a system is in a region of mainly diffusion control ($\overline{B} << 1$) or mainly hydrodynamic control ($\overline{B} >> 1$) . In examining the intermediate region, twelve different sets of the parameters V , G , $\overline{Ja}$, $\overline{B}$, γ and ϕ will be examined. It is an unrealistic task to examine all the parameters in detail and the twelve sets were selected carefully to show the more significant results. This selection is discussed further in Section 4.2.4 .

4.2.2 Method of solution

Equation 4.23, though complicated, is of a standard form and is a parabolic, linear partial differential equation. Considerable time and programming effort was saved by the use of a suitable existing programme from the library facilities at Imperial College.

The Harwell Subroutine Library (United Kingdom Atomic

Energy Authority (1973)) includes a subroutine named DP01A which solves a two point boundary value problem for a parabolic, linear partial differential equation, as described briefly below.

When the equation is of the form:

$$\frac{\partial C}{\partial t} = a(y,t)\frac{\partial^2 C}{\partial y^2} + b(y,t)\frac{\partial C}{\partial y} + c(y,t)\,C + d(y,t) \quad (4.26)$$

with initial and boundary conditions of the form:

$$b_1\frac{\partial C}{\partial t} = b_2 + b_3\,C + b_4\frac{\partial C}{\partial y} \quad (4.27)$$

then DP01A , given the solution, C_o , at $t = t_o$, finds the solution at $t = t_o + \delta t$.

The term $\frac{\partial C}{\partial t}$ is first replaced by the Crank-Nicolson formula:

$$\tfrac{1}{2}\left(\left.\frac{\partial C}{\partial t}\right|_{t_o} + \left.\frac{\partial C}{\partial t}\right|_{t_o+\delta t}\right) = \frac{\left[C|_{t_o+\delta t} - C|_{t_o}\right]}{\delta t} \quad (4.28)$$

The equation is then rewritten as an ordinary second order differential equation and is solved by calling a subroutine DD01A . This subroutine replaces the differential equation by a finite difference approximation. An initial approximation to C is obtained by ignoring third and higher differences. Successive approximations are then obtained by applying correction terms based upon the third and fourth differences of the previous values of C . Several other routines from the library (MA07A, TA03A, TD01A, TB04AA)

are called to be used during the solution.

The subroutine is called by arguments thus:

```
CALL DPO1A(C,YO,YN,NPT,TO,DT,CYO,CYN,DCDT,E,LIM,ERR,NUM)
```

NPT is the number of equally spaced points at which the solution is evaluated, in the range YO to YN and including them. C , DCDT and E are one dimensional arrays of length NPT . TO is the value of t at which the initial solution is given and DT is the value, δt , by which t is increased. TO returns with the value TO + DT .

When the routine is called, C contains the solution at the NPT points at time TO , that is:

$$\begin{aligned} C(\ 1\ ) &= C(YO,TO) \\ C(\ k\ ) &= C(Y_k,TO) \\ &\vdots \\ C(NPT) &= C(YN,TO) \end{aligned} \qquad (4.29)$$

On return, these values will be overwritten with the solution at time TO + DT .

If $\frac{\partial C}{\partial t}$ is known at the NPT points, at t = TO, then these values are placed in the array DCDT and the flag NUM is set to a number greater than zero. (If $\frac{\partial C}{\partial t}$ is not known then NUM is set equal to zero and the routine calculates its own approximation). On return DCDT will contain the values of $\frac{\partial C}{\partial t}$ at t = TO + DT .

CYO and CYN are one dimensional arrays of length four which contain the coefficients b_i of the boundary conditions

equation 4.27 :

<u>At YO</u> CYO(i) = b_i <u>at YN</u> CYN(k) = b_k

E contains, on exit from the routine, the difference between the solution obtained ignoring third and higher differences and the final solution obtained by taking these into account. E is ignored when the routine is entered.

ERR is the absolute value of the accuracy required.

LIM must be set to an integer greater than or equal to zero. If LIM equals zero, third and higher differences are never taken into account and the routine is left after solving the finite difference equations based on the first and second differences. In this case, both LIM and NUM are set to zero. If LIM is made greater than zero, then this value is the maximum number of times that correction terms based on the third and fourth differences are calculated. When the required accuracy is attained, NUM is set equal to the number of times the correction terms have been calculated and the routine is left. If the correction terms are calculated LIM times without reaching the required accuracy then the routine is left with NUM equal to -1 and DCDT equal to $\frac{\partial C}{\partial t}$ at t = TO .

So, if the required accuracy is attained within LIM steps, the routine is left in a condition ready to commence the next step immediately.

It is necessary to provide a subroutine FUNCTS to give the coefficients a , b , c , d of equation 4.26:

SUBROUTINE FUNCTS(A,B,C,D,T,Y,ID,IDU)

A, B, C and D are the a , b , c and d of equation 4.26. The arguments ID and IDU are dummies here; they are used in another routine DPO2A which solves a non-linear parabolic differential equation.

The routine uses an amount of COMMON storage as working space. (15*NPT + 6) spaces must be made available in an array W .

In order to test that the subroutine was working correctly, an equation with a known analytical solution was solved using it (see Appendix A.3) .

4.2.3 Computational procedure

There are two equations and their associated boundary conditions to be solved together. Equation 3.34 (or 3.50) is an ordinary differential equation and is solved in each time step by the Runge-Kutta-Nyström procedure. Equation 4.23 is a linear partial differential equation and is solved by routine DPO1A. The two are linked at the bubble surface by boundary condition 4.24f, $\Pi = C^*$.

Initially, Π is equal to unity and the first movement of the bubble surface must be limited by liquid properties. Subsequently, the concentration field around the bubble alters. The momentum equation is first solved to find a new A and $\frac{dA}{d\tau}$ at the end of a time interval. These new values are then substituted into the diffusion equation, and its boundary conditions, which is then solved to find the concentration field at the end of the time interval. This complete

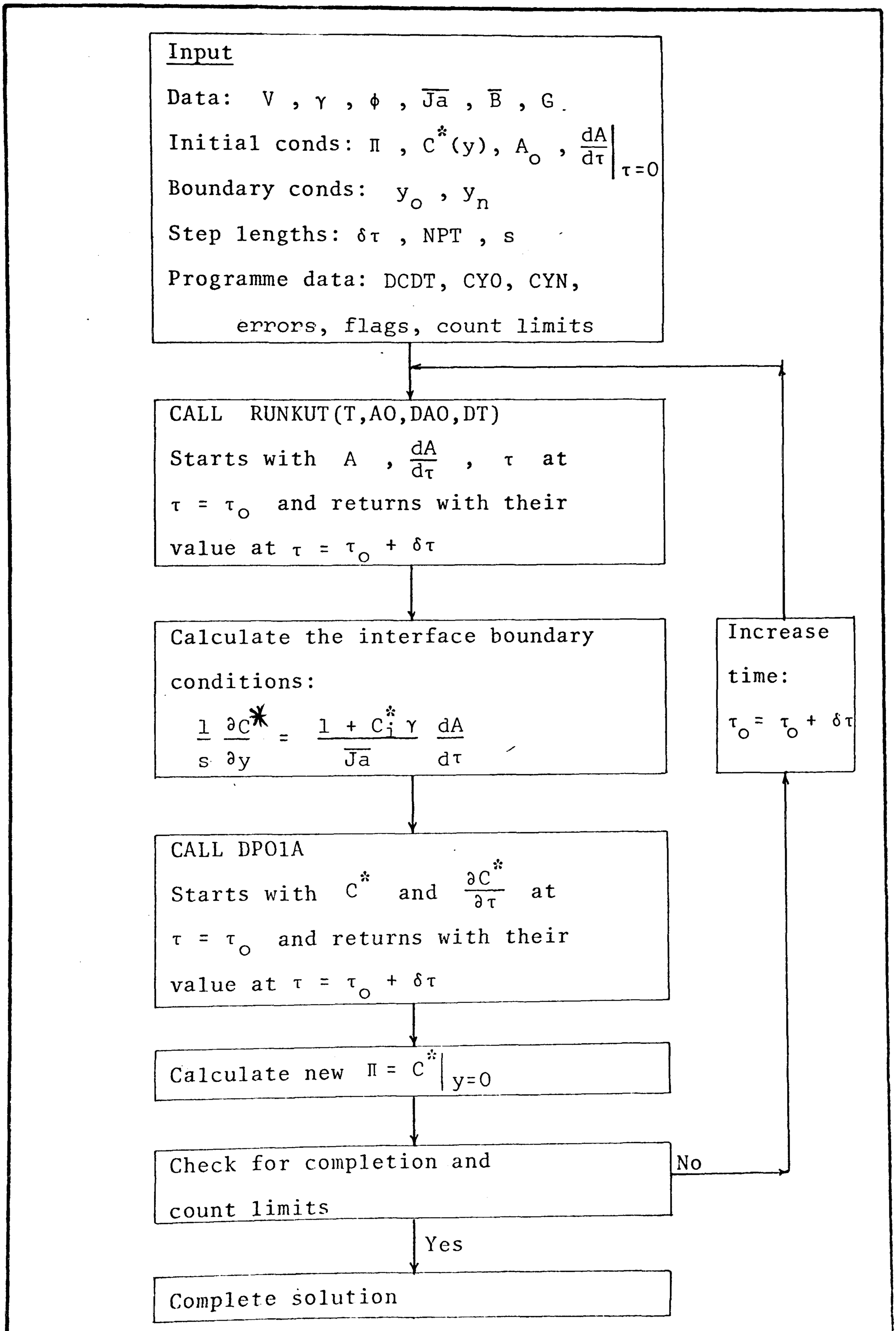
solution includes a new value of the interface concentration, C_i^* , which equals Π . The new value of Π determines the solution of the momentum equation during the next time step. The procedure is repeated. A flow diagram for the computational procedure is shown in Figure 4.16 .

There remained to determine three parameters which must be chosen optimally to give a stable, convergent and accurate solution. These are NPT , the number of points at which the solution is evaluated, DT , the time step length and s , which determines how closely the points are to the bubble in the original r-domain. Considerable numerical experimentation was necessary to determine these three parameters. The calculated values of the interface concentration C_i^* was used to compare results when examining various NPT , DT and s .

With regard to the number of points, NPT , experiments carried out using 21, 31, 41, 51 and 91 points showed that 51 points (50 intervals) were sufficient to realise accurate solutions at optimum s values.

The optimisation of the spacing parameter s was reasonably time consuming, involving experiments on all twelve sets of conditions and at several different time steps. Again, the calculated interface concentration C_i^* was used to compare results. Naturally, if the time step taken is zero, the calculated interface concentration would remain at unity. Similarly, if s is zero, y is always unity for any value of x and so C_i^* would be expected to remain at the

Figure 4.16 Flow diagram for the solution of the complete bubble growth equations



initial bubble surface value of unity. If s is very large, y is always zero and C_i^* would be expected to remain at the infinite boundary value, also unity. At intermediate values of s, C_i^* would be expected to take values less than unity. At the point where there is the minimum change in C_i^* with s (i.e. $\frac{\partial C_i^*}{\partial s} = 0$) the optimum s for a given time step and set of parameters is found.

Determination of this optimum s was carried out as follows. Starting with the initial conditions, solutions were found for a given time step and set of parameters at a number of values of s. The values of C_i^* versus s were plotted and the minimum point located, thus fixing the optimum s. The solution was then calculated for this optimum s and used as a starting point for a second set of solutions, again varying s. Another optimum s was found for the second time step. Obviously this procedure, when fully carried out for all sets of parameters, was a lengthy one but there was found a particularly simple relationship between the optimum value of s and the absolute time at the end of the time step, for all conditions:

$$s = 20\sqrt{\tau} \qquad (4.30)$$

As an illustration of the procedure, the curves of C_i^* versus s for two initial time steps and for a set of parameters are shown as Figure 4.17. A similar curve was examined for the second time step. The relationship between optimum s and τ is shown in Figure 4.18. This determination concluded the numerical experimentation.

Figure 4.17 Variation of interface concentration with spacing parameter, Set 4

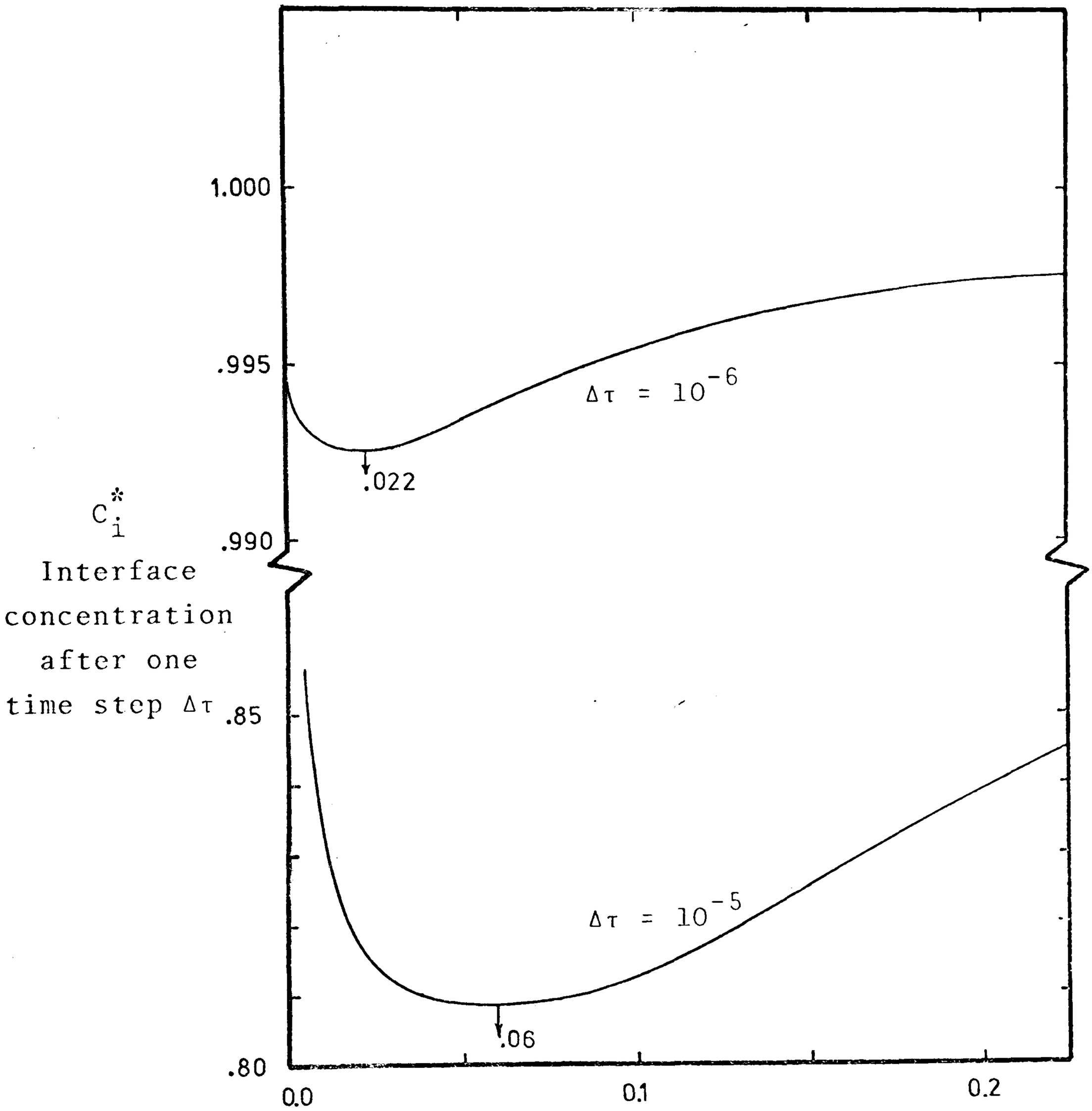
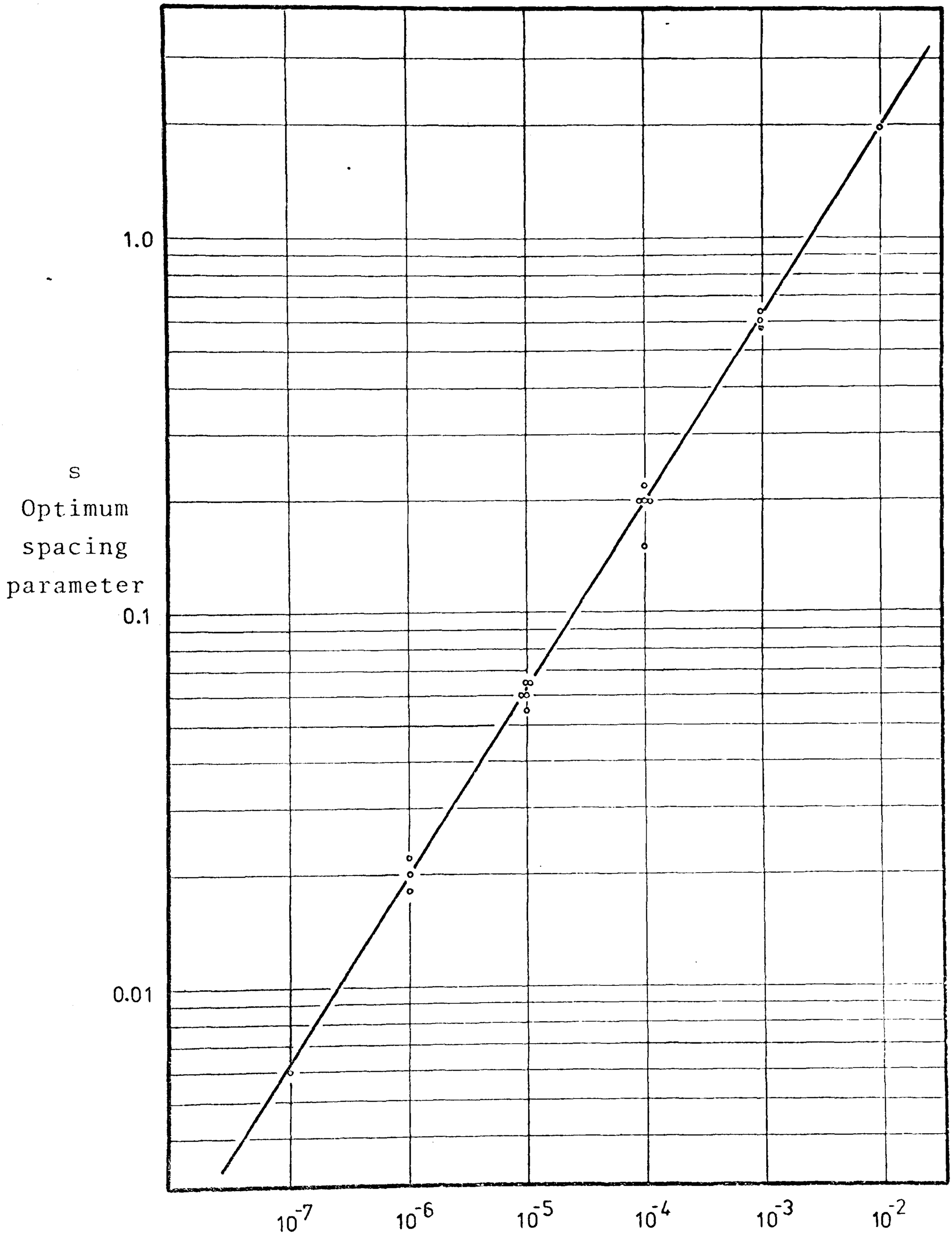


Figure 4.18 Optimum spacing parameter versus initial time steps, Sets 1 - 10



4.2.4 Selection of parameters for numerical solution

It is apparent that there are too many parameters in equations 3.34 or 3.50, 4.23, 4.24 and 4.25 for a systematic evaluation. Some of the less significant will be neglected or not varied; only the more important will be considered.

The surface tension parameter ϕ is less important since its effects are rapidly overcome as the bubble grows. It will be taken as zero in the numerical solutions.

The driving force parameter γ will be left constant at a value of 10 .

This leaves three parameters, $\overline{B}$, V and $\overline{Ja}$. V will be taken as either 0 (inviscid liquid) or 1 . $\overline{B}$ will be given four values to range over the expected regions, diffusion controlled to strongly inertial controlled. These will be 0.1 , 1 , 10 and 100 . $\overline{Ja}$ will take three different values 10 , 31.6 and 100.0 . (n.b. $31.6 = \sqrt{1000}$). The first would roughly correspond to a system of $\gamma = 10$ at atmospheric pressure and the last to the same system operating subatmospherically where the gas density is small. The value 31.6 is intermediate.

This leaves twelve sets of $\overline{B}$ and $\overline{Ja}$ to be examined at $V = 0$ and 1 and the sets where $V = 1$ to be examined with power law exponents of 0.5, 0.625 and 0.75 .

Table 4.1 shows the values of the dependent parameters for these sets of conditions.

Table 4.1 Parameters used in the numerical solutions

Set	$\overline{B}$	$\overline{Ja}$	G	γ	ϕ
1	0.1	100.0	10^{10}	10.0	0.0
2		31.6	10^{8}		
3		10.0	10^{6}		
4	1.0	100.0	10^{8}	10.0	0.0
5		31.6	10^{6}		
6		10.0	10^{4}		
7	10.0	100.0	10^{6}	10.0	0.0
8		31.6	10^{4}		
9		10.0	10^{2}		
10	100.0	100.0	10^{4}	10.0	0.0
11		31.6	10^{2}		
12		10.0	1		

4.2.5 Results of the numerical solution

The results for the numerical solutions are shown graphically in Figures 4.19 to 4.22 where the curves for $\overline{B}$ = 0.1, 1, 10 and 100 respectively are presented.

It was found that, at each $\overline{B}$, the shapes of the curves calculated for the three $\overline{Ja}$, at each V and power law exponent were not too different; only the time scale was different, but in the range up to A = 100 , the curves were only about 1% or less apart in the ordinate. Thus there is no detectable error in using only one graph to represent all the results of different $\overline{Ja}$ for a given $\overline{B}$. The whole family of $\overline{Ja}$ curves is also made available, not just those at the three values calculated.

Figure 4.19 Bubble growth curves for the general case, Sets 1,2,3

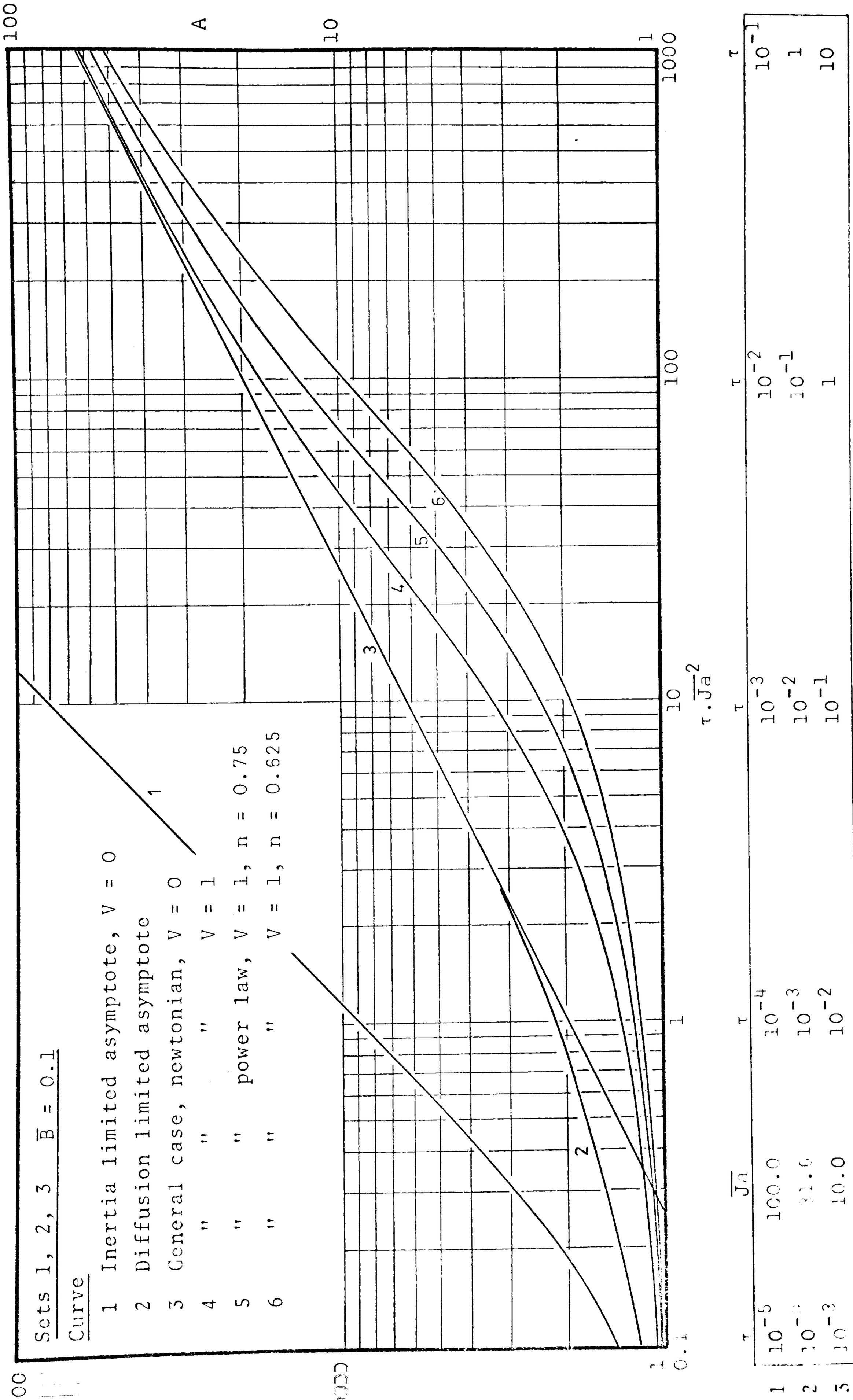
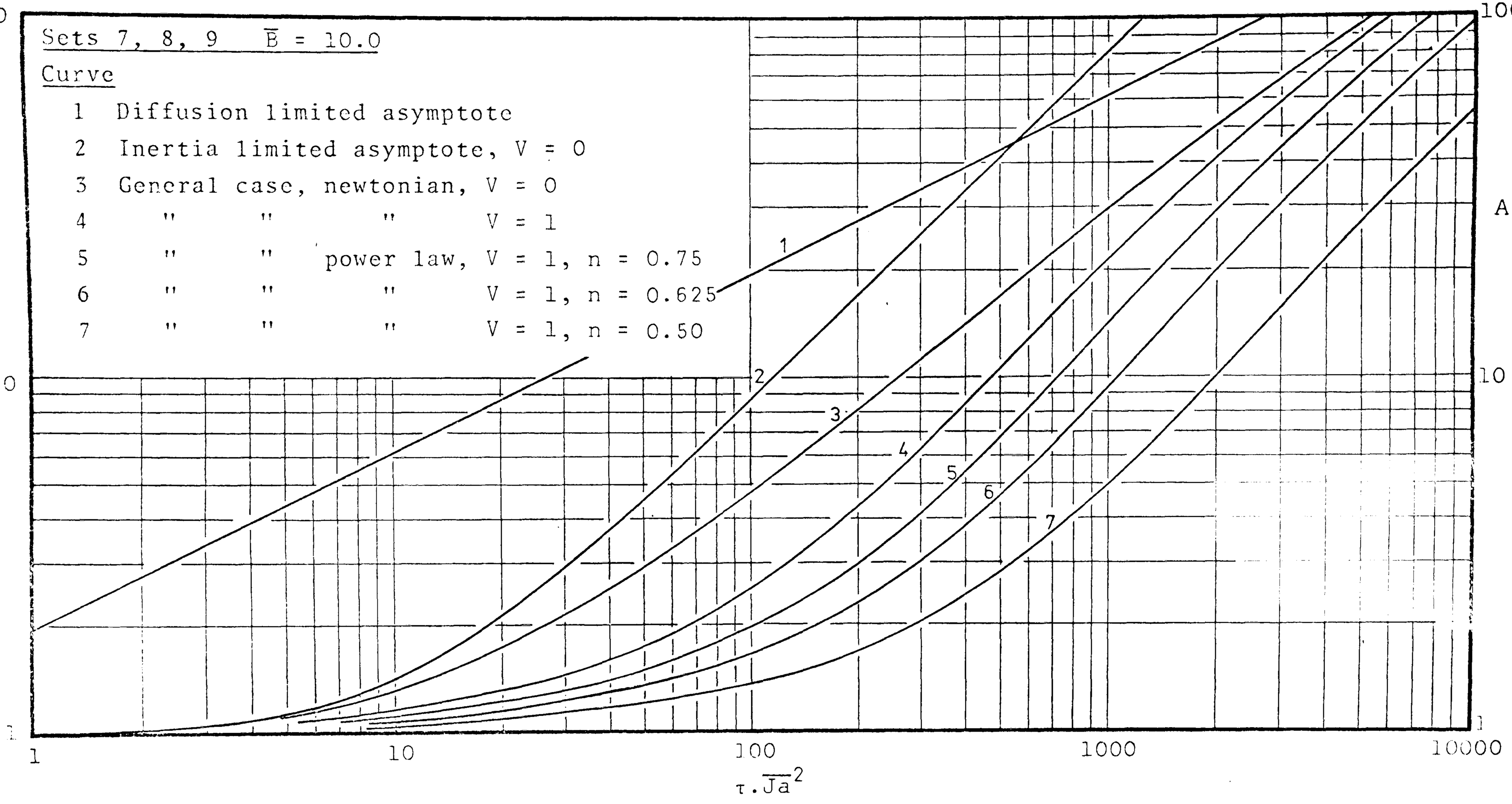


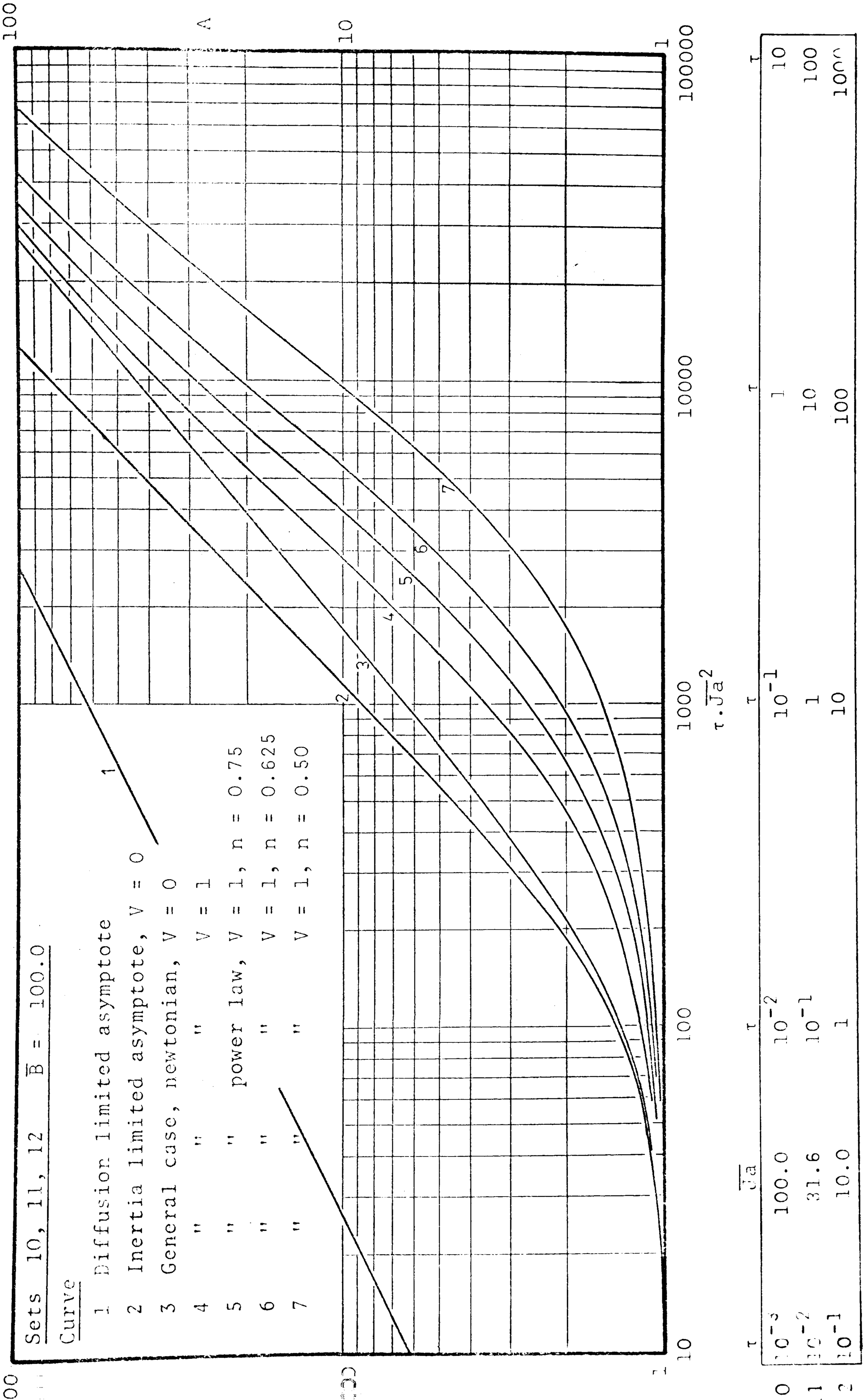
Figure 4.20 Bubble growth curves for the general case, Sets 4,5,6



	τ	$\overline{Ja}$	τ	τ	τ	τ
7	10^{-4}	100.0	10^{-3}	10^{-2}	10^{-1}	1
8	10^{-3}	31.6	10^{-2}	10^{-1}	1	10
9	10^{-2}	10.0	10^{-1}	1	10	100

Figure 4.21 Bubble growth curves for the general case, Sets 7,8,9

Figure 4.22 Bubble growth curves for the general case, Sets 10,11,12



4.2.6 Discussion of results

The implications of the results for the general case of growth in newtonian liquids have already been discussed by Szekely and Martins (1971) and by Florschuetz and Chao (1965), discussing the parameter $\overline{B}$. For completeness, their conclusions are summarised as:

(i) The parameter $\overline{B}$ provides a good characterisation of the regime. The larger $\overline{B}$ becomes, the more the system approaches hydrodynamic limitation; the smaller $\overline{B}$ becomes, the more the system is limited by diffusion.

(ii) In the earliest stages of every case, the growth rate is limited by factors other than diffusion. As time increases, there is a gradual approach to diffusive limitation. The rapidity of the approach depends on the value of $\overline{B}$.

(iii) Provided that $\overline{B} < 0.1$, the time taken to reach a certain size may be estimated without serious error by the asymptotic diffusion limited theory.

The general remarks above apply equally to the power law liquid with the addition that:

(iv) All else being equal, the growth curve of a power law liquid approaches that of a newtonian liquid of the same V and ϕ . The rate of growth and the radius at a given time decrease with decreasing power law exponent.

(v) As time proceeds, the solution for a power law liquid approaches that for a newtonian liquid;

they both approach the solution for an inviscid newtonian liquid and then all three approach the diffusion limited asymptote. The convergence to the diffusion limited asymptote is more rapid, the smaller the value of $\overline{B}$.

The same remarks made in Section 4.1.6 on the sensitivity of the parameters to R_o and the particular sensitivity of V^* to the power law exponent also apply here.

CHAPTER 5

EXPERIMENTAL - APPARATUS AND TECHNIQUES

In this chapter, the apparatus and techniques used in the experimental part of the work will be discussed. The justification for the experiments is found in Chapter 1.

The experiments were not difficult or complicated but care was taken in their execution and accurate records were made. The results obtained, presented and discussed in Chapter 6, justify the care taken.

5.1 Introduction

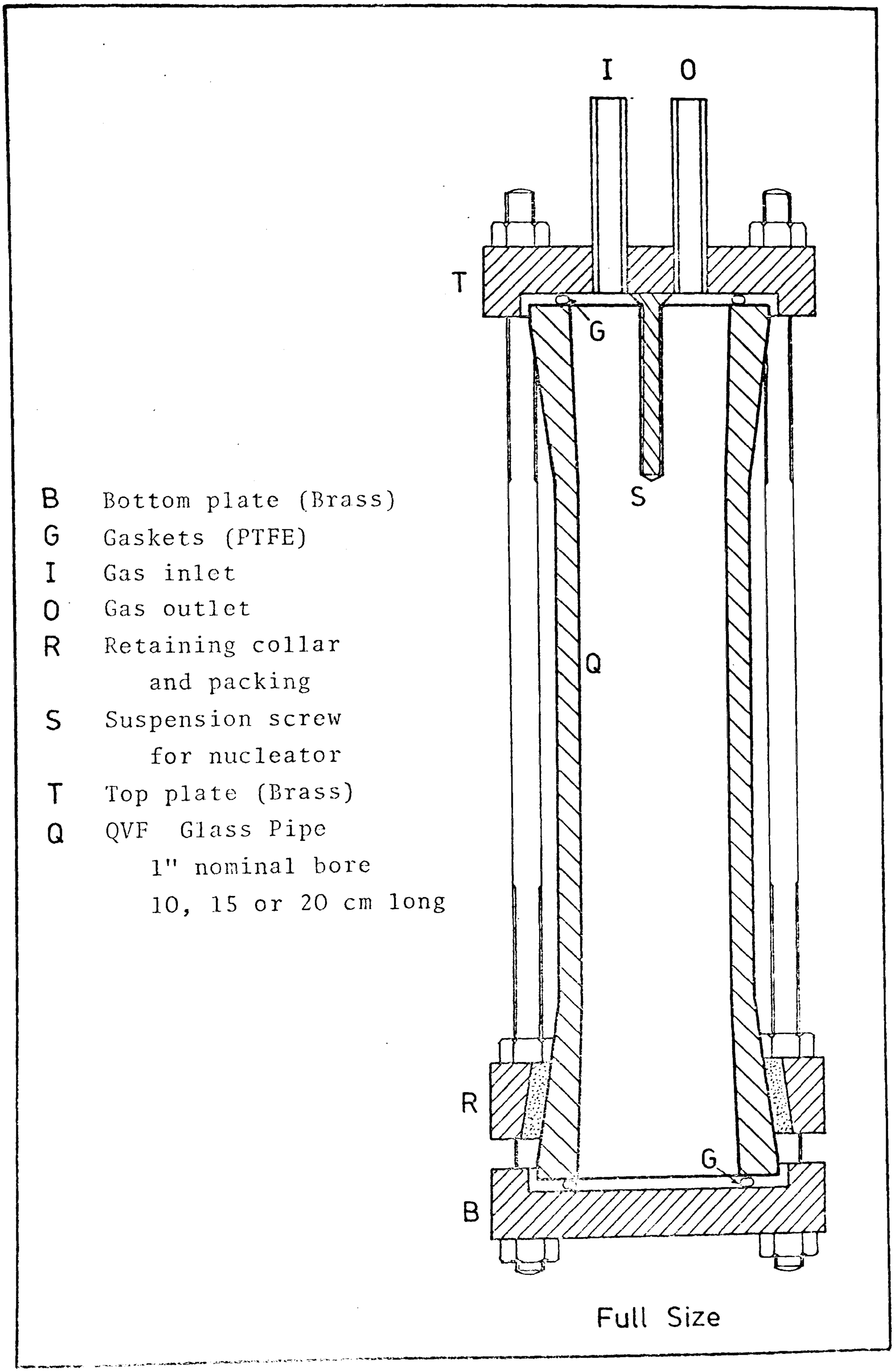
The experiments were designed to test the mass diffusion limited theory of Scriven (1959). Saturated solutions of carbon dioxide and of oxygen in water or glycerol solutions were prepared, at elevated pressures and at a constant temperature. When the pressure was released to atmosphere, a supersaturated solution of known concentration was obtained. It was then necessary to be able to reliably initiate bubbles of gas, desorbing from the supersaturated solution, to photograph the growing bubbles and to analyse the film.

5.2 Pressure vessel

A glass pressure vessel was necessary in order to be able to photograph the growing bubble. The vessel used (shown full size in half section in Figure 5.1) consisted of a standard length of QVF nominal one inch bore glass pipe, re-annealed before use. The brass end plates were square and bolted together with four lengths of $\frac{1}{4}$ inch threaded rod. A seal was provided by standard QVF teflon gaskets. Into the top brass plate were soldered two lengths of $\frac{1}{4}$ inch copper tubing to which the rest of the apparatus was joined by means of flexible terylene reinforced PVC tubing (which has a bursting pressure of around 800 psi). From the top plate, a bubble initiator was suspended on a screw thread.

Nominal one inch glass pipe has, according to the manufacturers specification, a safe working pressure of 100 psig. The vessel was hydrostatically tested to this

Figure 5.1 Half-Sectional view of pressure vessel



B Bottom plate (Brass)
G Gaskets (PTFE)
I Gas inlet
O Gas outlet
R Retaining collar and packing
S Suspension screw for nucleator
T Top plate (Brass)
Q QVF Glass Pipe
1" nominal bore
10, 15 or 20 cm long

pressure but in use the largest applied pressure was 60 psig.

5.3 Initiation of bubbles

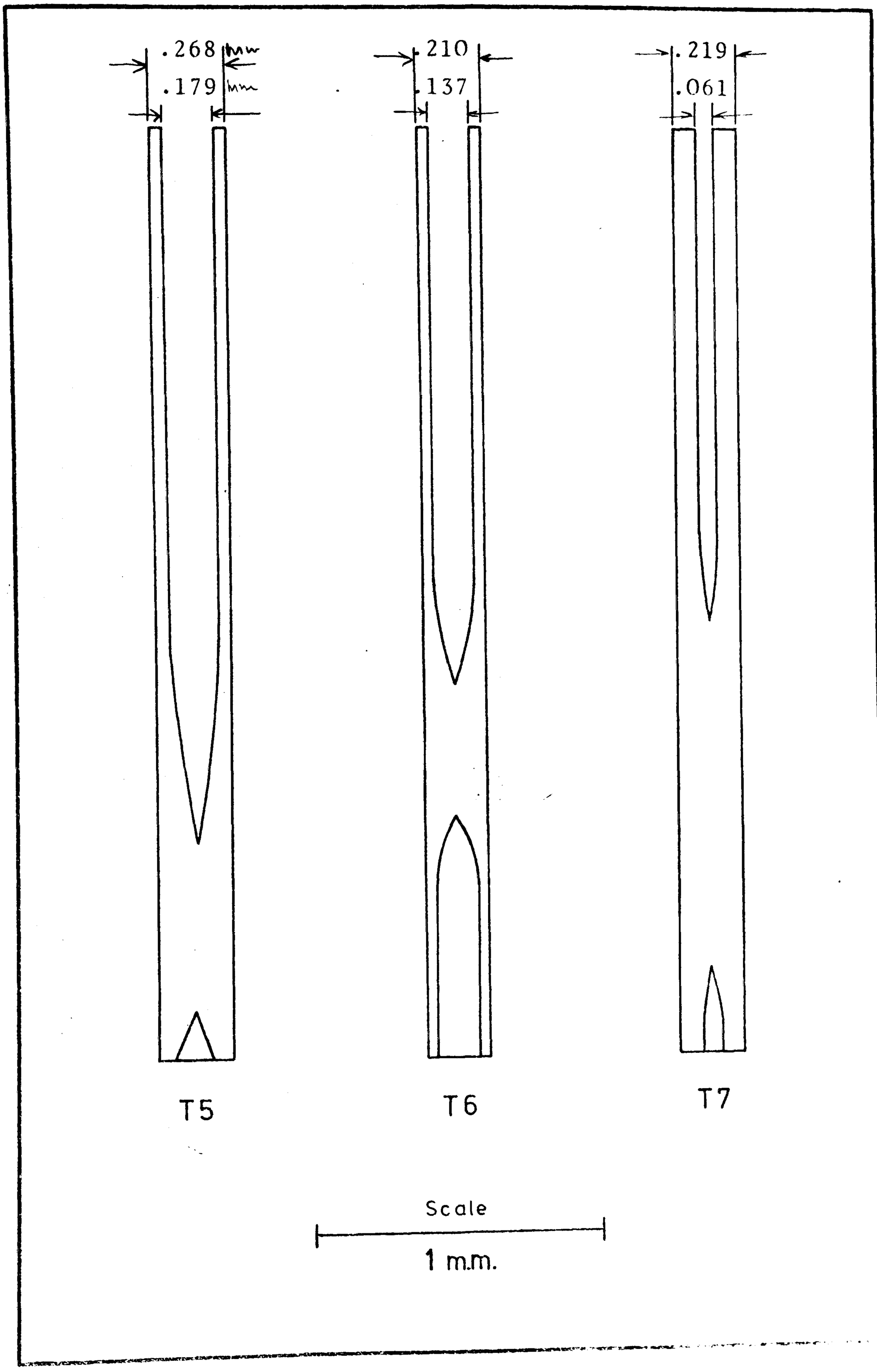
Bubbles in supersaturated or superheated liquids may be initiated relatively easily. Methods which have been used include a rapidly heated wire tip (Szekely and Martins (1971)), release of an entrapped portion of gas or vapour (Florschuetz and Chao (1965)), a drilled cavity (Buehl and Westwater (1966)), a sealed capillary (Saddy and Jameson (1971)) and a rough or discontinuous part of an otherwise smooth surface (Cole and Shulman (1966)). In addition it is possible to hope that a random nucleation site will occur in the field of view. These are all methods of heterogeneous nucleation; homogeneous nucleation is generally considered to be unimportant in all practical cases (Brinson (1966)). Presumably a microscopic speck of vapour or gas is provided, upon which the bubble grows.

The theoretical analysis assumes that the bubble is growing in a spherically symmetric, uniform concentration field so it is obviously desirable to approach this situation as closely as possible in experiments. One method of achieving this would be to initiate a bubble in space in a free falling apparatus so that the growing bubble would remain stationary, relative to the apparatus. This ambitious method was attempted by Florschuetz and Chao (1965) but was not particularly successful. Also their vapour bubbles were collapsing in a fraction of a second whereas the gas bubbles studied here took up to several minutes to evolve. Absolute

spherical symmetry is, unfortunately, ruled out. However, if a bubble is initiated on a plane and grows tangentially on it, it does not exhibit marked differences from spherically symmetric growth rates provided that the growth coefficient β is greater than unity. For very slow growth rates, the difference never exceeds 30.7% (Buehl and Westwater (1966)). So, if a bubble can be initiated at a point to which its surface remains fixed as it grows, the growth rates would be expected to be between the spherically symmetric case and the wall tangential case (and in any case exhibit no differences for β greater than unity).

Firstly, attempts were made to bring about initiation on a glass filament (less than 0.02 millimetre in diameter), the tip of which was rendered hydrophobic by the method of Blake and Kitchener (1972). The results were poor and consistent nucleation could not be obtained so it was decided to use a sealed capillary tip as the nucleating device. This provided a small reservoir of gas upon which the bubble grew and proved effective and absolutely reliable in use. A piece of glass tubing was first sharply necked to about one quarter of its original diameter and allowed to cool. The necked portion was then placed in a small hot flame and rapidly drawn, giving a very fine capillary close to a strong support. The fine tube was then nicked and broken off until a clean, square break was obtained. Then, using a micro flame, this small capillary was sealed about two millimetres from the open end and the whole device bent into an appropriate shape and size, ready for mounting inside the pressure vessel. The dimensions of three of the tips actually used in experim-

Figure 5.2 Bubble Initiating Tips



ents are shown in Figure 5.2, which is traced from a X50 photograph. The known dimensions, measured microscopically, were used as reference dimensions in the photographs of the experiments.

In the glycerol experiments, bubbles were initiated on the vessel surface by scratching the surface with a length of wire in an area upon which the camera had been previously focussed.

5.4 Photography

5.4.1 Camera

Since the time of evolution of some of the bubbles was long, it was not feasible to photograph them using a normal movie camera, which exposes a full thirty metre spool of film in only a few minutes at normal framing rates. The camera chosen was a Vinten Mark 3 "Scientific", 16mm camera. This instrument features a constant speed motor and a gear box giving framing speeds of 8, 16 or 24 frames per second. Alternatively it can be powered by an "intervalometer", an attachment using rotating notched cams to give a framing rate between one frame per 2 seconds and one frame per hour. The usual rate used in the experiments was one frame per two seconds for slower bubbles and eight frames per second for the more rapidly evolving ones.

The accuracy of the intervalometer cam was tested by photographing a digital timer accurate to 0.01 seconds. Over a period of several minutes the cam was consistent to $\pm$ 0.02 seconds with absolutely no drift.

The camera shutter is of the rotating blade type, adjustable between 20^{o} and 110^{o}. The lens mount is a standard C-mount. The photograph had first to be composed and focussed with a focussing telescope in position. This was later removed and replaced with a loaded film magazine.

In use, the camera was mounted on its side so that the longer side of the photograph was vertical.

5.4.2 Optics

As the pressure vessel was cylindrical, an amount of image distortion in one direction was unavoidable. This was minimised by placing the vessel in a water filled square perspex box (which also provided a constant temperature bath). Also the initiating tip was carefully made and positioned to be exactly radially aligned with the camera and the final bubble size was quite small, about one millimetre radius at most. Under these conditions, distortion was thought to be negligible but was checked by photographing an appropriately placed ruled graticule (1mm by 0.01mm). No measurable distortion was recorded.

Obviously, it was desirable to achieve a large magnification for accuracy and ease of analysis. This was accomplished by the use of extension tubes and a 25mm f1.4 Switar lens mounted in the reversed position. Reverse mounting of lenses in close-up situations gives better image quality, improved depth of field and a greater object-to-lens distance, an important point when the object is inside a vessel and approach is restricted. The combination was highly success-

ful. With forty millimetre extension tubes and reversed lens, approximately twice life size magnification was obtained; with seventy millimetres, approximately four times magnification. Yet the object-to-lens distance was around three centimetres, which approximates the film-to-lens distance in a normal situation. If the lens was in its normal mode, the object-to-lens distance with 70mm extension would be very small.

5.4.3 Illumination

The light source was a 1000 watt projector bulb illuminating a white card behind the pressure vessel. This provided sufficient light to enable an exposure of about $\frac{1}{250}$ second at an aperture of f16.

5.4.4 Films and Development

Kodak Plus-X negative film (80 ASA) was used in all runs and developed, for greater contrast, in Kodak D19 Developer, five minutes at $20^{o}C$.

5.5 Film Analysis

Films were analysed on a Vanguard Motion Analyser, Model C11 with projection head Model M16C. This instrument has a screen with moveable cross hairs which can be positioned to one thousandth of an inch and the co-ordinates read from two dials. During the course of the work, a P.C.D. Limited Digital Data Reader Model ZAE 3A was purchased by the Department. This instrument can be set as accurately as the Vanguard (and uses the same projector) but has the additional

advantages of variable electronic scaling and production of digitised co-ordinates on punched paper tape. This instrument was used only for examination of bubble growth in glycerol.

5.6 Chemicals used

Water used in the experiments was single distilled (stainless steel still) and reboiled. Thus it could not be considered free from surface active contaminants.

The glycerol used was Laboratory reagent grade, minimum 98% assay, from B.D.H. Chemicals Ltd.

Carbon dioxide was obtained from the Distiller's Company Limited and conformed to BS 4015 for fitness for use in laboratories. It contained not more than 0.20% by volume residual gases and not more than 0.05% by weight of water.

Oxygen was obtained from B.O.C. and was the standard laboratory grade.

5.7 Other apparatus used

During experiments, the temperature was maintained at $20^{o}C \pm 0.05^{o}C$ by a "Tempunit" water bath temperature controller which also circulated the water. The temperature was measured with a Sugden-Powell thermometer of range 0^{o}-$50^{o}C$ by $0.01^{o}C$ and certifed correct to $\pm 0.00^{o}C$ at $20^{o}C$.

Pressure was measured with one of two new Barnet Instruments Type 401-1 bourdon tube pressure gauges, calibrated in psig units and supplied with calibration certificates.

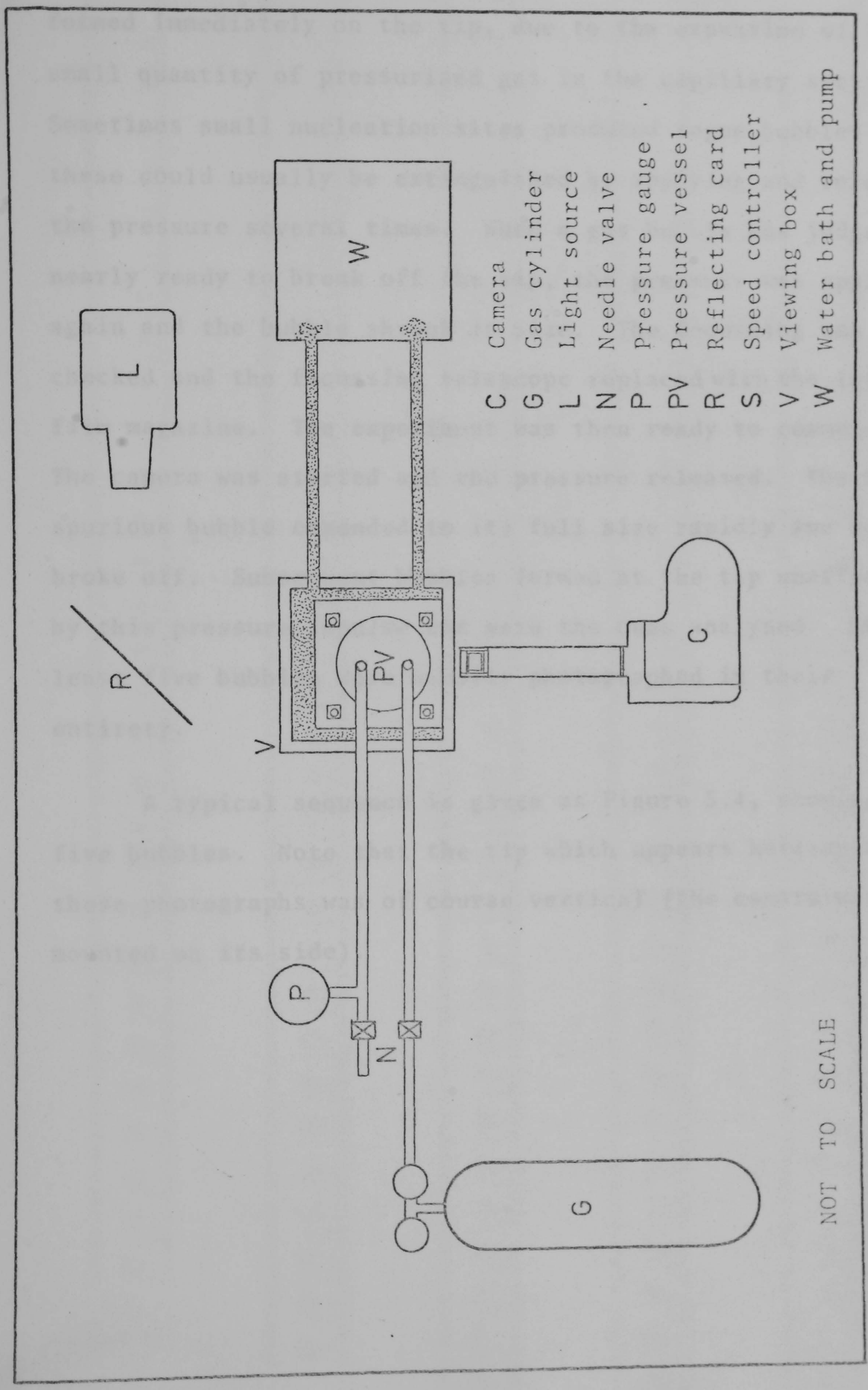
Viscosity of the glycerol solutions was determined with a Ferranti Viscometer Type VM which, immediately prior to its use had been overhauled and recalibrated by the manufacturer. Density of the solutions was measured with a 25ml pycnometer and all the correction terms were applied to yield an accuracy estimated at ± 0.05%.

5.8 Experimental procedure

A diagram of the complete experimental set-up is given in Figure 5.3.

When the capillary tip was made, it was carefully positioned inside the glass pressure vessel which was then assembled and made tight. The whole interior was then cleaned overnight (this was also done between runs) with a 5% solution of Decon 90, a rinseable surface active agent. Before any experiments, the vessel was thoroughly rinsed several times with distilled water and then enough reboiled water to cover the tip to a depth of about five centimetres was added. The vessel was connected to the carbon dioxide (or oxygen) cylinder and the pressure gauge with reinforced flexible PVC tubing and the air in the system purged by passing gas for about ten minutes. The vessel was then inclined so that the tip was out of the water and the required pressure applied. The vessel and contents under pressure were shaken in a water bath for eight hours to produce a saturated solution (at least 36 hours for the glycerol solutions). It was then removed from the bath and placed in the perspex viewing box and the camera, on a sturdy tripod, was positioned and focussed on the tip. Pressure was then released and a bubble

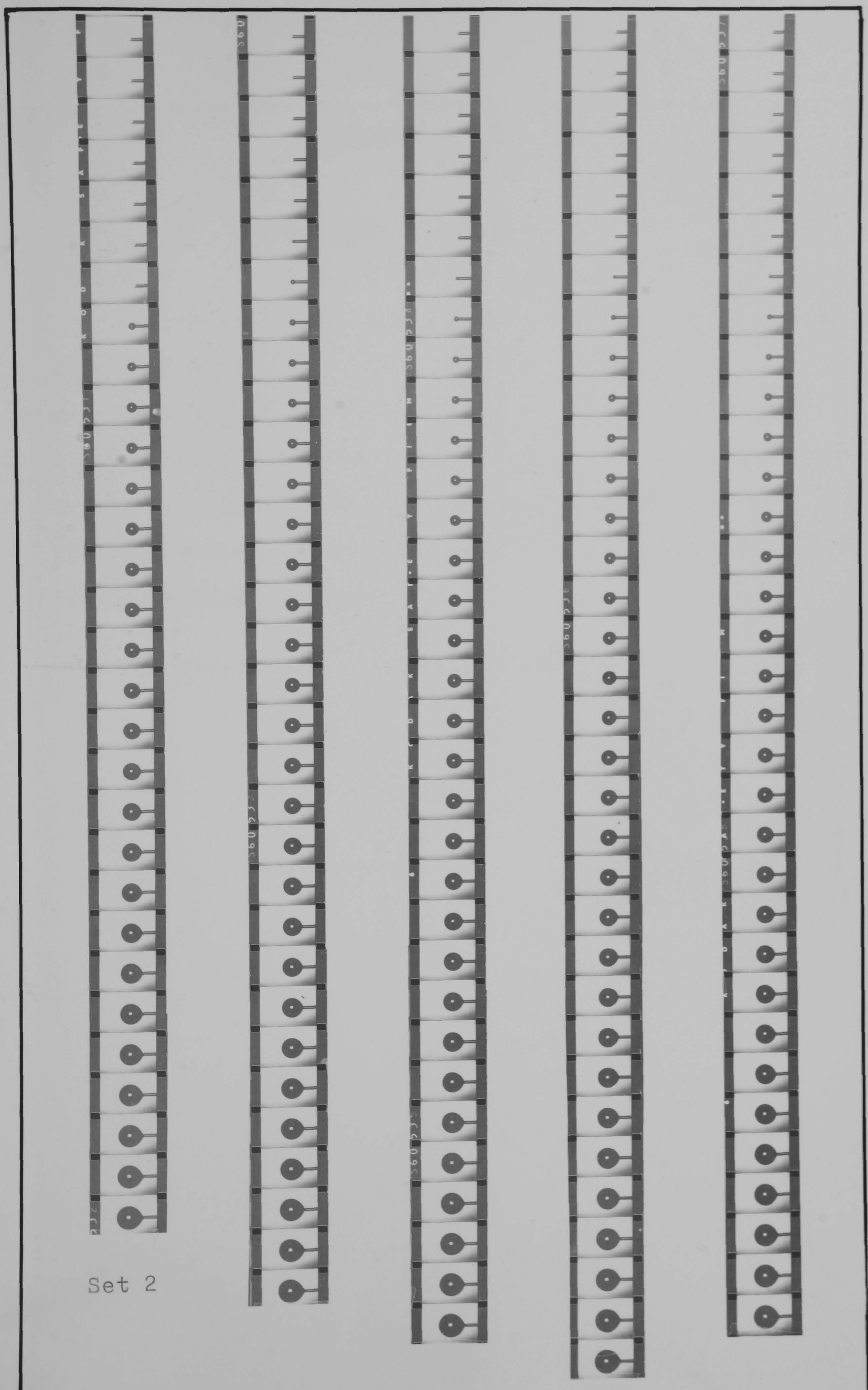
Figure 5.3 Diagram of experimental set-up



formed immediately on the tip, due to the expansion of the small quantity of pressurised gas in the capillary section. Sometimes small nucleation sites produced rogue bubbles but these could usually be extinguished by applying and releasing the pressure several times. When a gas bubble was judged nearly ready to break off the tip, the pressure was applied again and the bubble shrunk in size. The focussing was checked and the focussing telescope replaced with the loaded film magazine. The experiment was then ready to commence. The camera was started and the pressure released. The first spurious bubble expended to its full size rapidly and soon broke off. Subsequent bubbles formed at the tip unaffected by this pressure impulse and were the ones analysed. At least five bubbles were usually photographed in their entirety.

A typical sequence is given as Figure 5.4, showing five bubbles. Note that the tip which appears horizontal in these photographs was of course vertical (the camera was mounted on its side).

Figure 5.4 Typical bubble growth sequence



Set 2

CHAPTER 6

EXPERIMENTAL RESULTS

In this chapter, the sources of data used in calculations will be given. The conditions under which the experiments were carried out will be tabulated and calculations made to check that the experiments were carried out in the appropriate theoretical regime. Details of the analysis and statistical analysis will be given and the results presented graphically or in tabular form.

The results will then be discussed.

6.1 Data Sources

Data needed to calculate the theoretical parameters, given the experimental conditions, were taken from the literature.

For the solubility of carbon dioxide in water, the data of Houghton et al (1957) were used. They provide useful tabulations of the Bunsen absorption coefficient and the mole fraction of dissolved carbon dioxide in water at nine temperatures between $0^{o}C$ and $100^{o}C$ and at nineteen pressures from one atmosphere to thirty-six atmospheres. The results have been taken from several sources and are claimed to have an accuracy better than 3%. At $20^{o}C$ and in the range 0 to 10 atmospheres, the data correlates as:

$$x = 0.6971\ P - 0.005321\ P^2 \qquad (6.1)$$

where x is the mole fraction of carbon dioxide and P is the pressure in atmospheres.

Data for the solubility of oxygen in water at a number of temperatures are given by Perry (1963) in the form of a Henry's law constant. At $20^{o}C$ $H = 4.01 \times 10^4$ atmospheres per mole fraction oxygen.

Data for the solubility of carbon dioxide in glycerol solution was interpolated between two sources. In Lawrie (1928) data are found giving the Bunsen absorption coefficient at $15^{o}C$ against weight percent of glycerol in water; in Seidell (1940) data are found giving the Ostwald coefficient at $25^{o}C$ against the number of gram moles of glycerol per

litre of solution. These data may be found in Appendix A.4 where they are recalculated to the same basis and an interpolation made to give results at $20^{o}C$.

In calculating the solubilities from the known gas pressure and atmospheric pressure of the experiments, the vapour pressure of water at $20^{o}C$ (approximately 17mm mercury) was neglected.

Diffusivity data for carbon dioxide in water were taken from Pratt et al (1973) and Davidson and Cullen (1957) who were also the source of data for the diffusivity of oxygen in water. At $20^{o}C$:

$$D_{CO_2} = 1.65 \times 10^{-5} \ cm^2/sec$$

$$D_{O_2} = 2.00 \times 10^{-5} \ cm^2/sec$$

Reported results for diffusivities of sparingly soluble gases vary greatly. The values for carbon dioxide seem to suffer less from this variability than those of oxygen. The above should be considered as "best estimates". No attempt was made to include corrections for the effect of concentration on diffusivity. Diffusivity data for carbon dioxide in glycerol solutions were harder to come by but some are given by Astarita (1964). This data had to be extrapolated to be used for one of the experiments so must be considered only moderately reliable. (No other data supporting Astarita's values were found).

The relationship between viscosity and weight percent glycerol was found in Kaye and Laby (1966). Values of

specific gravity versus weight percent glycerol were taken from the International Critical Tables, Volume III.

It was assumed that the dissolved gas could be considered undissociated or that the time constant for the carbonic acid-carbon dioxide reaction was an insignicant factor compared to the rates at which the bubbles were evolving (Quinn and Jones (1936)).

6.2 Experimental Conditions

All experiments were conducted at $20^{o}C \pm 0.05^{o}C$. Table 6.1 gives the conditions for the experiments involving carbon dioxide and oxygen in water; Table 6.2 gives the conditions for the carbon dioxide in glycerol experiments. The carbon dioxide - water system was the most fully examined since it is an everyday system yet no reliable results are known to have been reported for it. The results of Buehl and Westwater (1966) are by their own admission not very satisfactory, exhibiting strange discontinuities and much more rapid growth than had been expected. (See Figure 2.2 which is their Figure 4).

At this stage, the assumptions of Scriven's asymptotic theory should be justified, that is the viscous, inertial and surface tension forces should be negligible with the growth simply controlled by mass diffusion. In terms of the parameters previously defined, it has to be shown that $\bar{B} << 1$, $V << 1$,and $\phi << 1$.

Take, as an example, conditions slightly more severe than those encountered in the experiments. Consider a

bubble growing at ambient pressure from carbon dioxide solution previously saturated at six atmospheres and using the smallest initiation tip, radius 0.03 millimetres. Take the surface tension of water as 70 dynes/cm and the viscosity as 1 centipoise. Then:

$$\Delta P = 5 \text{ atm}$$

$$\Delta C = 8.1 \times 10^{-3} \text{ g/cm}^3$$

$$\rho_g = 1.86 \times 10^{-3} \text{ g/cm}^3$$

$$\overline{Ja} = \frac{\Delta C}{\rho_g} = 4.4$$

$$\phi = \frac{2\sigma}{R_o \Delta P} = 9.6 \times 10^{-3}$$

$$G = \frac{R_o^2 \Delta P}{\rho_\ell D^2} = 16.7 \times 10^{10}$$

$$G^{\frac{1}{2}} = 4.1 \times 10^5$$

$$Sc = \frac{\nu}{D} = 6.1 \times 10^2$$

$$V = \frac{Sc}{G^{\frac{1}{2}}} = 1.5 \times 10^{-3}$$

$$\overline{B} = \frac{\overline{Ja}}{G^{\frac{1}{2}}} = 4.9 \times 10^{-5}$$

The values of $\overline{B}$, V and ϕ are all much less than unity so the experiments lie well within the domain of a Scriven solution.

Table 6.1 Experimental conditions

Experiment	1	2	3	4	5	6	7
Gas	CO_2	CO_2	CO_2	CO_2	CO_2	CO_2	CO_2
Capillary Tip	T4	T5	T5	T5	T6	T6	T6
Framing Rate (Frames per sec)	0.5	0.5	0.5	0.5	0.5	0.5	0.5
Gas Pressure P_o (psig)	20.2	20.2	25.5	31.3	11.0	20.1	29.5
Atm. Pressure P_∞ (mm Hg)	770	778	777	777	766	766	765
ΔP (atmospheres)	1.36	1.35	1.71	2.11	0.74	1.36	2.00
C_o $gm/cm^3 \times 10^3$	3.96	3.96	4.55	5.19	2.94	3.95	4.99
C_{sat} $gm/cm^3 \times 10^3$	1.71	1.73	1.73	1.73	1.70	1.70	1.70
ΔC $gm/cm^3 \times 10^3$	2.25	2.23	2.82	3.46	1.24	2.25	3.29
Calculated $\Phi\{\varepsilon,\beta\} = \overline{Ja}$	1.21	1.19	1.50	1.84	0.67	1.21	1.78
Calculated β	1.54	1.51	1.84	2.18	0.97	1.54	2.12

Table 6.1 (continued) Experimental conditions

Experiment	8	9	10	11	12	13	14
Gas	CO_2	CO_2	CO_2	CO_2	CO_2	CO_2	O_2
Capillary Tip	T6	T6	T6	T6	T6	T6	T7
Framing Rate (Frames per sec)	0.5	8	8	8	8	8	0.5
Gas Pressure P_o (psig)	40.3	29.3	39.7	49.6	35.1	45.0	50.0
Atm. Pressure P_∞ (psig)	765	756	768	770	763	768	774
ΔP (atmospheres)	2.73	2.00	2.69	3.36	2.38	3.05	3.38
C_o $gm/cm^3 \times 10^3$	6.17	4.97	6.11	7.18	5.61	6.68	0.195
C_{sat} $gm/cm^3 \times 10^3$	1.70	1.68	1.71	1.71	1.70	1.71	0.045
ΔC $gm/cm^3 \times 10^3$	4.47	3.29	4.40	5.47	3.91	4.97	0.150
Calculated $\Phi\{\varepsilon,\beta\} = \overline{Ja}$	2.42	1.80	2.37	2.93	2.12	2.68	0.129
Calculated β	2.75	2.14	2.71	3.27	2.46	3.01	0.320

Table 6.2 Experimental conditions for carbon dioxide and glycerol system

Experiment	15	16
Filming rate (frames per sec)	0.2	0.2
Glycerol density (d_4^{20})	1.2415	1.2169
Glycerol viscosity (centipoise)	380	86.4
Weight % glycerol	92.5	83.5
Diffusivity coeff. (cm^2/sec x 10^7)	1.56	4.50
Bunsen absorption coefficient	0.35	0.36
Gas pressure P_o (psig)	60.0	20.0
Atmospheric pressure (mm Hg) P_∞	758	761
ΔP (atm)	4.08	1.36
C_o (gm/cm^3 x 10^3)	3.28	1.57
C_{sat} (gm/cm^3 x 10^3)	0.65	0.67
ΔC (gm/cm^3 x 10^3)	2.63	0.90
Calculated $\Phi\{\varepsilon,\beta\} = \overline{Ja}$	1.44	0.49
Calculated β	1.83	0.77

6.3 Analysis of experimental results

The instrument used for the analysis of the film was a Vanguard Motion Analyser (see Section 5.5). In the case of carbon dioxide and oxygen in water, the glass initiating tip provided a known dimension which was used as a reference. For the glycerol experiments where much smaller bubbles were growing on the glass wall of the vessel, the reference dimension was the wire of known diameter used to initiate the bubble by scratching the wall. During the early and middle stages of the growth, the bubble had a spherical surface. As the bubble reached a certain size, bouyancy forces caused it to become slightly elongated in the vertical direction, before the forces overcame the surface tension forces holding the bubble to the tip and caused it to break off. This elongation occurred in about the last 20% of the growth period (see Figure 5.4). The diameter measured was the average of the two principal diameters.

In all cases the exact zero time is unknown. The Scriven solution forces the bubble to have zero radius at zero time but obviously the bubbles here had an initial size equal to the radius of the glass tip. In the absence of any limitation except for mass diffusion the growth soon approaches the asymptotic solution so the zero time, or the hypothetical time at which the bubble would have had zero radius may be inferred from the values of the radius at later times. Thus it is the shape of the measured radius versus time curve which is important, rather than the absolute values of the time.

The statistical analysis of the data was directed first

towards an examination of the exponent term of the bubble growth equation:

$$R = 2\beta (D t)^n \qquad (3.19)$$

In the Scriven solution n is $\frac{1}{2}$ but, in experiments in boiling Saddy and Jameson (1971) had found exponents up to 1.0 and report that other authors had made similar observations. An explanation offered was that the translational motion of the growing bubble caused a more rapid growth; this conflicts with the calculations of Buehl and Westwater (1966) who show that whilst the growth coefficient β could be affected by the motion of a tangentially growing bubble, the exponent would not be. Another explanation is that the radiant heating system used (also used by Dergarabedian (1953), (1960)) could have heated the vapour in the bubble and caused it to expand. In any case, it was decided to examine the present data with a model of the form:

$$R = 2\beta\sqrt{D}\,(t_e - t_o)^n \qquad (6.3)$$

where t_e is the experiment time and t_o a notional correction to force a co-incidence with the asymptotic solution. The growth coefficient β , the exponent n and t_o are all treated as unknown parameters. This model presents a need for data fitting by a non-linear regression method and the procedure of Law and Bailey (1963) was adopted. (See Appendix A.5 for more details).

The results of this examination are given in Table 6.3.

Table 6.3 Experimental values of the bubble growth exponent

Experiment Set	Number of Bubbles	Value of exponent		
		Minimum	Maximum	Average
1	3	.52	.57	.55
2	5	.50	.58	.55
3	5	.53	.59	.56
4	5	.51	.56	.55
5	6	.55	.56	.55
6	6	.56	.57	.56
7	8	.55	.58	.56
8	6	.53	.59	.57
9	9	.46	.56	.52
10	4	.55	.57	.56
11	4	.55	.60	.57
12	5	.52	.66	.57
13	6	.56	.63	.60
14	4	.46	.60	.55

It is plain that the exponent is not significantly different from 0.5, especially considering the slight distortions to the smaller measured radii that the tip must make.

Having examined this aspect, it was assumed that the growth could be satisfactorily represented by the square root law so the data were recalculated to determine the growth coefficients β . This time a small correction was included to account for the effect of the tip. The area of the bubble surface available for diffusion is, approximately:

$$A_{exp} = 4\pi R_{exp}^2 - \pi r_t^2 \qquad (6.4)$$

where r_t is the inside radius of the tip and πr_t^2 the non-diffusing portion of the apparent bubble area. This is not an exact correction but in any case its effect soon dies away as the bubble expands. So, for the examination of β , the model fitted was:

$$R = \sqrt{4\ \beta^2\ D(t_e - t_o) - \frac{r_t^2}{4}} \qquad (6.5)$$

with β and t_o as parameters.

For the glycerol experiments there was no tip to be concerned with and the model fitted was:

$$R = 2\ \beta \sqrt{D\ (t_e - t_o)} \qquad (6.6)$$

The results for the sixteen series of experiments are presented in Figures 6.1 to 6.16. The expected growth curve (Scriven solution) is shown on each figure as a dashed

line and the curve of best fit from the model (Equation 6.5 or 6.6) is shown for each bubble as a full line. It should be noted that the time scale is floating and only the shapes of the curves are important when comparing theoretical predictions and experiment. The values of the growth coefficients in the experiments are compared with the theoretical predictions in Figure 6.17 and in Table 6.4 .

Figure 6.1 Experimental Results -Radius vs Time- Set 1

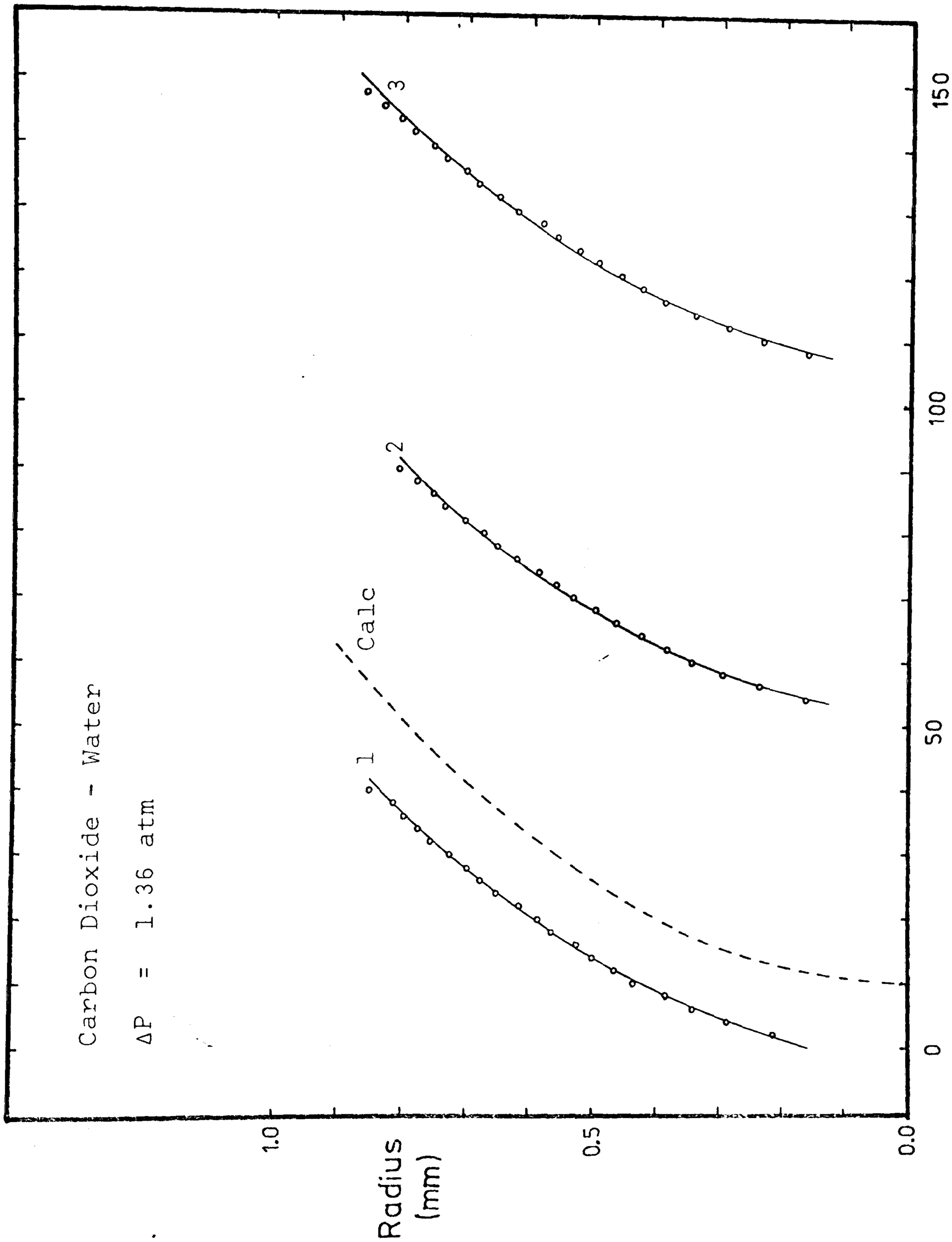


Figure 6.2 Experimental Results -Radius vs Time- Set 2

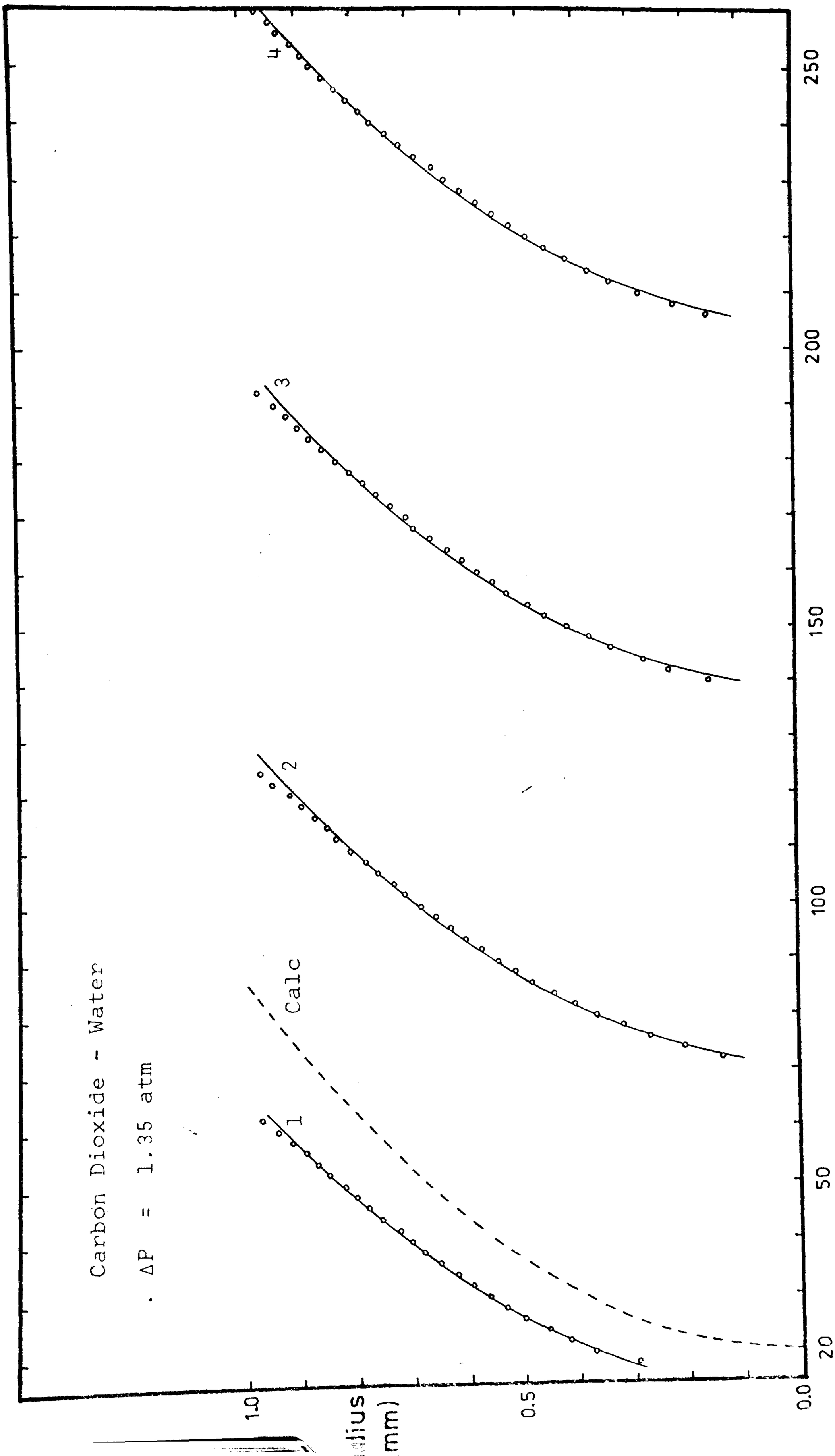


Figure 6.3 Experimental Results -Radius vs Time- Set 3

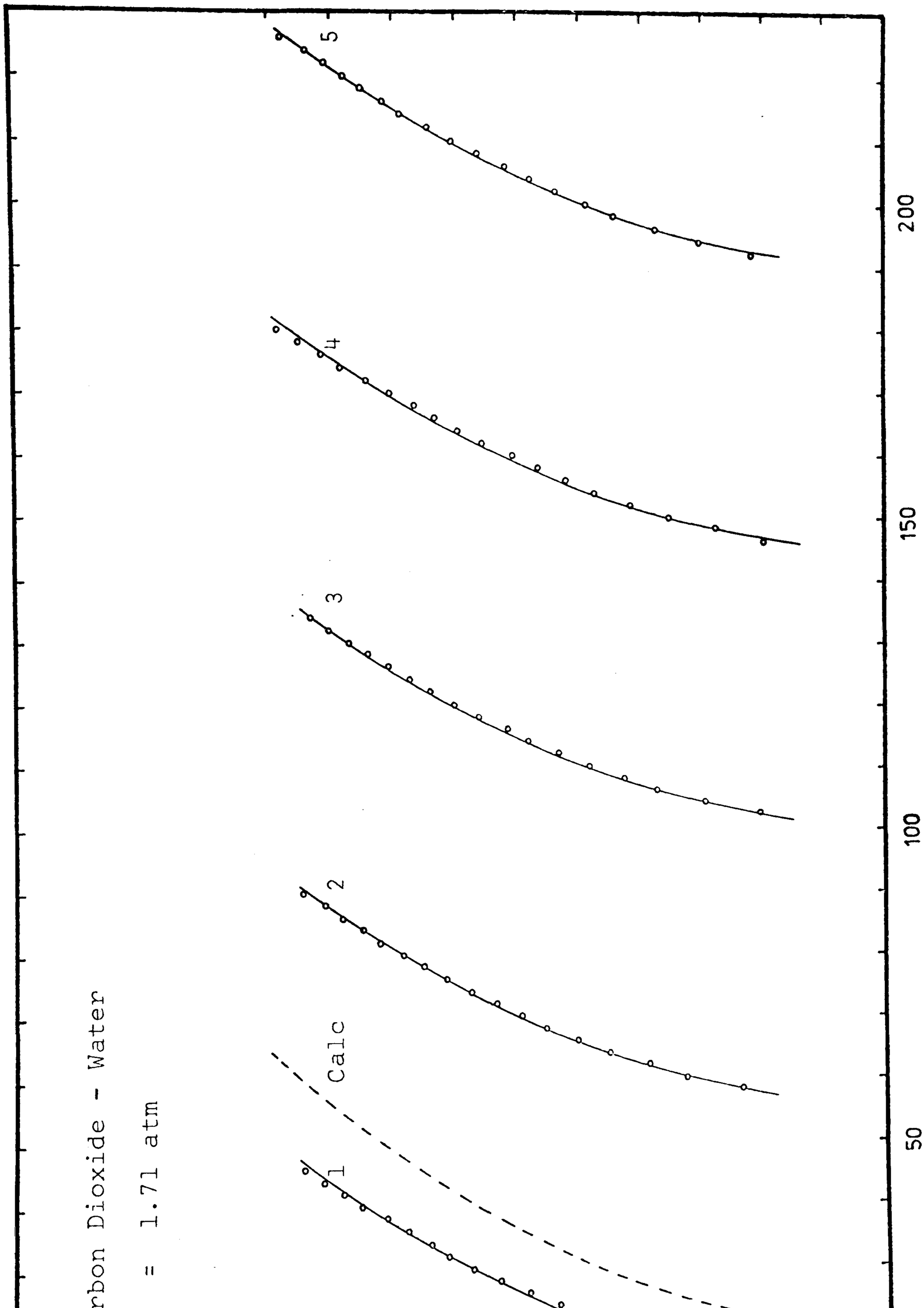


Figure 6.4 Experimental Results -Radius vs Time- Set 4

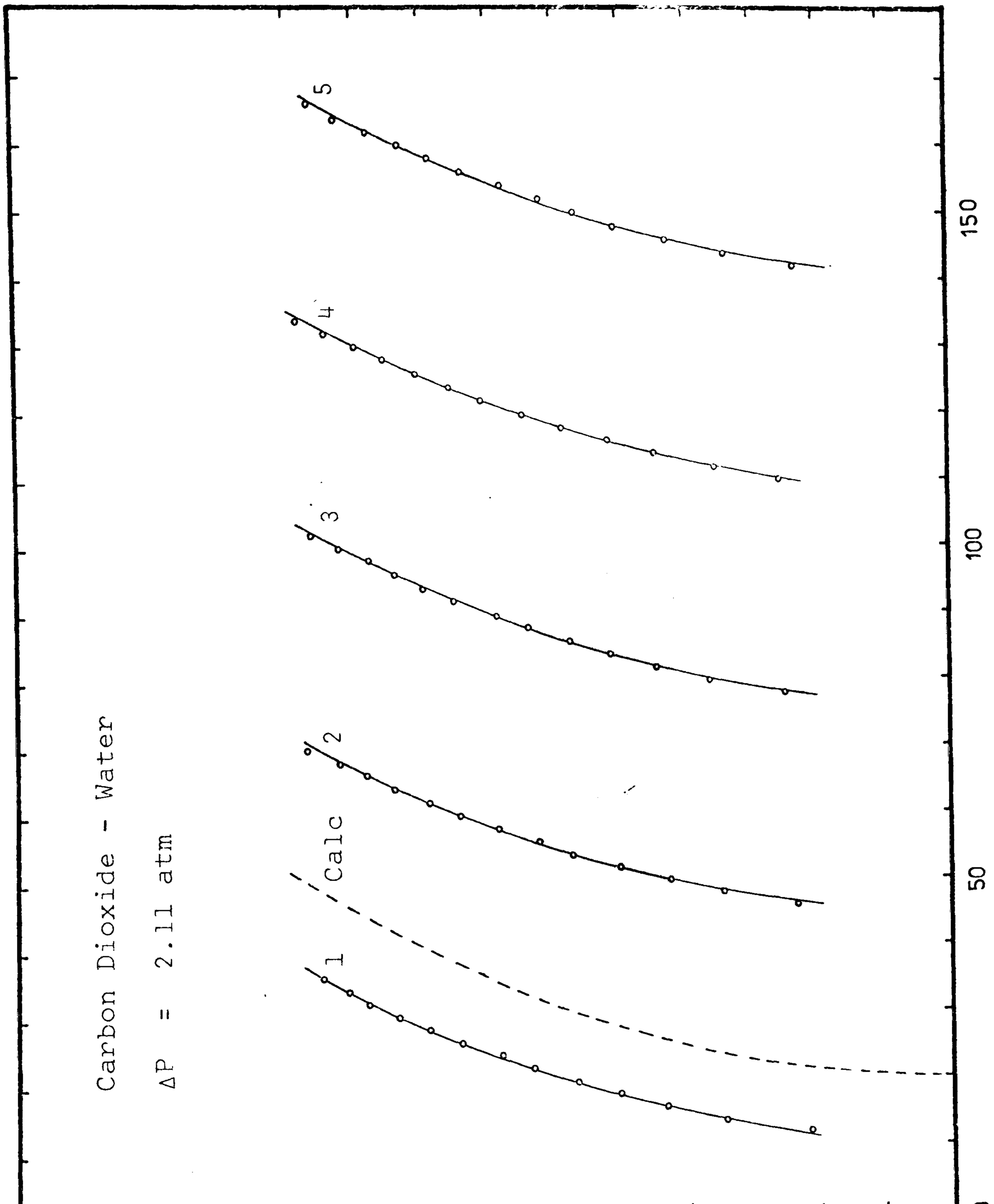


Figure 6.5 Experimental Results -Radius vs Time- Set 5

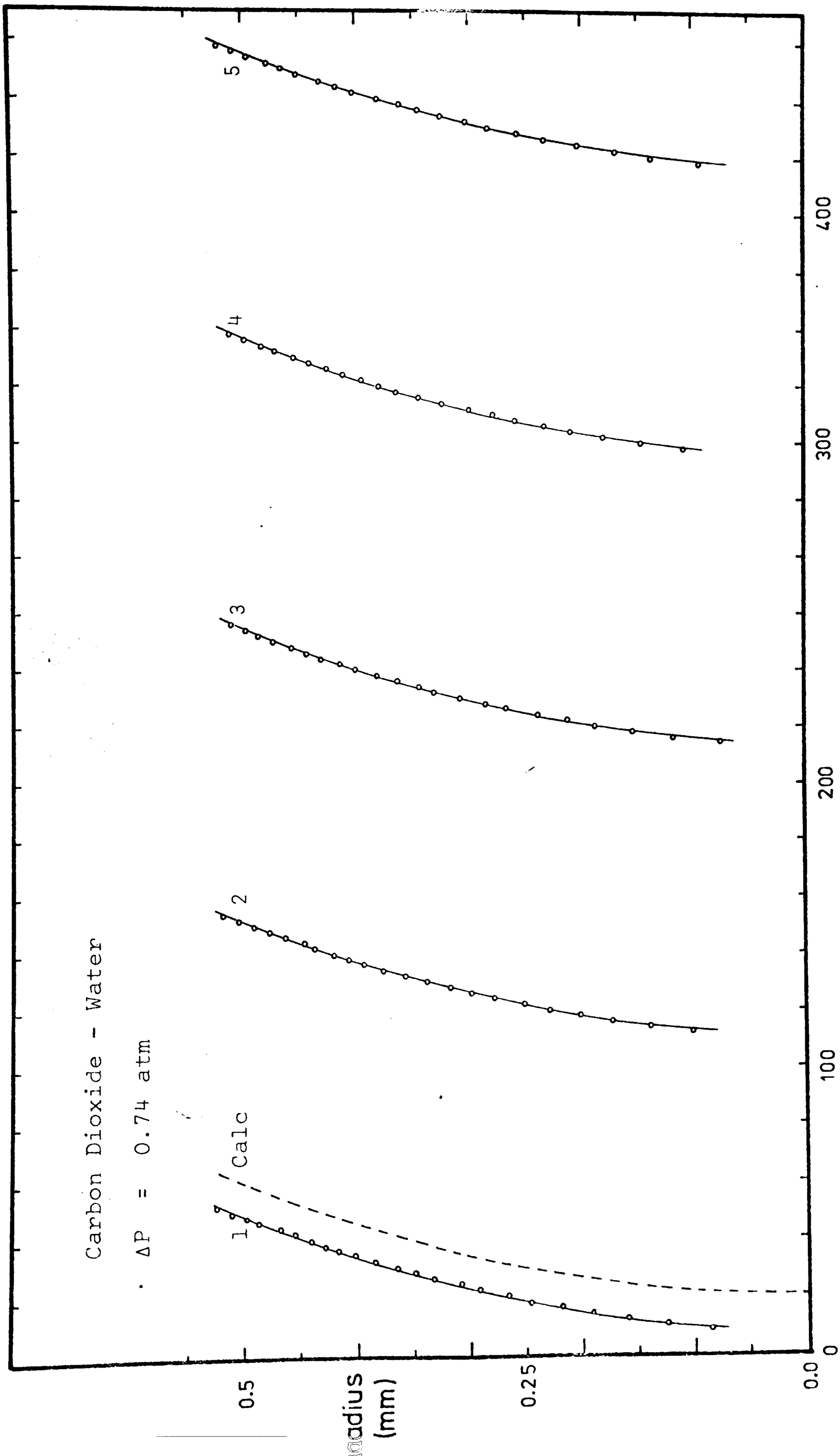


Figure 6.6 Experimental Results -Radius vs Time- Set 6

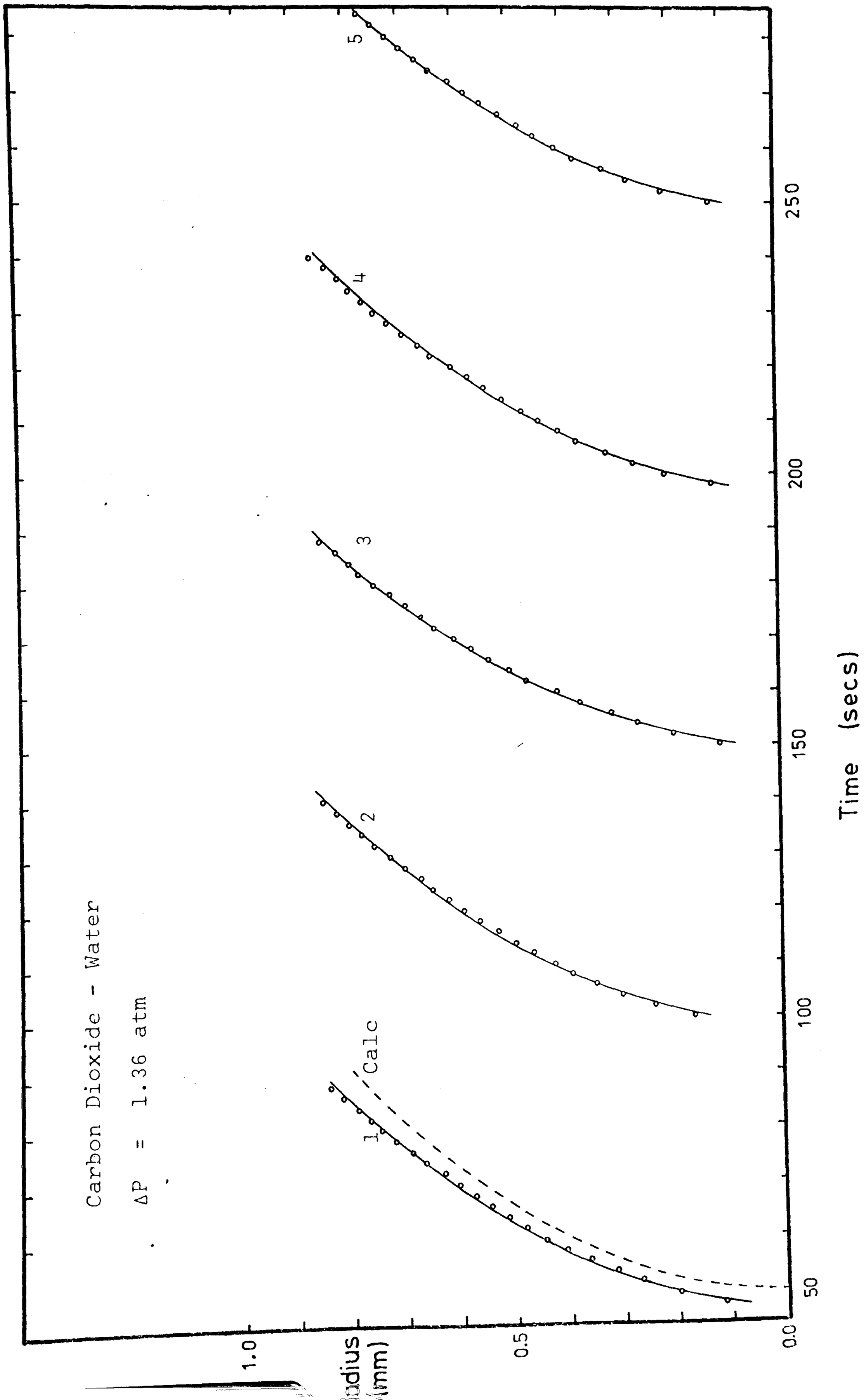


Figure 6.7 Experimental Results -Radius vs Time- Set 7

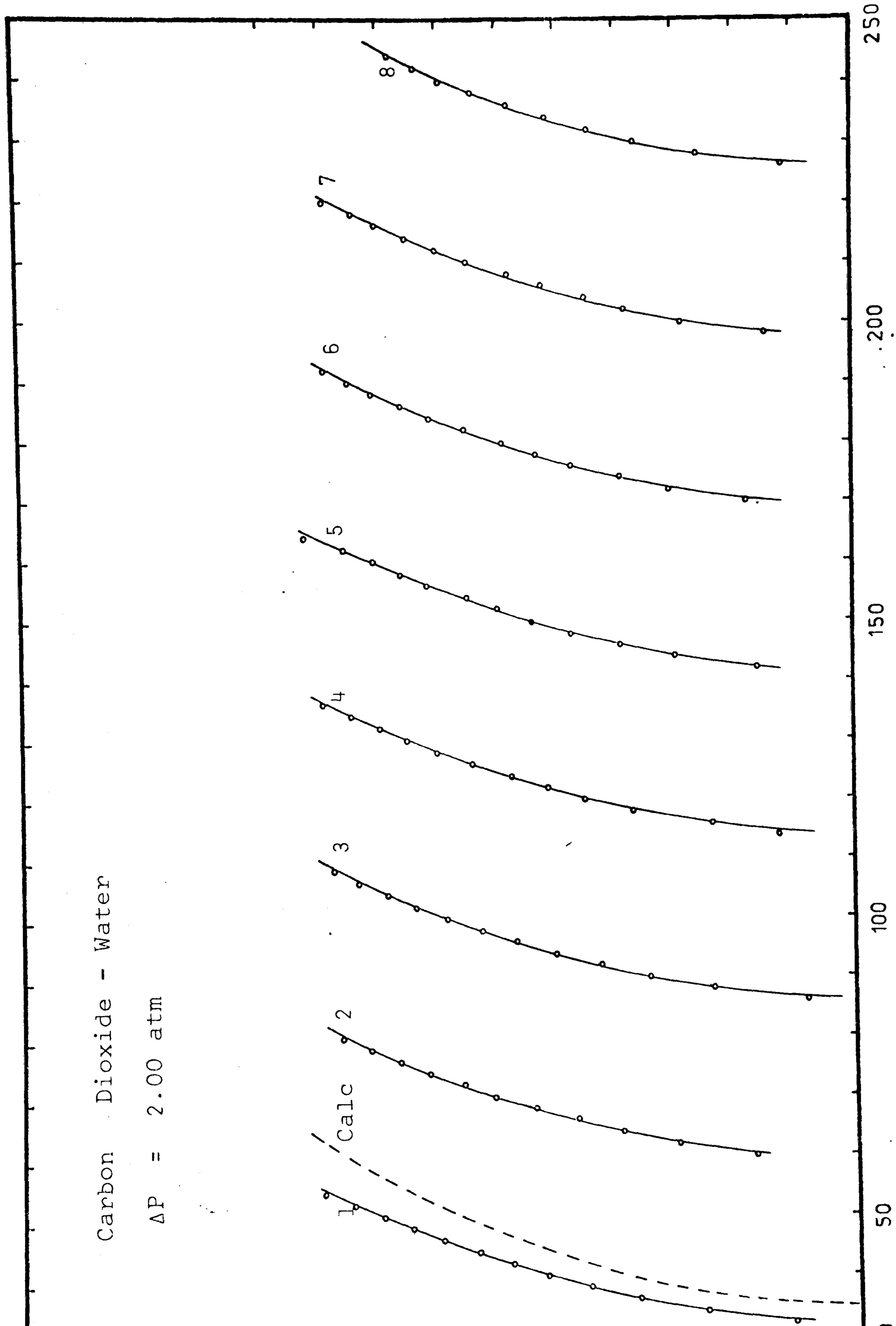


Figure 6.8 Experimental Results -Radius vs Time- Set 8

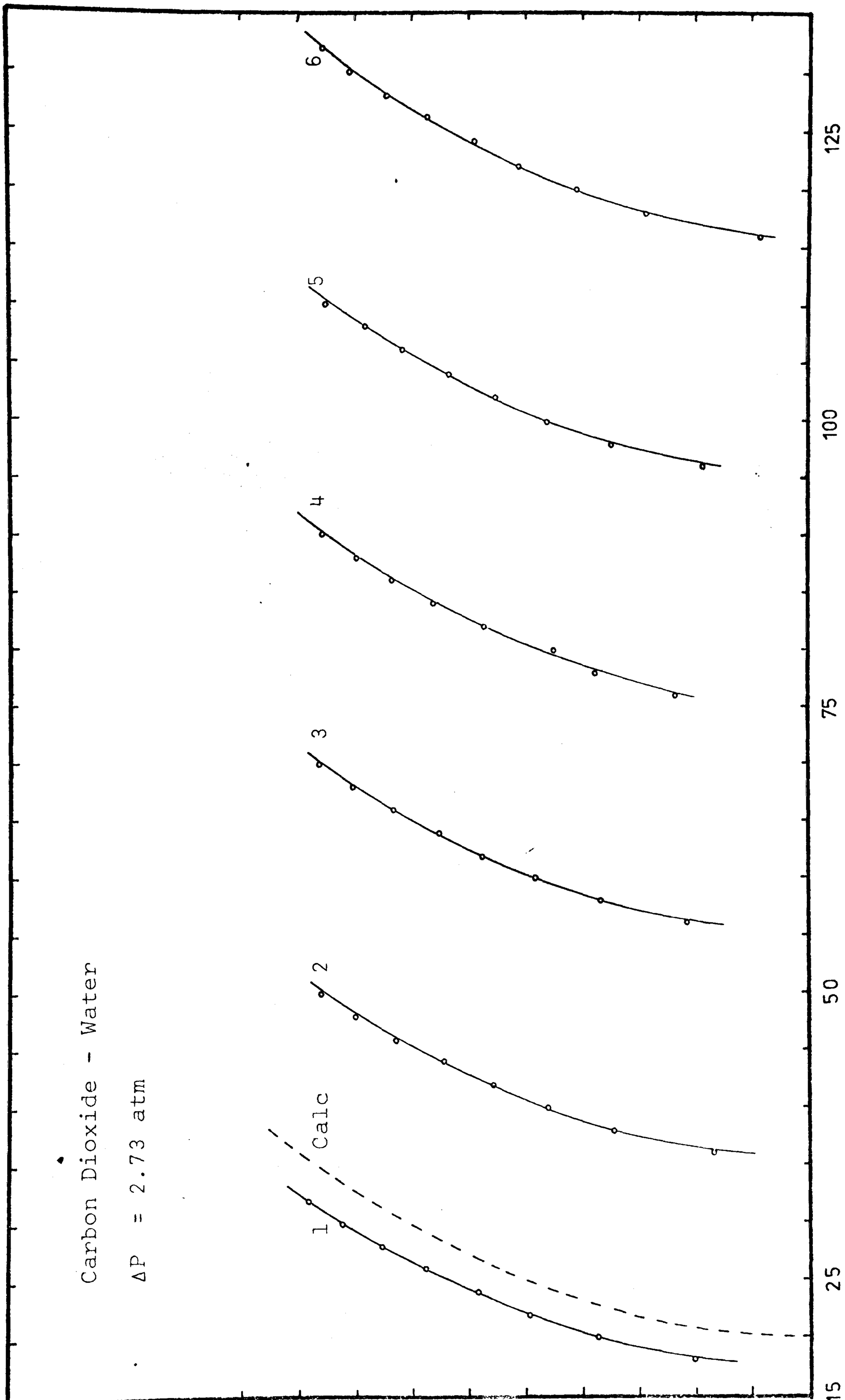


Figure 6.9 Experimental Results -Radius vs Time- Set 9

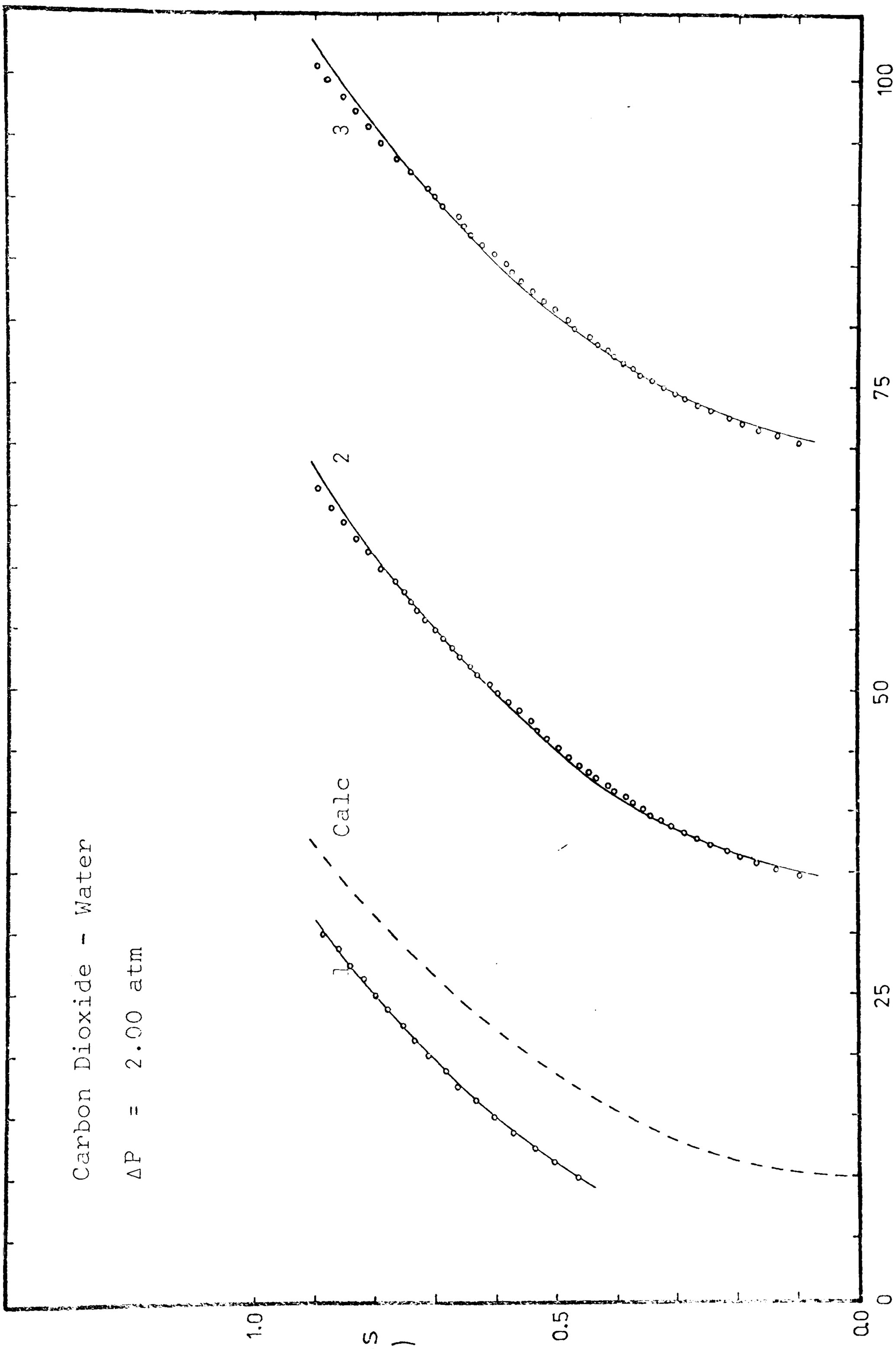


Figure 6.10 Experimental Results -Radius vs Time- Set 10

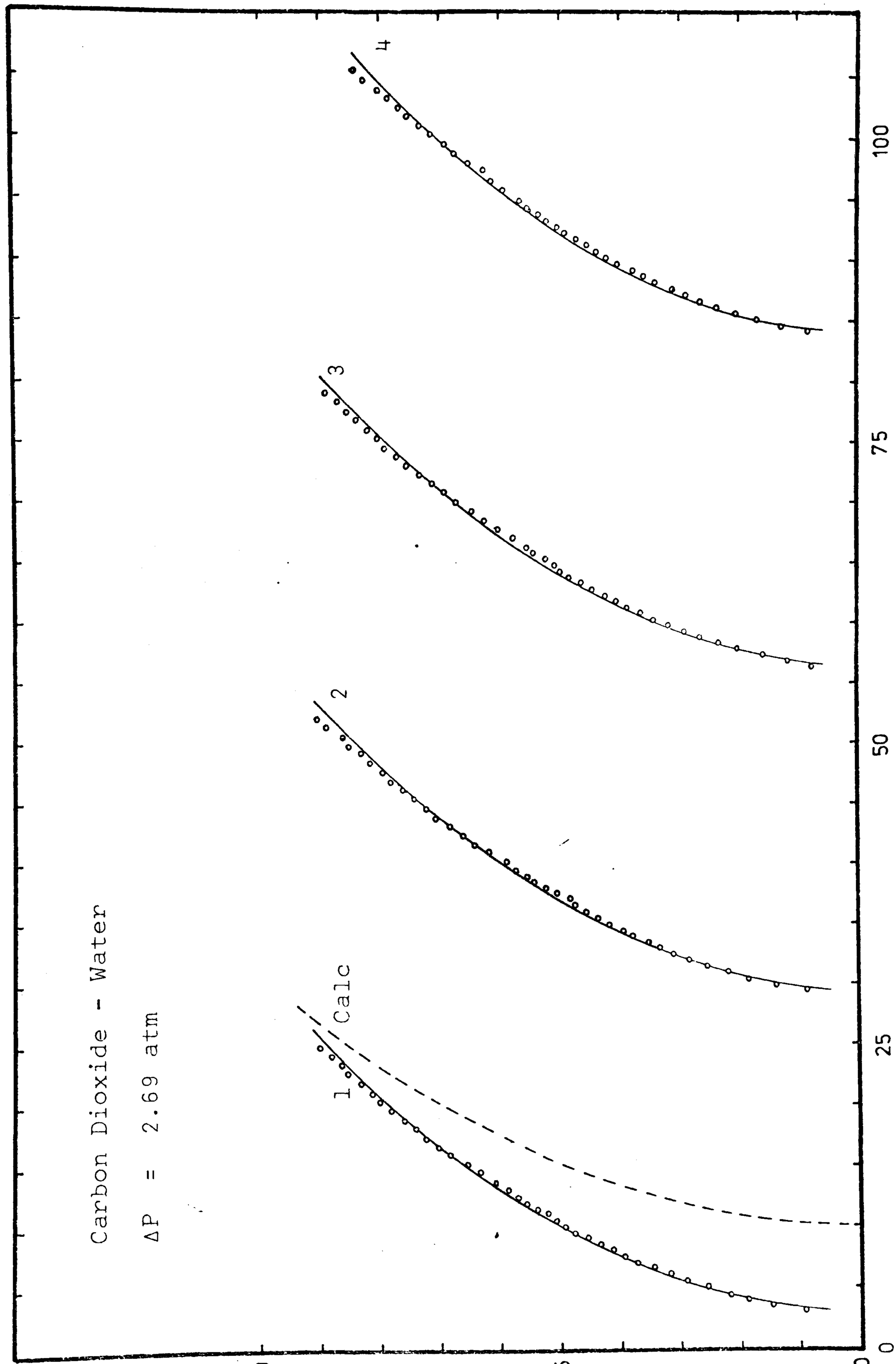


Figure 6.11 Experimental Results -Radius vs Time- Set 11

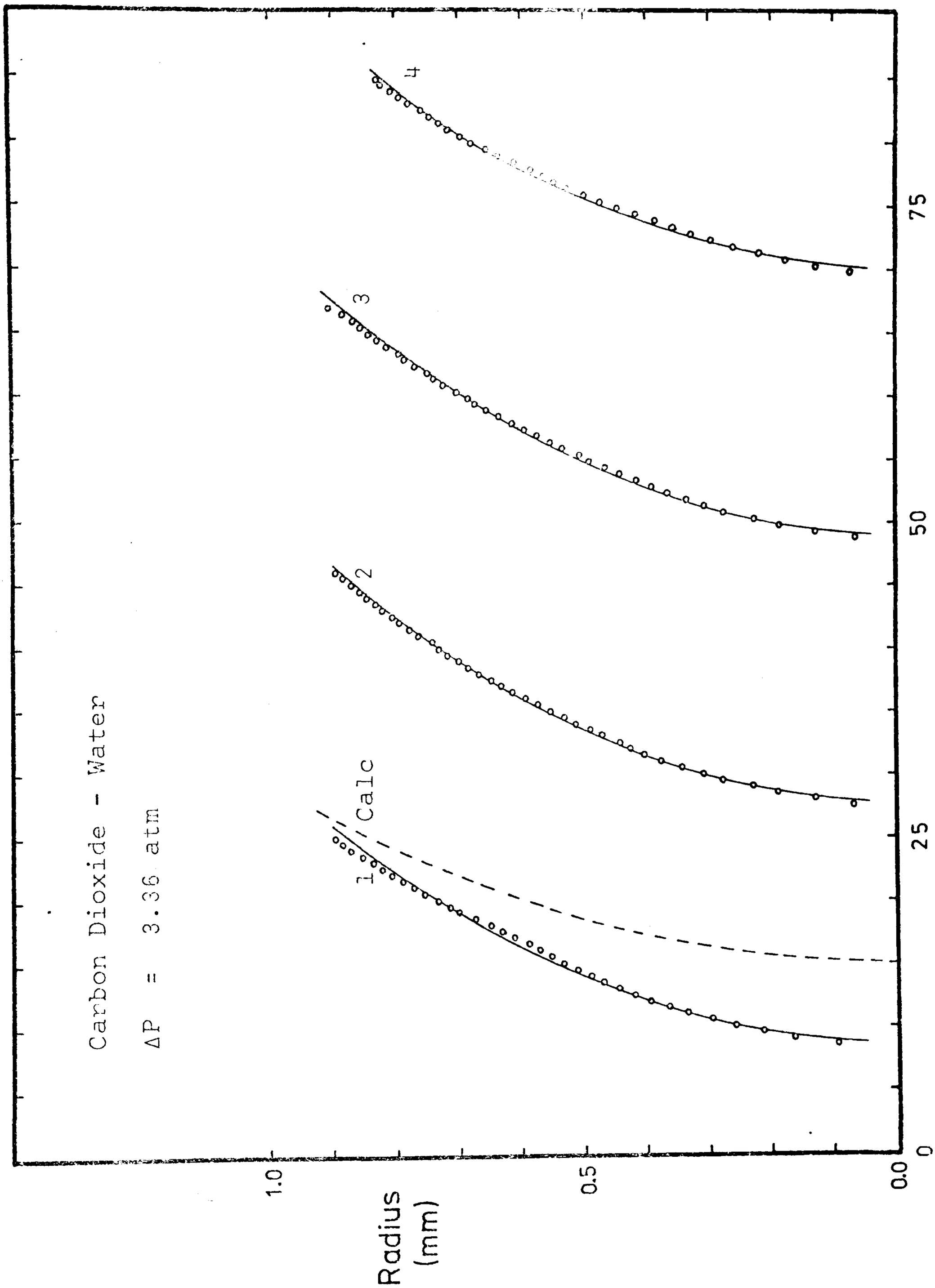


Figure 6.12 Experimental Results -Radius vs Time- Set 12

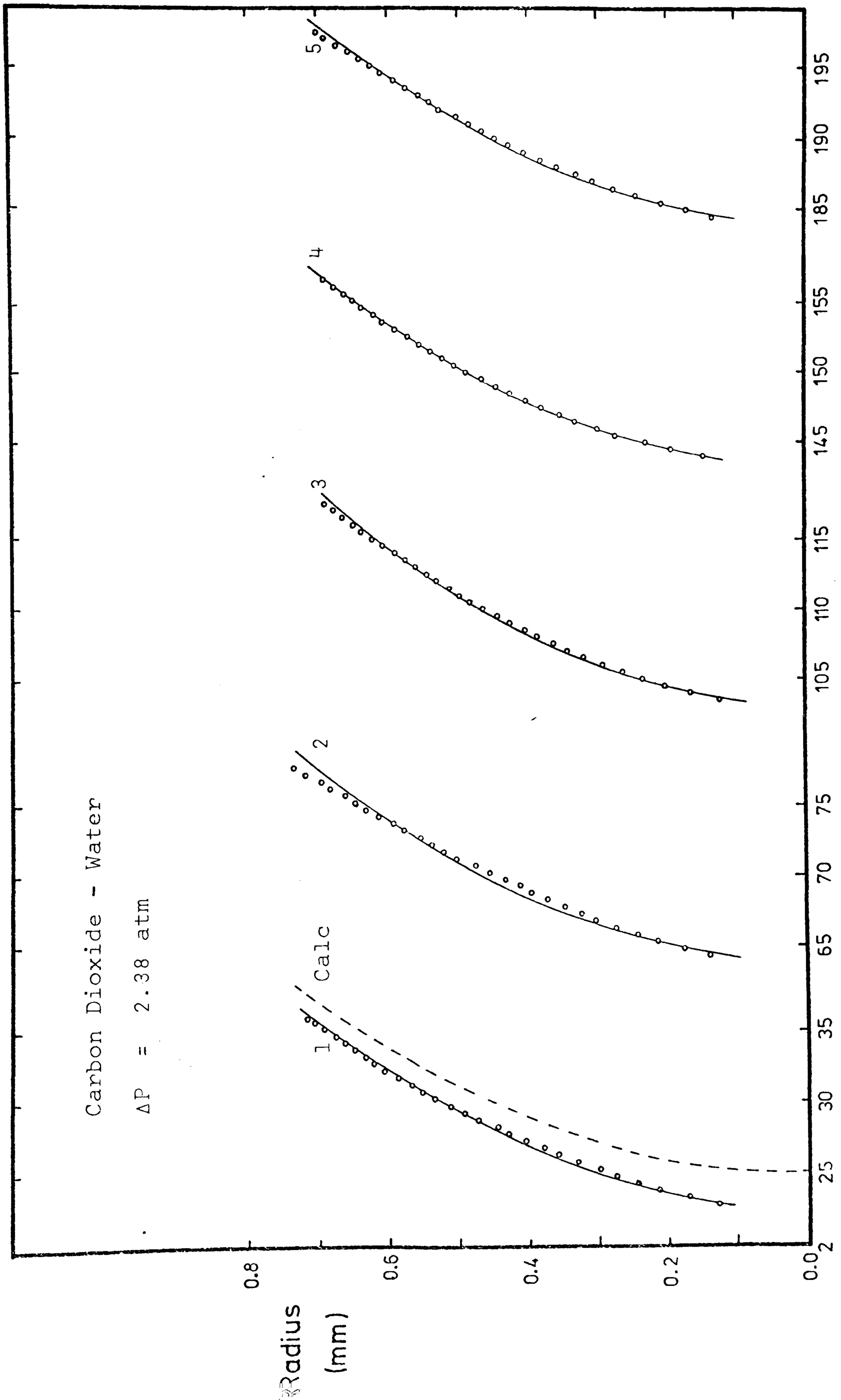


Figure 6.13 Experimental Results -Radius vs Time- Set 13

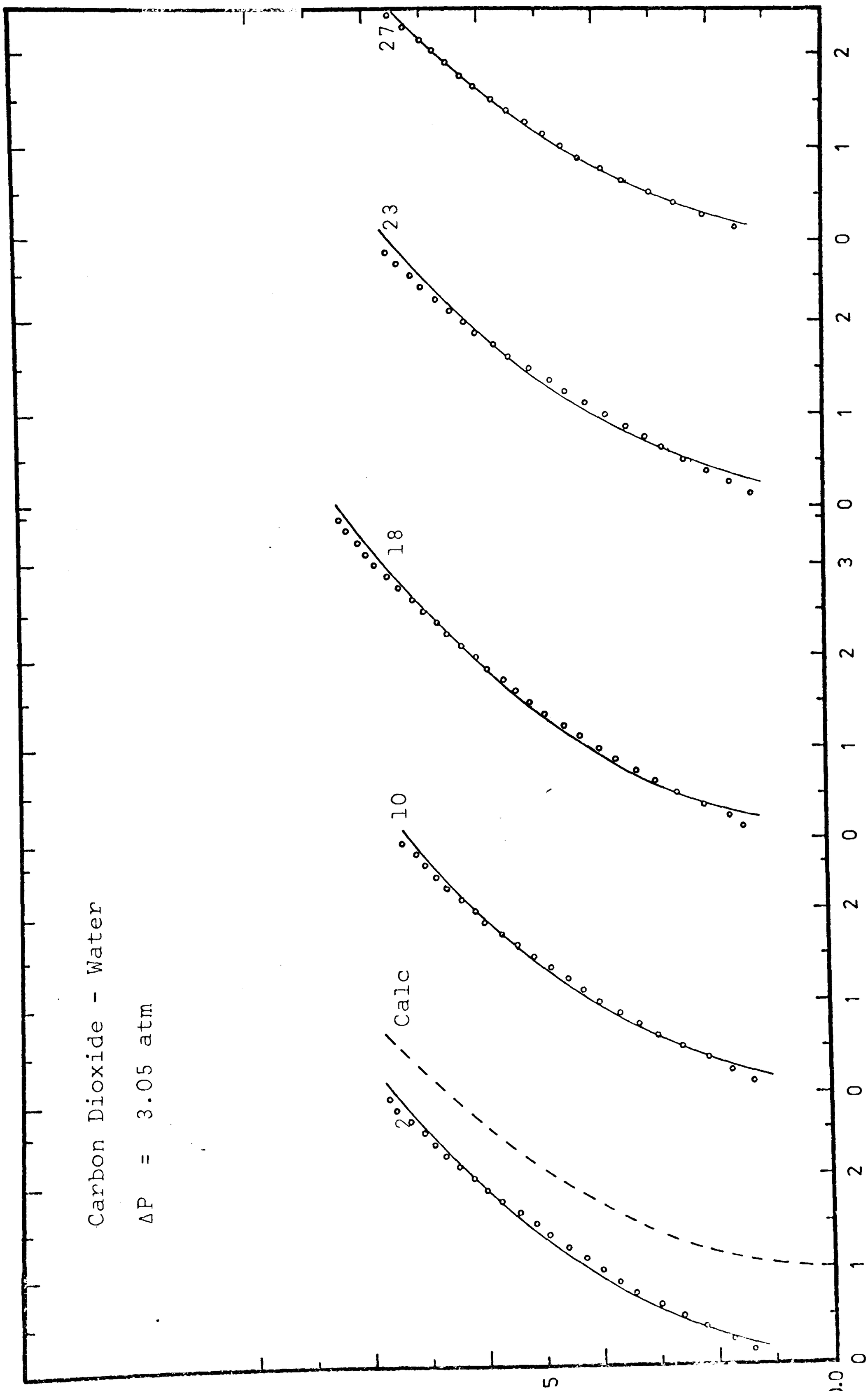


Figure 6.14 Experimental Results -Radius vs Time- Set 14

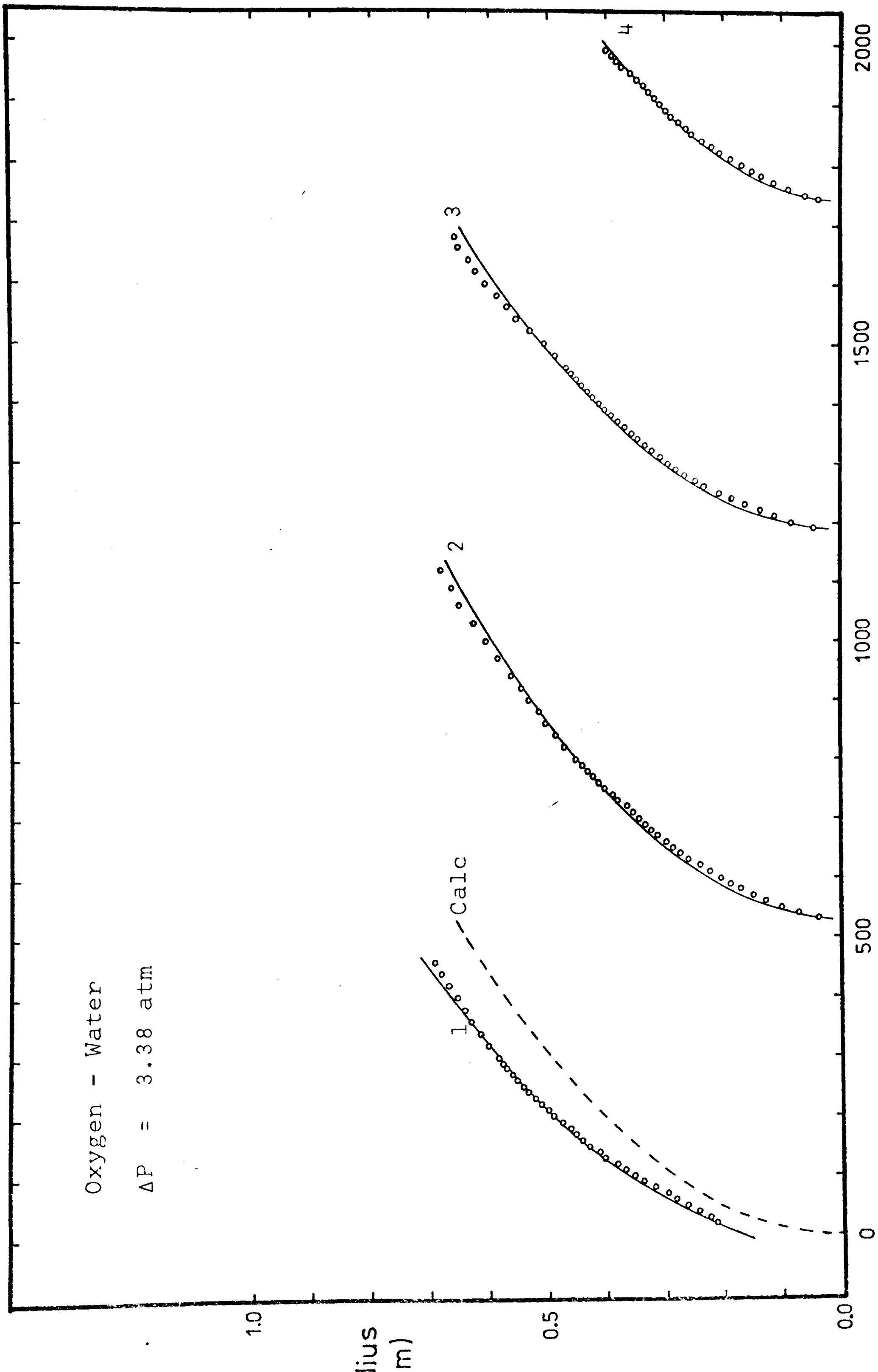


Figure 6.15 Experimental Results -Radius vs Time- Set 15

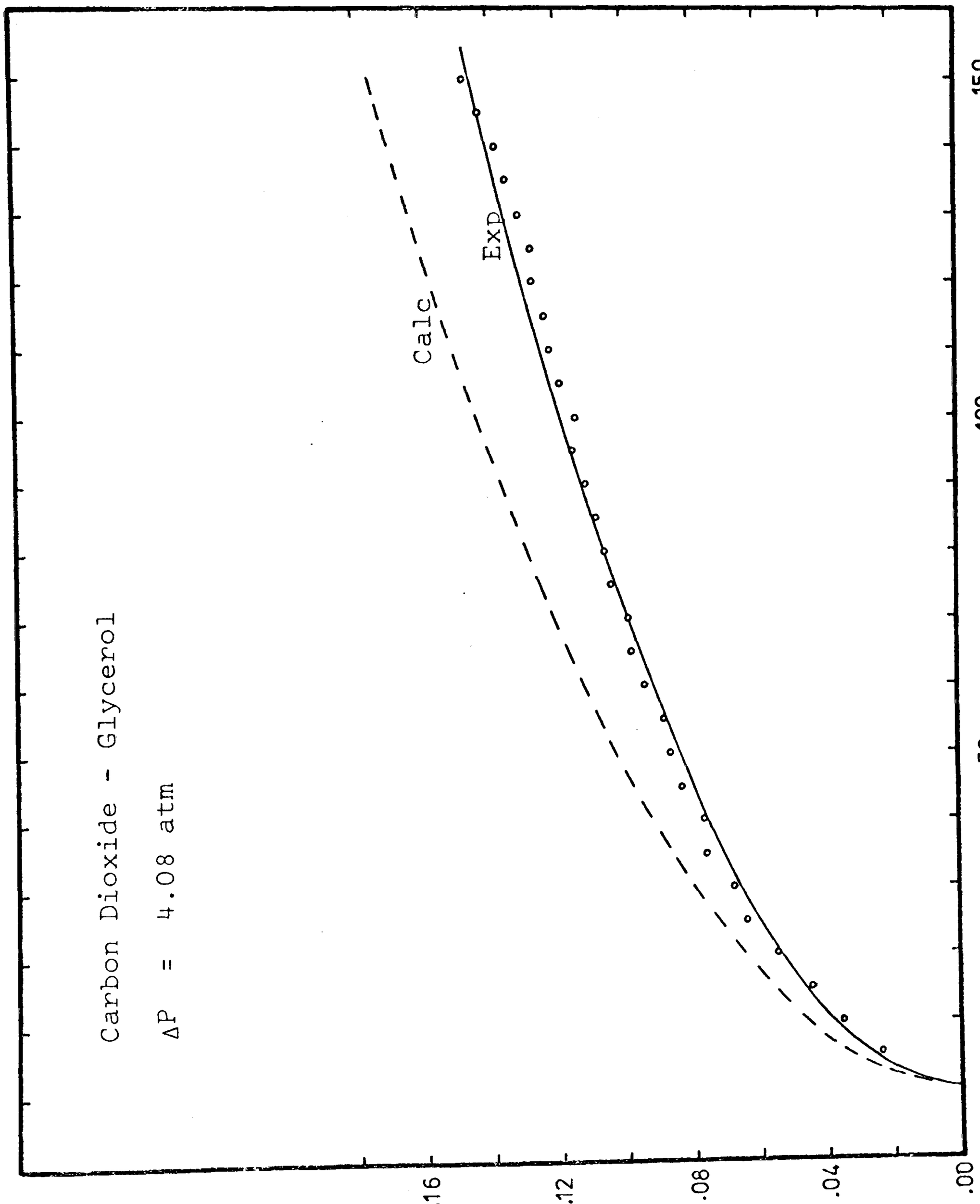
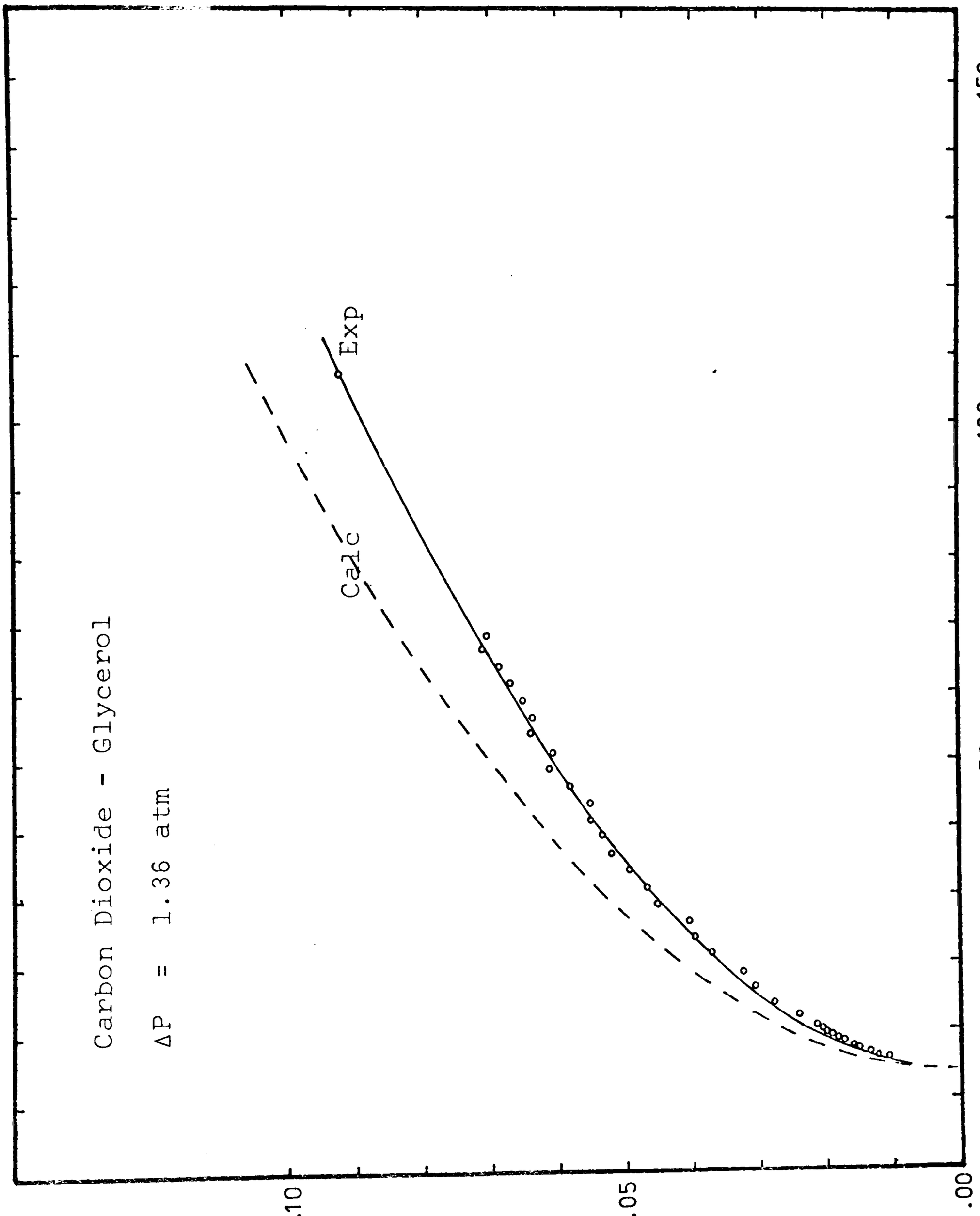


Figure 6.16 Experimental Results -Radius vs Time- Set 16



6.4 Discussion of results

The previous pages have shown graphically the results for the sixteen sets of experiments. Table 6.4 shows the calculated and experimental values of the dimensionless growth coefficient for consecutive bubbles and these values are represented graphically in Figure 6.17 .

The greatest deviation between experimental and theoretical growth coefficient is in Set 15, carbon dioxide in glycerol, where the experimental value is 25% less than expected. It is not the error which is surprising but the agreement, considering the uncertainty of the solubility and diffusivity of carbon dioxide in glycerol. Where these figures are known accurately, for carbon dioxide - water and oxygen - water, the results are most encouraging. Only two bubbles out of the seventy examined show more than 20% deviation and inspection of Figure 6.17 shows that there does not appear to be any consistent direction to the deviation from the theory.

The following conclusions are drawn from the experiments:

(i) The Scriven function $\Phi\{\varepsilon,\beta\}$, calculated from the liquid and gas properties is accurate and reliable as a predictor of the dimensionless growth coefficient β . This has not been conclusively established previously.

(ii) The growth is well described by the parabolic law. This has never really been questioned except in some experiments in boiling.

(iii) The growth was in all cases steady, continuous and consistent. There were none of the alarming and unexplained discontinuities exhibited in previously reported results.

(iv) There was no consistent increase or decrease in growth coefficient from one bubble to the next; in fact it is surprising how consistent the results are within each set. The maximum deviations of β_{exp} from the mean are, for carbon dioxide - water, in Set 13 where for bubble 28, β is 5.1% greater than the mean; for oxygen - water in Set 14 where for bubble 1, β is 13.2% greater than the mean.

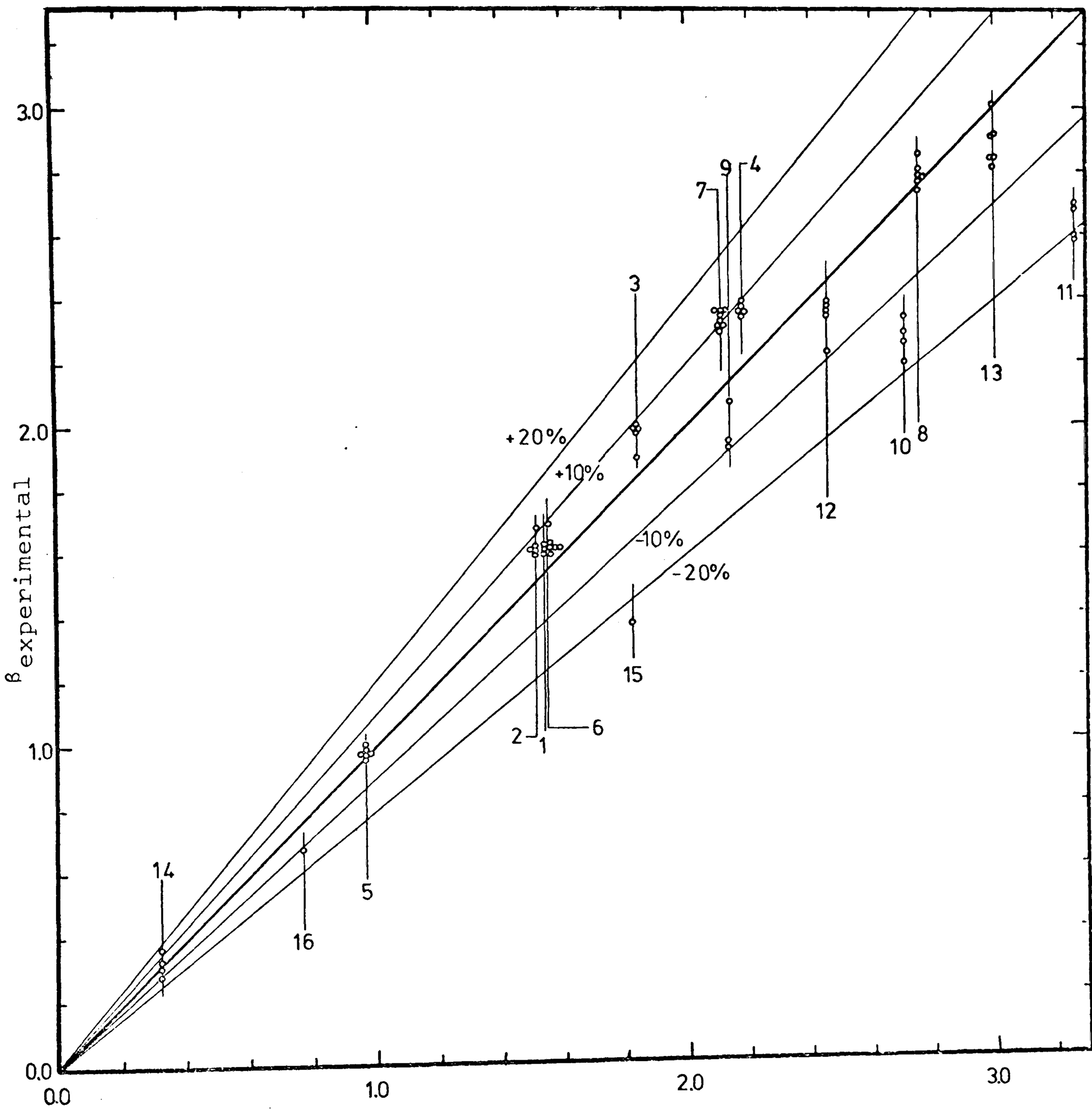
Table 6.4 Calculated and experimental values of the dimensionless growth coefficient for consecutive bubbles

Set	β		Set	β		Set	β	
	Calc.	Exp.		Calc.	Exp.		Calc.	Exp.
1	1.54	1.62	6	1.54	1.62	10	2.71	2.34
		1.61			1.62			2.29
		1.63			1.69			2.26
2	1.51	1.68			1.61			2.20
		1.62			1.61	11	3.27	2.68
		1.61			1.60			2.58
		1.60	7	2.12	2.35			2.59
		1.60			2.36			2.69
3	1.84	1.97			2.33	12	2.46	2.38
		1.99			2.36			2.37
		1.90			2.36			2.23
		2.02			2.31			2.36
		2.00			2.31			2.35
4	2.18	2.35			2.39	13	3.01	2.84 *
		2.37	8	2.75	2.86			2.91 *
		2.34			2.80			2.81 *
		2.40			2.79			2.84 *
		2.35			2.76			2.91 *
5	0.97	0.96			2.74			3.04 *
		0.97			2.68	14	0.32	0.36
		0.97	9	2.14	2.07			0.31
		0.98			1.93			0.32
		1.00			1.95			0.28
		0.98				15	1.83	1.38
						16	0.77	0.67

* Not consecutive bubbles: Bubble numbers 2,10,18,23,27,28.

Calculated values from 3.22, p 43.

Figure 6.17 Calculated and experimental values of the dimensionless growth coefficient



CHAPTER 7

CONCLUSIONS

The theoretical and experimental results have been discussed in detail in appropriate places in the text, see Sections 4.1.6, 4.2.6 and 6.4 .

In concluding, we may say that, for the theoretical study of bubble growth in power law liquids:

(i) The previously defined parameters G , V , ϕ , $\overline{B}$ and $\overline{Ja}$ are as useful in characterising the behaviour of bubbles in a power law liquid as in a newtonian liquid.

(ii) When $\overline{B} << 1$, the growth approaches limitation by diffusion only and there is no difference between bubble behaviour in newtonian and power law liquids.

(iii) When $\overline{B} >> 1$, the growth approaches limitation by hydrodynamic forces only and the rheological properties of the liquid begin to have a dominant effect. All else being equal, a bubble will grow more slowly in a power law liquid than in a newtonian liquid. The smaller the characteristic exponent of the power law liquid, the slower the growth.

(iv) When $\overline{B}$ is in the critical region, 0.1 to 10 , neither the diffusion limited solution nor the hydrodynamically limited solution are particularly accurate. The effect of the exponent in the power law solution is noticeable.

For the experimental study of gas bubbles evolving from supersaturated solutions:

(v) A parabolic law, radius proportional to the square root of time, is followed.

(vi) It has not been previously established conclusively that the constant of proportionality in the parabolic law is that given by Scrivens asymptotic solution. This has now been done.

(vii) Growth of bubbles can be expected to be steady and consistent and, within reasonable limits, show little effect of solute depletion.

(viii) In calculations for processes using growing bubbles, where their growth is limited by diffusion only, the Scriven solution may be used with confidence and accuracy.

APPENDICES

APPENDIX A.1

Table showing the relationship between the dimensionless growth coefficient, the Jakob number and the Sherwood number for an expanding bubble

Dimensionless Growth Coefficient β	Instantaneous Jakob number Ja	Instantaneous Sherwood number Sh
0.08	0.01120	2.286
0.10	0.01697	2.357
0.15	0.03546	2.538
0.2	0.05881	2.721
0.3	0.1166	3.087
0.4	0.1850	3.459
0.6	0.3420	4.211
0.8	0.5152	4.969
1.0	0.6977	5.733
1.5	1.175	7.660
2.0	1.668	9.592
3.0	2.671	13.48
4.0	3.683	17.38
6.0	5.719	25.18
8.0	7.760	32.99
10.0	9.803	40.80

APPENDIX A.2

Mass diffusivity in highly viscous newtonian liquids and in non-newtonian liquids.

The expression of Wilke and Chang (1955) has been widely used in predicting diffusivities of gases in newtonian liquids but has not been found entirely satisfactory for systems involving a small solute gas molecule such as hydrogen or helium or for systems having viscosities greater than a few centipoise. (Akgerman and Gainer (1972) proposed a new equation for these situations and claimed to be able to predict diffusivities more accurately in high viscosity solutes). The Wilke-Chang expression predicts that diffusivity is inversely proportional to viscosity, all else being equal. The experimental results of Astarita (1964) for the diffusivity of carbon dioxide in glycerol solutions, in the range 1 to 100 centipoise, showed that:

$$D \propto (\mu)^{-0.72}$$

Use of the Wilke-Chang expression would soon lead to serious error so the experimental results of Astarita (1964) were used in the present work although some extrapolation was necessary.

In the text, the equations for the growth of a gas bubble in a non-newtonian liquid were derived. In that derivation, it was assumed that the diffusivity coefficient of the gas in the liquid was constant. Now, a non-newtonian liquid is often a solution of a polymer and the apparent viscosity can change as a result of the polymer concentration

as well as the shear applied to a given solution. Osmers and Metzner (1972) and Astarita (1965) measured diffusivities in polymer solutions with different concentrations of polymer and found that in no case was the decrease in diffusivity as strong as the increase in apparent viscosity; in some cases the diffusivity even increased slightly with increasing apparent viscosity. Clough et al (1962) measured the effect of applied shear on the diffusivity in solutions of polymers and slurries and found that there was no significant change. It was concluded by all that the macroscopic viscosity is not a suitable index of resistance to the molecular motions of diffusion.

On the basis of the experimental evidence, it was concluded that the assumption of constant diffusivity made in Chapter 3 is justified.

APPENDIX A.3

Testing the computer programme DP01A.

DP01A is a Fortran Subroutine used for solving a linear parabolic partial differential equation. The manner in which this routine was used to solve the diffusion equation has already been described in the text. (See Section 4.2.2).

The routine was however first tested by using it to solve an equation with a known analytical solution. A suitable "known" equation is presented by Smith (1965), where both an analytical solution and numerical solutions, using various explicit and implicit methods of solution, are described and the results tabulated.

The equation is a simple one:

$$\frac{\partial U}{\partial t} = \frac{\partial^2 U}{\partial x^2} \qquad (A.3.1)$$

This is a dimensionless equation which represents the distribution of U (say, temperature) at a distance x from the end of a thin uniform rod after time t . If the initial distribution of U is:

$$\begin{aligned} U &= 2x && 0 \leq x \leq \tfrac{1}{2} : t = 0 \\ U &= 2(1 - x) && \tfrac{1}{2} \leq x \leq 1 : t = 0 \end{aligned} \qquad (A.3.2)$$

and the boundary conditions are:

$$\begin{aligned} U &= 0 && x = 0 : \text{all } t > 0 \\ U &= 0 && x = 1 : \text{all } t > 0 \end{aligned} \qquad (A.3.3)$$

then the analytical solution is known to be:

$$U = \frac{8}{\pi} \sum_{n=1}^{\infty} \frac{1}{n^2} (\sin\tfrac{1}{2}n\pi)(\sin n\pi x)\exp(-n^2\pi^2 t) \qquad (A.3.4)$$

Such an equation and set of initial conditions and boundary conditions provide a reasonable test because there is a discontinuity in the initial value of $\partial U/\partial x$, from +2 to -2 at $x = 0.5$. Comparison of the calculated U's will be made at $x = 0.5$.

Equations A.3.1, 2, 3 were prepared in the form required for routine DP01A and the equation solved with various time steps and with ten x-intervals in the range $0 \leqslant x \leqslant 1.0$.

The results of the investigation are tabulated in Table A.3.1 . Inspection of the table shows that the routine DP01A is indeed as accurate as the Crank-Nicolson implicit method of solution for similar time steps; both methods are computationally more rapid, and more accurate, than the explicit methods. The routine DP01A was thus confidently applied to the solution of the diffusion equation, subject of course to appropriate numerical experimentation to determine suitable step lengths and other factors pertinent to that particular equation.

Table A.3.1 Values of U at x = 0.5 for the solution of equations A.3.1,2,3 by various methods.

Time t	Analytical Solution	DP01A Δt = .001	DP01A Δt = .005	DP01A Δt = .01	Smith 1 Δt = .01	Smith 2 Δt = .001	Smith 3 Δt = .005
0.00	1.0000	1.0000	1.0000	1.0000	1.0000	1.0000	1.0000
0.01	.7743	.7853	.7842	.7700	.7691	.7687	.8000
0.02	.6809	.6873	.6874	.6904	.6921	.6981	.7000
0.10	.3021	.3047	.3049	.3050	.3069	.3056	.3071

Smith 1 : Crank-Nicolson Implicit Method

Smith 2 : Explicit method

Smith 3 : Explicit method

APPENDIX A.4

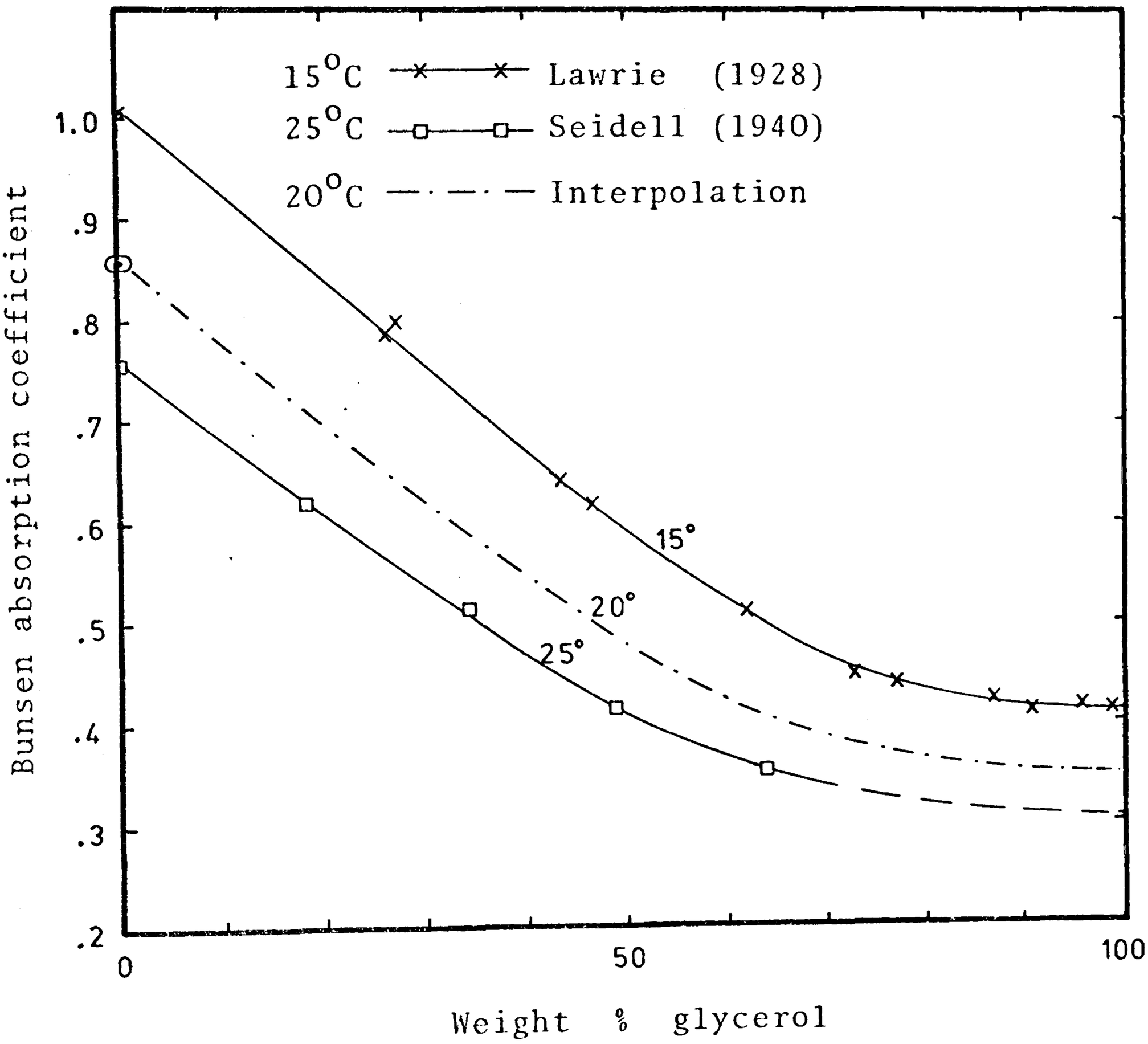
Solubility of carbon dioxide in glycerol solutions

Seidell's Data (1940)		Calculated from Seidell	
Moles glycerol per litre soln	Ostwald Coeff at 25°C	Weight % glycerol	Bunsen Coeff at 25°C
0.0	0.826	0.0	0.756
2.0	0.666	18.0	0.610
4.0	0.516	34.0	0.474
6.0	0.453	49.0	0.414
8.0	0.384	63.5	0.352

Lawrie's Data (1928)			
Weight % glycerol	Bunsen Coeff at 15°C	Weight % glycerol	Bunsen Coeff at 15°C
0.0	1.003	73.4	0.449
26.1	0.785	77.8	0.430
26.7	0.800	87.4	0.422
43.7	0.639	90.8	0.404
46.6	0.620	96.6	0.415
62.1	0.511	99.3	0.410

Houghton et al Data (1957)	
Temperature °C	Bunsen Coeff (pure water)
15	0.990
20	0.855
25	0.749

Figure A.4.1 Solubility of carbon dioxide in glycerol



APPENDIX A.5

Statistical analysis of data

A.5.1 The procedure of Law and Bailey (1965)

It has been necessary to fit different mathematical models to a large number of data to determine experimental parameters, for comparison with theoretical predictions. A usual approach is to apply a "least squares" method to the determination of the parameters. That is, the sum of squares of the deviations between the observed and predicted values is minimised by the appropriate choice of parameters in a given model.

The linear least squares regression regression is perhaps the most widely known statistical method. Even when the original equation to be fitted is non-linear, it is often possible to transform the variables to yield a linear form (Miller and Freund (1965)). However, an important model fitted in this work had the following non-linear form, (equation 6.3) :

$$R = 2\beta \sqrt{D}\,(t_e - t_o)^n \qquad (A.5.1)$$

where β , t_o and n had to be selected to minimise the sum of :

$$(R_{observed} - R_{predicted})^2$$

If the equation was transformed by taking the logarithm of both sides, the parameter t_o would still be included in a non-linear term. In addition, the transformation of variables automatically weights the data in some way. Taking the logarithm would lend increased importance to the smaller

values of the data. It was therefore decided to apply a non-linear regression technique, due to Law and Bailey (1963).

A computer programme (Program P3) was written to perform the non-linear least squares regression. A description of the method of Law and Bailey (1963) follows, along with the flowsheet presented in their paper.

Supposing we wish to fit an equation of the form:

$$Y_i = \Phi\{X_i, B_k\} \pm e_y \qquad (A.5.2)$$

where Y_i = the dependent variable

X_i = the independent variable

B_k = the unknown parameters

i = 1,2,.....,P P = the number of data points

k = 1.2,.....,m m = the number of parameters

e_y = experimental error in the Y_i, assumed normally distributed.

If Φ is a linear function, the parameters B_k can be determined by standard methods in one step; if Φ is non-linear, the best parameters must be found by iterative calculations.

In the function Φ is differentiable with respect to the parameters and if it is desired to seek an unrestricted minimum of the sums of squares of the deviations, then Law and Bailey show that m simultaneous equations can be obtained and represented in matrix from, for the j-th iteration as:

$$Z\,b = C \qquad (A.5.3)$$

where:

$$Z = \begin{bmatrix} \sum_{i=1}^{P} Z_1 Z_1 & \cdots & \sum_{i=1}^{P} Z_1 Z_m \\ \vdots & & \vdots \\ \sum_{i=1}^{P} Z_m Z_1 & \cdots & \sum_{i=1}^{P} Z_m Z_m \end{bmatrix} \qquad (A.5.4)$$

$$Z_k = \left(\frac{\partial \Phi}{\partial \beta_k} \right)_j \qquad (A.5.5)$$

$$b = \begin{bmatrix} \Delta B_1 \\ \vdots \\ \Delta B_m \end{bmatrix} \qquad (A.5.6)$$

$$\Delta B_k = (B_k)_{j+1} - (B_k)_j \qquad (A.5.7)$$

$$C = \begin{bmatrix} C_1 \\ \vdots \\ C_m \end{bmatrix} \qquad (A.5.8)$$

$$C_k = \left(\sum_{i=1}^{P} S_i Z_k \right)_j \qquad (A.5.9)$$

and

$$S_i = (Y_i - \Phi_i) \qquad (A.5.10)$$

From Equation A.5.3:

$$b = Z^{-1} C \qquad (A.5.11)$$

which enables the vector of ΔB's to be determined and thus, since $(B_k)_j$ is known, allows $(B_k)_{j+1}$ to be found. This new value can then be used in the next iteration until the

correction terms ΔB_k become negligibly small.

Law and Bailey then describe how convergence can be assured from any starting values of B_k , if there is a unique solution. They show that, if the corrections ΔB_k are restricted by a fraction α thus:

$$\Delta B_{kr} = \alpha(\Delta B_k) \qquad \text{(A.5.12)}$$

and if:

$$D_t = \sum_{k=1}^{m} D_k = \sum_{k=1}^{m} (\Delta B_k C_k) \qquad \text{(A.5.13)}$$

then:

$$\Delta S^2_{lr} = (2\alpha - \alpha^2) D_t \qquad \text{(A.5.14)}$$

where ΔS^2_{lr} is the change in the sum of squares for a linear function over the restricted range.

Defining:

$$\Delta S^2_{ar} = (S^2_a)_j - (S^2_{ar})_{j+1} \qquad \text{(A.5.15)}$$

= actual change in sum of squares for the restricted range

and $$\Delta S^2_a = (S^2_a)_j - (S^2_a)_{j+1} \qquad \text{(A.5.16)}$$

= actual change in sum of squares for the unrestricted range

where $$S^2_a = \sum_{i=1}^{P} (Y_i - \Phi_i)^2 = \sum_{i=1}^{P} S^2_i \qquad \text{(A.5.17)}$$

= actual sum of squares

and S^2_{ar} = actual sum of squares using the restricted parameters.

Finally, Law and Bailey state their convergence criteria:

1. D_t in equation A.5.13 must be positive. If it is negative, the signs of all the ΔB_k must be changed.
2. If ΔS_a^2 is positive, the unrestricted calculation is converging. If negative, it is diverging and the corrections must be restricted. However, the convergence may be slow. A criterion

$$\Delta S_{ar}^2 - \beta \Delta S_{lr}^2 \geq 0 \qquad \text{(A.5.18)}$$

ensures convergence and avoids a slow convergence.

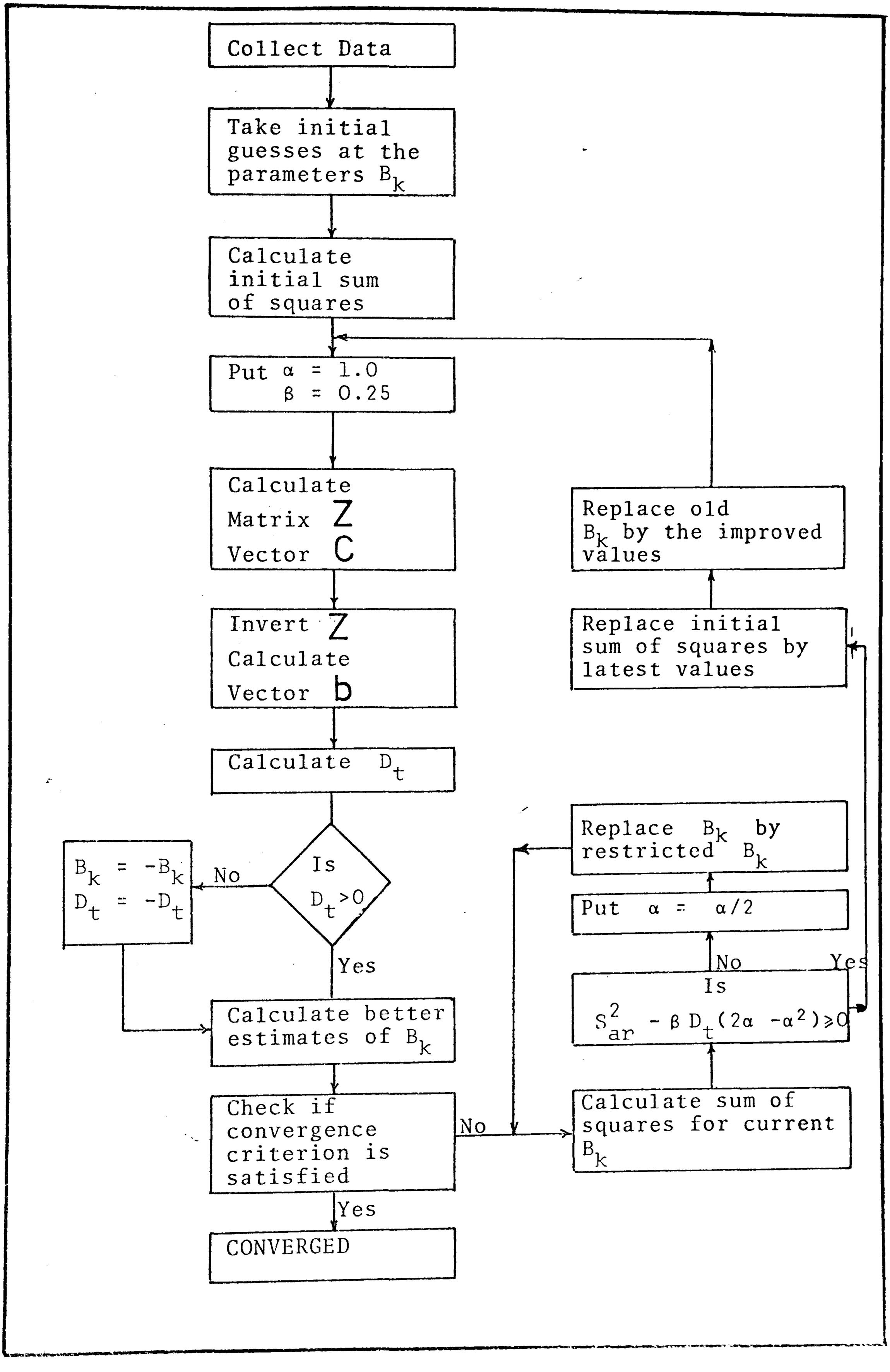
Law and Bailey recommend that divergent calculations be restricted by a successive halving of α until convergence is obtained, and that a suitable value for β in equation A.5.18 is 0.25.

The flow diagram for the procedure is shown as Figure A.5.1 and the computer programme is number P3. The nomenclature of Law and Bailey has been followed as closely as possible above and in the programme.

A.5.2 Using the computer programme

The above procedure was programmed in the FORTRAN IV language. The programme was in the form of a subroutine called BAILEY and information is passed to and from the subroutine by arguments. Because of the use of variable dimensions, any number of data points may be manipulated but, as written, the programme can handle up to only five parameters and five constants in the model fitted. Only DIMENSION statements must be altered to accommodate more than five parameters and constants. Labelled COMMON is used

Figure A.5.1 Flow diagram for the non-linear regression technique



within the routine in two blocks known as /LAWA/ and /LAWB/ . No blank COMMON is used.

Matrix inversion in the programme, required by equation A.5.11 , is performed by the algorithm of Crout, described by Lapidus (1962). This is a fairly suitable method if the matrix of Z's is likely to be dense and without zero elements on the principal diagonal.

Within the programme, a check is kept on the number of iterations made in both the unrestricted and restricted loops of Law and Bailey's method. If more than twenty iterations are needed, the programme is stopped. No more than five or six iterations have usually been found necessary to achieve the required convergence, provided that the starting values of the parameters are intelligent estimates and at least within an order of magnitude of the converged values.

A subroutine called MODEL must be supplied to give the values of the calculated Y_i's and the Z_k's for any required model.

The subroutine is called as follows:

```
CALL  BAILEY(Y,X,ND,B,TOL,NP,CON,YCAL)
```

where:

Y is a one dimensional array of the experimental values of the dependent variable,

X is a one dimensional array of the experimental values of the independent variable,

ND is the integer number of data points,

B is an array of the parameters. It contains the starting estimates on entry and is overwritten

on exit with the converged values,

TOL is an array of the relative (per unit) tolerances for each parameter, used as the convergence criteria,

NP is the integer number of parameters,

CON is an array of any constants used in the model,

YCAL is a one dimensional array, output from BAILEY, giving the calculated values of the dependent variable using the converged parameters.

The subroutine MODEL must be specified similarly:

```
SUBROUTINE  MODEL(I,Y,X,ND,CON,B)
```

where:

I represents the i-th data point

and other arguments are as above.

In subroutine MODEL the function:

$$Y_i = \Phi(X_i, B_k, CON_j)$$

and the derivatives:

$$Z_k = \frac{\partial \Phi}{\partial B_k} \qquad k = 1,2,.....,NP$$

must be written as:

$$PHI = (X_i, B_k, CON_j)$$

$$Z(1) = \frac{\partial \Phi}{\partial B_k}$$

$$\vdots$$

$$Z(k) = \frac{\partial \Phi}{\partial B_k}$$

and the results put in a labelled COMMON block:

```
COMMON /LAWA/ PHI,Z
```

APPENDIX A.6

Tables of experimental results

Time (secs)	Radius (mm)	Time (secs)	Radius (mm)	Time (secs)	Radius (mm)	Time (secs)	Radius (mm)
Set 1		78.0	.653	26.0	.501	104.0	.713
1/1		80.0	.675	28.0	.534	106.0	.732
2.0	.212	82.0	.701	30.0	.569	108.0	.761
4.0	.289	84.0	.736	32.0	.599	110.0	.787
6.0	.341	86.0	.752	34.0	.625	112.0	.813
8.0	.386	88.0	.788	36.0	.657	114.0	.839
10.0	.434	90.0	.810	38.0	.683	116.0	.856
12.0	.466	1/3		40.0	.706	118.0	.878
14.0	.502	108.0	.161	42.0	.729	120.0	.901
16.0	.527	110.0	.232	44.0	.761	122.0	.921
18.0	.563	112.0	.289	46.0	.787	124.0	.953
20.0	.588	114.0	.341	48.0	.804	126.0	.976
22.0	.617	116.0	.392	50.0	.826	2/3	
24.0	.653	118.0	.424	52.0	.856	140.0	.153
26.0	.679	120.0	.460	54.0	.875	142.0	.228
28.0	.698	122.0	.495	56.0	.895	144.0	.277
30.0	.724	124.0	.527	58.0	.921	146.0	.332
32.0	.756	126.0	.560	60.0	.947	148.0	.374
34.0	.775	128.0	.585	62.0	.976	150.0	.413
36.0	.797	130.0	.624	2/2		152.0	.456
38.0	.817	132.0	.653	74.0	.137	154.0	.488
40.0	.852	134.0	.682	76.0	.208	156.0	.524
1/2		136.0	.704	78.0	.270	158.0	.550
54.0	.167	138.0	.733	80.0	.319	160.0	.579
56.0	.238	140.0	.756	82.0	.368	162.0	.605
58.0	.296	142.0	.788	84.0	.407	164.0	.631
60.0	.347	144.0	.807	86.0	.446	166.0	.664
62.0	.386	146.0	.836	88.0	.482	168.0	.693
64.0	.428	148.0	.862	90.0	.514	170.0	.709
66.0	.466	Set 2		92.0	.543	172.0	.735
68.0	.498	2/1		94.0	.576	174.0	.761
70.0	.531	18.0	.293	96.0	.602	176.0	.787
72.0	.560	20.0	.374	98.0	.631	178.0	.810
74.0	.588	22.0	.420	100.0	.660	180.0	.833
76.0	.624	24.0	.459	102.0	.683	182.0	.859

Time (secs)	Radius (mm)	Time (secs)	Radius (mm)	Time (secs)	Radius (mm)	Time (secs)	Radius (mm)
184.0	.882	2/5		22.0	.487	108.0	.428
186.0	.901	274.0	.150	24.0	.537	110.0	.484
188.0	.921	276.0	.218	26.0	.583	112.0	.534
190.0	.944	278.0	.273	28.0	.632	114.0	.586
192.0	.976	280.0	.325	30.0	.675	116.0	.619
2/4		282.0	.374	32.0	.711	118.0	.665
206.0	.153	284.0	.413	34.0	.741	120.0	.702
208.0	.218	286.0	.449	36.0	.781	122.0	.741
210.0	.280	288.0	.485	38.0	.817	124.0	.777
212.0	.332	290.0	.511	40.0	.853	126.0	.810
214.0	.374	292.0	.537	42.0	.883	128.0	.843
216.0	.413	294.0	.569	44.0	.919	130.0	.873
218.0	.452	296.0	.595	46.0	.949	132.0	.906
220.0	.488	298.0	.628	3/2		134.0	.952
222.0	.514	300.0	.651	58.0	.231	3/4	
224.0	.547	302.0	.680	60.0	.323	146.0	.198
226.0	.576	304.0	.706	62.0	.389	148.0	.277
228.0	.602	306.0	.729	64.0	.451	150.0	.352
230.0	.634	308.0	.752	66.0	.501	152.0	.415
232.0	.657	310.0	.781	68.0	.553	154.0	.474
234.0	.687	312.0	.800	70.0	.593	156.0	.520
236.0	.713	314.0	.826	72.0	.636	158.0	.567
238.0	.739	316.0	.843	74.0	.678	160.0	.609
240.0	.765	318.0	.872	76.0	.715	162.0	.659
242.0	.787	320.0	.901	78.0	.751	164.0	.698
244.0	.810	322.0	.914	80.0	.787	166.0	.731
246.0	.830	324.0	.944	82.0	.823	168.0	.767
248.0	.852	326.0	.970	84.0	.850	170.0	.804
250.0	.875	Set 3		86.0	.886	172.0	.846
252.0	.888	3/1		88.0	.912	174.0	.886
254.0	.908	12.0	.138	90.0	.949	176.0	.916
256.0	.934	14.0	.237	3/3		178.0	.952
258.0	.947	16.0	.313	102.0	.207	180.0	.985
260.0	.970	18.0	.382	104.0	.296	3/5	
		20.0	.441	106.0	.375	192.0	.214

Time (secs)	Radius (mm)	Time (secs)	Radius (mm)	Time (secs)	Radius (mm)	Time (secs)	Radius (mm)
194.0	.300	50.0	.428	128.0	.856	40.0	.442
196.0	.372	52.0	.501	130.0	.899	42.0	.455
198.0	.441	54.0	.573	132.0	.942	44.0	.468
200.0	.487	56.0	.626	134.0	.988	46.0	.488
202.0	.534	58.0	.685	4/5		48.0	.498
204.0	.576	60.0	.744	142.0	.231	50.0	.511
206.0	.619	62.0	.790	144.0	.339	52.0	.524
208.0	.662	64.0	.843	146.0	.428	5/2	
210.0	.705	66.0	.886	148.0	.504	112.0	.100
212.0	.741	68.0	.929	150.0	.563	114.0	.139
214.0	.784	70.0	.972	152.0	.619	116.0	.173
216.0	.817	4/3		154.0	.738	118.0	.202
218.0	.850	78.0	.250	156.0	.787	120.0	.229
220.0	.876	80.0	.362	158.0	.830	122.0	.252
222.0	.909	82.0	.445	160.0	.876	124.0	.279
224.0	.939	84.0	.511	162.0	.929	126.0	.299
226.0	.978	86.0	.576	164.0	.962	128.0	.319
Set 4		88.0	.639	Set 5		130.0	.339
4/1		90.0	.688	5/1		132.0	.359
12.0	.214	92.0	.751	8.0	.083	134.0	.378
14.0	.343	94.0	.797	10.0	.123	136.0	.395
16.0	.435	96.0	.840	12.0	.159	138.0	.408
18.0	.507	98.0	.879	14.0	.189	140.0	.422
20.0	.570	100.0	.929	16.0	.219	142.0	.438
22.0	.636	102.0	.965	18.0	.246	144.0	.448
24.0	.688	4/4		20.0	.266	146.0	.465
26.0	.744	110.0	.254	22.0	.292	148.0	.478
28.0	.794	112.0	.359	24.0	.309	150.0	.491
30.0	.840	114.0	.448	26.0	.332	152.0	.505
32.0	.883	116.0	.517	28.0	.349	154.0	.518
34.0	.919	118.0	.583	30.0	.365	5/3	
36.0	.955	120.0	.642	32.0	.385	214.0	.073
4/2		122.0	.705	34.0	.402	216.0	.116
46.0	.231	124.0	.754	36.0	.418	218.0	.153
48.0	.346	126.0	.807	38.0	.428	220.0	.186

Time (secs)	Radius (mm)	Time (secs)	Radius (mm)	Time (secs)	Radius (mm)	Time (secs)	Radius (mm)
222.0	.212	350.0	.455	530.0	.292	84.0	.793
224.0	.239	352.0	.471	532.0	.312	86.0	.823
226.0	.266	354.0	.485	534.0	.332	88.0	.846
228.0	.285	356.0	.498	536.0	.352	6/2	
230.0	.309	358.0	.511	538.0	.375	100.0	.166
232.0	.332	5/5		540.0	.392	1o2.0	.239
234.0	.345	418.0	.093	542.0	.405	104.0	.299
236.0	.365	420.0	.136	544.0	.418	106.0	.345
238.0	.382	422.0	.169	546.0	.435	108.0	.392
240.0	.402	424.0	.202	548.0	.451	110.0	.425
242.0	.415	426.0	.232	550.0	.465	112.0	.465
244.0	.432	428.0	.256	552.0	.478	114.0	.498
246.0	.445	430.0	.282	554.0	.491	116.0	.531
248.0	.458	432.0	.302	556.0	.511	118.0	.564
250.0	.475	434.0	.325	558.0	.521	120.0	.591
252.0	.488	436.0	.345	Set 6		122.0	.624
254.0	.498	438.0	.362	6/1		124.0	.654
256.0	.511	440.0	.382	48.0	.113	126.0	.677
5/4		442.0	.402	50.0	.199	128.0	.707
318.0	.106	444.0	.418	52.0	.266	130.0	.730
320.0	.146	446.0	.432	54.0	.315	132.0	.760
322.0	.179	448.0	.451	56.0	.365	134.0	.780
324.0	.209	450.0	.465	58.0	.408	136.0	.807
326.0	.232	452.0	.478	60.0	.448	138.0	.830
328.0	.259	454.0	.495	62.0	.481	140.0	.853
330.0	.279	456.0	.508	64.0	.518	6/3	
332.0	.299	458.0	.521	66.0	.548	150.0	.110
334.0	.325	5/6		68.0	.578	152.0	.199
336.0	.345	516.0	.073	70.0	.607	154.0	.266
338.0	.365	518.0	.113	72.0	.637	156.0	.312
340.0	.378	520.0	.156	74.0	.671	158.0	.339
342.0	.395	522.0	.186	76.0	.694	160.0	.418
344.0	.412	524.0	.219	78.0	.727	162.0	.471
346.0	.425	526.0	.246	80.0	.750	164.0	.505
348.0	.442	528.0	.269	82.0	.770	166.0	.541

Time (secs)	Radius (mm)	Time (secs)	Radius (mm)	Time (secs)	Radius (mm)	Time (secs)	Radius (mm)
168.0	.574	6/5		324.0	.591	78.0	.828
170.0	.607	250.0	.120	326.0	.617	80.0	.871
172.0	.644	252.0	.206	328.0	.654	7/3	
174.0	.667	254.0	.272	330.0	.684	86.0	.080
176.0	.697	256.0	.319	332.0	.710	88.0	.239
178.0	.727	258.0	.372	334.0	.734	90.0	.349
180.0	.754	260.0	.408	336.0	.760	92.0	.432
182.0	.783	262.0	.445	338.0	.783	94.0	.509
184.0	.800	264.0	.478	340.0	.803	96.0	.572
186.0	.823	266.0	.511	342.0	.830	98.0	.632
188.0	.853	268.0	.544	344.0	.853	100.0	.691
6/4		270.0	.574	Set 7		102.0	.748
198.0	.120	272.0	.601	7/1		104.0	.794
200.0	.209	274.0	.641	32.0	.106	106.0	.844
202.0	.269	276.0	.664	34.0	.259	108.0	.887
204.0	.319	278.0	.694	36.0	.372	7/4	
206.0	.372	280.0	.720	38.0	.452	114.0	.126
208.0	.408	282.0	.744	40.0	.525	116.0	.239
210.0	.445	284.0	.770	42.0	.588	118.0	.372
212.0	.478	286.0	.800	44.0	.645	120.0	.455
214.0	.511	288.0	.817	46.0	.705	122.0	.519
216.0	.544	290.0	.837	48.0	.758	124.0	.578
218.0	.574	292.0	.866	50.0	.808	126.0	.648
220.0	.604	6/6		52.0	.854	128.0	.705
222.0	.644	302.0	.093	54.0	.904	130.0	.758
224.0	.667	304.0	.179	7/2		132.0	.801
226.0	.697	306.0	.246	60.0	.170	134.0	.851
228.0	.724	308.0	.312	62.0	.299	136.0	.901
230.0	.750	310.0	.352	64.0	.396	7/5	
232.0	.770	312.0	.398	66.0	.472	142.0	.160
234.0	.793	314.0	.432	68.0	.545	144.0	.299
236.0	.813	316.0	.468	70.0	.612	146.0	.392
238.0	.837	318.0	.501	72.0	.668	148.0	.475
240.0	.866	320.0	.531	74.0	.728	150.0	.542
		322.0	.561	76.0	.774	152.0	.602

Time (secs)	Radius (mm)	Time (secs)	Radius (mm)	Time (secs)	Radius (mm)	Time (secs)	Radius (mm)
154.0	.658	232.0	.442	70.0	.866	16.25	.633
156.0	.721	234.0	.512	8/4		17.50	.666
158.0	.768	236.0	.578	76.0	.232	18.75	.686
160.0	.814	238.0	.638	78.0	.378	20.00	.713
162.0	.868	240.0	.691	80.0	.451	21.25	.739
164.0	.931	242.0	.741	82.0	.578	22.50	.759
7/6		244.0	.791	84.0	.661	23.75	.782
170.0	.179	246.0	.831	86.0	.734	25.00	.802
172.0	.309	248.0	.877	88.0	.800	26.25	.821
174.0	.392	Set 8		90.0	.860	27.50	.844
176.0	.475	8/1		8/5		28.75	.864
178.0	.538	18.0	.202	96.0	.186	30.00	.891
180.0	.595	20.0	.375	98.0	.349	9/2	
182.0	.658	22.0	.495	100.0	.461	34.75	.096
184.0	.715	24.0	.598	102.0	.551	35.25	.132
186.0	.768	26.0	.677	104.0	.637	35.75	.165
188.0	.814	28.0	.754	106.0	.714	36.25	.191
190.0	.854	30.0	.827	108.0	.783	36.75	.218
192.0	.894	32.0	.886	110.0	.853	37.25	.244
7/7		8/2		8/6		37.75	.264
198.0	.143	36.0	.169	116.0	.083	38.25	.287
200.0	.283	38.0	.345	118.0	.289	38.75	.310
202.0	.382	40.0	.461	120.0	.412	39.25	.327
204.0	.455	42.0	.558	122.0	.511	39.75	.343
206.0	.525	44.0	.644	124.0	.591	40.25	.356
208.0	.582	46.0	.730	126.0	.677	40.75	.376
210.0	.651	48.0	.800	128.0	.747	41.25	.389
212.0	.705	50.0	.863	130.0	.810	41.75	.406
214.0	.755	8/3		132.0	.866	42.25	.419
216.0	.801	56.0	.212	Set 9		42.75	.435
218.0	.848	58.0	.368	9/1		43.25	.449
220.0	.891	60.0	.481	10.00	.465	43.75	.462
7/8		62.0	.578	11.25	.505	44.50	.482
226.0	.113	64.0	.657	12.50	.538	45.25	.498
228.0	.259	66.0	.737	13.75	.571	46.00	.518
230.0	.366	68.0	.807	15.00	.604	46.75	.534

Time (secs)	Radius (mm)	Time (secs)	Radius (mm)	Time (secs)	Radius (mm)	Time (secs)	Radius (mm)
47.50	.544	76.50	.376	4.50	.219	10/2	
48.25	.564	77.00	.396	5.00	.259	29.38	.086
49.00	.581	77.50	.409	5.50	.289	29.87	.139
49.75	.600	78.00	.419	6.00	.315	30.37	.182
50.50	.617	78.50	.439	6.50	.342	30.87	.219
51.25	.633	79.00	.449	7.00	.371	31.37	.252
52.00	.647	79.75	.475	7.50	.391	31.88	.282
52.75	.666	80.50	.488	8.00	.411	32.37	.308
53.50	.676	81.25	.508	8.50	.434	32.87	.332
54.25	.693	82.00	.528	8.00	.454	33.37	.352
55.00	.706	82.75	.541	9.50	.474	33.87	.378
55.75	.722	83.50	.561	10.00	.491	34.38	.395
56.50	.736	84.25	.574	10.50	.507	34.87	.418
57.25	.746	85.00	.587	11.00	.521	35.37	.438
58.00	.759	85.75	.607	11.50	.541	35.87	.458
58.75	.772	86.50	.630	12.00	.554	36.37	.471
60.00	.795	87.25	.647	12.50	.570	36.88	.481
61.25	.818	88.00	.660	13.00	.587	37.37	.407
62.50	.838	88.75	.676	13.75	.610	37.87	.524
63.75	.858	89.50	.693	14.50	.637	38.37	.541
65.00	.877	90.25	.706	15.25	.657	38.87	.554
66.25	.901	91.00	.719	16.00	.683	39.37	.574
9/3		92.25	.749	16.75	.703	40.12	.590
70.50	.099	93.50	.769	17.50	.726	40.87	.620
71.00	.132	94.75	.792	18.25	.743	41.62	.647
71.50	.165	96.00	.808	19.00	.763	42.37	.667
72.00	.191	97.25	.835	19.75	.786	43.13	.687
72.50	.218	98.50	.854	20.50	.803	43.87	.710
73.00	.244	99.75	.881	21.25	.816	44.62	.726
73.50	.270	101.00	.897	22.00	.836	45.37	.746
74.00	.290	Set 10		22.75	.856	46.12	.766
74.50	.307	10/1		23.50	.866	46.88	.786
75.00	.327	3.00	.090	24.25	.885	47.62	.799
75.50	.343	3.50	.143	25.00	.902	48.37	.819
76.00	.363	4.00	.186			49.12	.832

Time (secs)	Radius (mm)	Time (secs)	Radius (mm)	Time (secs)	Radius (mm)	Time (secs)	Radius (mm)
49.87	.856	73.75	.773	98.62	.677	20.0	.737
50.63	.866	74.50	.793	99.38	.693	20.5	.757
51.37	.892	75.25	.803	100.12	.716	21.0	.773
52.12	.909	76.00	.822	100.87	.733	21.5	.793
10/3		76.75	.842	101.62	.756	22.0	.810
56.25	.073	77.50	.856	102.37	.769	22.5	.826
56.75	.116	78.25	.872	103.13	.789	23.0	.840
57.25	.159	79.00	.892	103.87	.806	23.5	.856
57.75	.199	10/4		104.62	.829	24.0	.873
58.25	.232	84.12	.080	105.37	.846	24.5	.889
58.75	.262	84.62	.126	Set 11		24.87	.899
59.25	.289	85.12	.169	11/1		11/2	
59.75	.318	85.63	.202	8.5	.093	27.5	.063
60.25	.342	86.12	.235	9.0	.163	28.0	.123
60.75	.365	86.62	.262	9.5	.216	28.5	.183
61.25	.385	87.12	.289	10.0	.259	29.0	.229
61.75	.405	87.62	.312	10.5	.299	29.5	.275
62.25	.425	88.13	.338	11.0	.335	30.0	.309
62.75	.444	88.62	.358	11.5	.365	30.5	.342
63.25	.464	89.12	.378	12.0	.395	31.0	.375
63.75	.481	89.62	.401	12.5	.421	31.5	.402
64.25	.497	90.12	.421	13.0	.448	32.0	.425
64.75	.507	90.63	.438	13.5	.478	32.5	.445
65.25	.524	91.12	.454	14.0	.491	33.0	.471
65.75	.544	91.62	.474	14.5	.511	33.5	.491
66.25	.557	92.12	.491	15.0	.534	34.0	.514
67.00	.580	92.62	.501	15.5	.551	34.5	.531
67.75	.607	93.13	.521	16.0	.571	35.0	.554
68.50	.630	93.62	.534	16.5	.591	35.5	.574
69.25	.650	94.12	.554	17.0	.614	36.0	.594
70.00	.673	94.87	.567	17.5	.631	36.5	.617
70.75	.693	95.63	.594	18.0	.650	37.0	.631
71.50	.713	96.37	.614	18.5	.677	37.5	.650
72.25	.736	97.37	.630	19.0	.700	38.0	.670
73.00	.756	97.87	.653	19.5	.717	38.5	.687

Time (secs)	Radius (mm)	Time (secs)	Radius (mm)	Time (secs)	Radius (mm)	Time (secs)	Radius (mm)
39.0	.700	58.75	.657	78.75	.640	33.75	.649
39.5	.720	59.25	.674	79.25	.654	34.25	.664
40.0	.733	59.75	.687	79.75	.680	34.75	.679
40.5	.747	60.25	.704	80.25	.697	35.25	.694
41.0	.767	60.75	.723	80.75	.713	35.75	.709
41.5	.780	61.25	.740	81.25	.730	36.12	.718
42.0	.796	61.75	.750	81.75	.743	12/2	
42.5	.806	62.25	.770	82.25	.760	64.75	.175
43.0	.823	62.75	.786	82.75	.780	65.25	.211
43.5	.836	63.25	.793	83.25	.796	65.75	.241
44.0	.850	63.75	.816	83.75	.806	66.25	.272
44.5	.860	64.25	.830	84.25	.823	66.75	.302
45.0	.876	64.75	.843	84.50	.830	67.25	.323
45.5	.889	65.25	.856	Set 12		67.75	.347
45.87	.899	65.75	.869	12/1		68.25	.371
11/3		66.25	.886	23.25	.169	68.75	.395
48.75	.070	66.88	.903	23.75	.214	69.25	.411
49.25	.129	11/4		24.25	.244	69.75	.435
49.75	.186	69.75	.070	24.75	.278	70.25	.456
50.25	.226	70.25	.123	25.25	.296	70.75	.477
50.75	.275	70.75	.176	25.75	.329	71.25	.504
51.25	.305	71.25	.219	26.25	.356	71.75	.522
51.75	.338	71.75	.256	26.75	.377	72.25	.537
52.25	.368	72.25	.292	27.25	.404	72.75	.555
52.75	.392	72.75	.325	27.75	.426	73.25	.580
53.25	.418	73.25	.358	28.25	.444	73.75	.595
53.75	.441	73.75	.385	28.75	.471	74.25	.616
54.25	.468	74.25	.418	29.25	.492	74.75	.634
54.75	.491	74.75	.445	29.75	.513	75.25	.649
55.25	.508	75.25	.475	30.25	.534	75.75	.664
55.75	.534	75.75	.489	30.75	.552	76.25	.685
56.25	.551	76.25	.524	31.25	.567	76.75	.697
56.75	.574	76.75	.544	31.75	.589	77.25	.721
57.25	.597	77.25	.564	32.25	.607	77.75	.736
57.75	.617	77.75	.587	32.75	.622	12/3	
58.25	.637	78.25	.617	33.25	.634	104.0	.163

Time (secs)	Radius (mm)	Time (secs)	Radius (mm)	Time (secs)	Radius (mm)	Time (secs)	Radius (mm)
104.5	.202	148.0	.401	193.0	.555	13/10	
105.0	.235	148.5	.426	193.5	.574	31.50	.084
105.5	.263	149.0	.447	194.0	.592	31.62	.111
106.0	.293	149.5	.465	194.5	.610	31.75	.135
106.5	.320	150.0	.489	195.0	.625	31.88	.159
107.0	.344	150.5	.504	195.5	.640	32.00	.177
107.5	.362	151.0	.522	196.0	.655	32.13	.195
108.0	.386	151.5	.540	196.5	.673	32.25	.213
108.5	.404	152.0	.555	197.0	.691	32.37	.231
109.0	.426	152.5	.574	197.37	.697	32.50	.246
109.5	.444	153.0	.592	Set 13		32.63	.264
110.0	.465	153.5	.610	13/2		32.75	.279
110.5	.483	154.0	.622	4.75	.090	32.87	.291
111.0	.490	154.5	.640	4.88	.114	33.00	.306
111.5	.513	155.0	.652	5.00	.132	13/18	
112.0	.531	155.5	.661	5.13	.153	20.25	.087
112.5	.546	156.0	.679	5.25	.174	20.37	.108
113.0	.561	156.62	.694	5.38	.189	20.50	.132
113.5	.577	12/5		5.50	.204	20.63	.153
114.0	.592	185.0	.169	5.63	.219	20.75	.168
114.5	.610	185.5	.205	5.75	.234	20.88	.186
115.0	.625	186.0	.241	5.88	.249	21.00	.204
115.5	.640	186.5	.275	6.00	.261	21.12	.219
116.0	.652	187.0	.305	6.13	.276	21.25	.231
116.5	.667	187.5	.332	6.25	.291	21.38	.246
117.0	.679	188.0	.356	6.38	.303	21.50	.261
117.5	.694	188.5	.380	6.50	.315	21.62	.276
12/4		189.0	.404	6.63	.627	21.75	.288
144.5	.193	189.5	.426	6.75	.340	21.88	.303
145.0	.229	190.0	.447	6.88	.349	22.00	.312
145.5	.272	190.5	.465	7.00	.358	22.13	.324
146.0	.299	191.0	.483	7.13	.370	22.25	.337
146.5	.332	191.5	.501	7.25	.382	22.37	.346
147.0	.353	192.0	.525	7.38	.388	22.50	.355
147.5	.380	192.5	.540			22.63	.364

Time (secs)	Radius (mm)	Time (secs)	Radius (mm)	Time (secs)	Radius (mm)	Time (secs)	Radius (mm)
22.75	.376	54.00	.192	20.0	.214	440.0	.681
13/23		54.12	.210	30.0	.229	458.0	.697
35.50	.084	54.25	.228	40.0	.249	14/2	
35.63	.108	54.38	.240	50.0	.265	532.0	.034
35.75	.132	54.50	.258	60.0	.284	540.0	.070
35.88	.150	54.63	.276	70.0	.299	550.0	.099
36.00	.168	54.75	.288	80.0	.321	560.0	.127
36.12	.186	54.87	.306	90.0	.340	570.0	.150
36.25	.201	55.00	.315	100.0	.355	580.0	.170
36.38	.219	55.13	.327	110.0	.370	590.0	.189
36.50	.231	55.25	.340	120.0	.386	600.0	.204
36.62	.249	55.37	.352	130.0	.404	610.0	.222
36.75	.261	55.50	.361	140.0	.417	620.0	.240
36.88	.273	55.63	.373	150.0	.432	630.0	.260
37.00	.285	55.75	.382	160.0	.443	640.0	.273
37.13	.300	13/28		170.0	.454	650.0	.286
37.25	.309	59.63	.129	180.0	.465	660.0	.300
37.37	.321	59.75	.150	190.0	.480	670.0	.311
37.50	.334	59.87	.174	200.0	.493	680.0	.323
37.63	.343	60.00	.192	210.0	.502	690.0	.331
37.75	.355	60.13	.213	220.0	.512	700.0	.344
37.87	.364	60.25	.228	230.0	.521	710.0	.355
38.00	.376	60.37	.243	240.0	.534	720.0	.368
38.13	.385	60.50	.258	250.0	.545	730.0	.382
38.25	.397	60.63	.276	260.0	.555	740.0	.391
38.38	.403	60.75	.288	270.0	.562	750.0	.403
38.50	.412	60.88	.303	280.0	.571	760.0	.413
38.62	.421	61.00	.315	290.0	.581	770.0	.422
38.75	.427	61.12	.327	300.0	.588	780.0	.432
13/27		61.25	.337	320.0	.605	790.0	.441
53.38	.102	61.38	.349	340.0	.618	800.0	.453
53.50	.123	61.50	.364	360.0	.633	820.0	.462
53.62	.141	61.62	.376	380.0	.644	840.0	.489
53.75	.156	Set 14		400.0	.659	860.0	.505
53.88	.174	14/1		420.0	.671	880.0	.517

Time (secs)	Radius (mm)	Time (secs)	Radius (mm)	Time (secs)	Radius (mm)	Time (secs)	Radius (mm)
900.0	.533	1450.0	.462	1950.0	.360	150.0	.141
920.0	.547	1460.0	.469	1960.0	.373	Set 16	
940.0	.463	1480.0	.488	1970.0	.383	5.88	.011
970.0	.589	1500.0	.507	1980.0	.390	6.38	.013
1000.0	.608	1520.0	.532	1990.0	.402	6.88	.014
1030.0	.628	1540.0	.553	Set 15		7.38	.015
1060.0	.651	1560.0	.570	5.0	.024	7.88	.016
1090.0	.663	1580.0	.588	10.0	.036	8.38	.018
1120.0	.686	1600.0	.609	15.0	.045	8.88	.019
14/3		1620.0	.621	20.0	.055	9.38	.019
1190.0	.042	1640.0	.633	25.0	.064	9.88	.020
1200.0	.079	1660.0	.651	30.0	.068	10.37	.021
1220.0	.137	1676.0	.658	35.0	.077	10.87	.023
1230.0	.161	14/4		40.0	.077	11.37	.021
1240.0	.186	1744.0	.034	45.0	.084	11.87	.022
1250.0	.206	1750.0	.059	50.0	.087	12.50	.024
1260.0	.232	1760.0	.085	55.0	.089	14.37	.028
1270.0	.249	1770.0	.110	60.0	.095	16.25	.031
1280.0	.263	1780.0	.131	65.0	.099	18.75	.033
1290.0	.280	1790.0	.149	70.0	.100	21.25	.037
1300.0	.293	1800.0	.167	75.0	.105	23.75	.040
1310.0	.308	1810.0	.183	80.0	.107	26.25	.041
1320.0	.322	1820.0	.202	85.0	.109	28.75	.045
1330.0	.334	1830.0	.220	90.0	.111	31.25	.041
1340.0	.346	1840.0	.235	95.0	.116	33.75	.050
1350.0	.359	1850.0	.251	100.0	.115	36.25	.052
1360.0	.370	1860.0	.262	105.0	.119	38.75	.054
1370.0	.380	1870.0	.276	110.0	.123	41.25	.055
1380.0	.392	1880.0	.288	115.0	.124	43.75	.055
1390.0	.402	1890.0	.298	120.0	.128	46.25	.058
1400.0	.412	1900.0	.308	125.0	.128	51.25	.061
1410.0	.423	1910.0	.317	130.0	.131	56.25	.064
1420.0	.434	1920.0	.329	135.0	.136	61.25	.067
1430.0	.447	1930.0	.338	140.0	.139	66.25	.071
1440.0	.452	1940.0	.349	145.0	.143	107.0	.093

COMPUTER PROGRAMMES

Programs P 1

Solution of the hydrodynamically limited bubble growth equations

```
      PROGRAM NEWT   (INPUT,OUTPUT,TAPE5=INPUT,TAPE6=OUTPUT)
C**   NEWTONIAN FLUID
C**   INTEGRATING THE EQUATION WITH SUITABLE STEP LENGTH
      COMMON /CMNN/ P,S,PL
      READ(5,2000) NRESULT
      DO 100 NRES=1,NRESULT
      READ(5,2001) P,S,H
      PL = 1.0
      WRITE(6,1001)
      WRITE(6,1005)
      WRITE(6,1000)
      WRITE(6,1002)
      WRITE(6,1003) P,S,H
      WRITE(6,1004)
      CALL RUNKUT(H)
      WRITE(6,1005)
  100 CONTINUE
 1000 FORMAT(     10X,'DIFFUSIONAL BUBBLE GROWTH LIMITED BY HYDRODYNAMI
     1FORCES'/)
 1001 FORMAT(1H1)
 1002 FORMAT(10X,'NEWTONIAN FLUID'/)
 1003 FORMAT(10X,'SURFACE TENSION PARAMETER 9',F6.3/
     1        10X,'VISCOUS/INERTIA PARAMETER 9',F6.3/
     2        10X,'ITERATION STEP LENGTH(DT) 9',F6.3/)
 1004 FORMAT( 9X,5(3X,'T',5X,'A',4X)/)
 1005 FORMAT(//////////)
 2000 FORMAT(I5)
 2001 FORMAT(3F10.5)
      STOP
      END
```

```
      FUNCTION F(T,A,DA)
C**
C**   THIS IS THE HYDRODYNAMICALLY LIMITED EQUATION
C**   FOR A NEWTONIAN FLUID
C**
      COMMON /CMNN/ P,S,PL
      T1 = 1.5*(1.0-P/A)
      T2 = 1.5*DA*DA
      T3 = (SQRT(24.0)*S*DA)/A
      F  = (T1-T2-T3)/A
      RETURN
      END
```

```
      PROGRAM POWLAW(INPUT,OUTPUT,TAPE5=INPUT,TAPE6=OUTPUT)
C**   POWER LAW FLUID
C**   INTEGRATING THE EQUATION WITH SUITABLE STEP LENGTH
      COMMON /CMNN/ P,S,PL
      READ(5,2000) NRESULT
      DO 100 NRES=1,NRESULT
      READ(5,2001) PL,P,S,H
      WRITE(6,1001)
      WRITE(6,1005)
      WRITE(6,1000)
      WRITE(6,1002) PL
      WRITE(6,1003) P,S,H
      WRITE(6,1004)
      CALL RUNKUT(H)
      WRITE(6,1005)
  100 CONTINUE
 1000 FORMAT(     10X,'DIFFUSIONAL BUBBLE GROWTH LIMITED BY HYDRODYNAMI(
     1FORCES'/)
 1001 FORMAT(1H1)
 1002 FORMAT(10X,'POWER LAW FLUID  EXPONENT 9',F6.3/)
 1003 FORMAT(10X,'SURFACE TENSION PARAMETER 9',F6.3/
     1       10X,'VISCOUS/INERTIA PARAMETER 9',F6.3/
     2       10X,'ITERATION STEP LENGTH(DT) 9',F6.3/)
 1004 FORMAT( 9X,5(3X,'T',5X,'A',4X)/)
 1005 FORMAT(////////////)
 2000 FORMAT(I5)
 2001 FORMAT(4F10.5)
      STOP
      END



      FUNCTION F(T,A,DA)
C**
C**   THIS IS THE HYDRODYNAMICALLY LIMITED EQUATION
C**   FOR BUBBLE GROWTH IN A NON-NEWTONIAN FLUID
C**   OF THE POWER LAW KIND.
C**   P IS THE SURFACE TENSION PARAMETER
C**   S IS THE VISCOUS/INERTIA PARAMETER
C**   PL IS THE POWER LAW EXPONENT
C**
      COMMON /CMNN/ P,S,PL
      T1 = 1.5*(1.0-P/A)
      T2 = 1.5*DA*DA
      T3 = (SQRT(3.0)*(2.0)**(1.5*PL)*S*(DA/A)**PL)/PL
      F = (T1-T2-T3)/A
      RETURN
      END
```

```
      SUBROUTINE RUNKUT(H)
      DIMENSION XP(5),YP(5),ZP(5)
      X = 0.0
      Y = 1.0
      Z = 0.0
      HN = 2.0/H + 0.5
      NH = HN
      DO 104 I=1,10
      DO 103 II=1,5
      DO 102 J=1,NH
      AN = H*F(X,Y,Z)/2.0
      BE = H*(Z + AN/2.0)/2.0
      XX = X + H/2.0
      YY = Y + BE
      ZZ = Z + AN
      BN = H*F(XX,YY,ZZ)/2.0
      ZZ = Z + BN
      CN = H*F(XX,YY,ZZ)/2.0
      DE = H*(Z + CN)
      XX = X + H
      YY = Y + DE
      ZZ = Z + 2.0*CN
      DN = H*F(XX,YY,ZZ)/2.0
      X  = X + H
      Y  = Y+ H*(Z+(AN+BN+CN)/3.0)
      Z  = Z+(AN+2.0*BN+2.0*CN+DN)/3.0
  102 CONTINUE
      XP(II) = X
      YP(II) = Y
      ZP(II) = Z
  103 CONTINUE
      WRITE(6,1001) (XP(K),YP(K), K=1,5)
      WRITE(6,1002) (ZP(K), K=1,5)
  104 CONTINUE
      RETURN
 1001 FORMAT( 9X,5(F5.1,F7.2,2X))
 1002 FORMAT(9X,5(1PE14.2))
      END
```

Program P 2

Solution of the general case of bubble growth

```
      PROGRAM AASPL(INPUT,OUTPUT,TAPE5=INPUT,TAPE6=OUTPUT)
      DIMENSION C(51),DCDT(51),E(51),CYO(4),CYN(4),W(800),TITLE(5)
      COMMON W
      COMMON /CMN1/ SC,G,PI,PHI
      COMMON /CMN2/ A,DA,S
      COMMON /POWER/ PL
      REAL JABAR
      NPT = 51
      READ(5,1004) PL
 1004 FORMAT(F10.5)
      READ(5,1000) NSETS
      DO 400 NSET = 1,NSETS
      READ(5,1001) (TITLE(IT), IT = 1,5)
      READ(5,1002) V,GAMMA,PHI,JABAR,BBAR,G
      READ(5,1003) KLIM,DT,AMAX,ERROR
      SC = V*(G**(1.0-PL/2.0))
      DO 100 I = 1,NPT
      DCDT(I) = 0.0
  100 C(I) = 1.0
      PI = 1.0
      YO = 0.0
      YN = 1.0
      AO = 1.0
      DAO= 0.0
      A  = AO
      DA = DAO
      T  = 0.0
      DY = (YN-YO)/FLOAT(NPT-1)
      NUM = 2
      LIM = 4
      KOUNT = 0
      CYO(1) = 0.0
      CYN(1) = 0.0
      CYN(2) =-1.0
      CYN(3) = 1.0
      CYN(4) = 0.0
      TMCON= 4.0*JABAR*JABAR/3.14159
      TICON= SQRT(2.0*G/3.0)
      SL = DT
      S  = 20.0 * SQRT(DT)
      WRITE(6,2000)
      WRITE(6,2001)
      WRITE(6,2002) (TITLE(IT), IT=1,5), PL
 2002 FORMAT(1X,5A10*EXPONENT =*F7.3)
      WRITE(6,2003) SC,NPT,G,GAMMA,DT,V,TICON,PHI,TMCON,JABAR,BBAR,ERROI
      WRITE(6,2001)
      WRITE(6,2004)
      WRITE(6,2005) KOUNT,T,A,DA,SL,S,C(1)
  200 CALL RUNKUT(T,AO,DAO,SL)
      A  = AO
      DA = DAO
      S  = 20.0 * SQRT(T)
      T  = T - SL
      CYO(2) = -DA/JABAR
      CYO(3) = -GAMMA*DA/JABAR
      CYO(4) = 1.0/S
      CALL DP01A(C,YO,YN,NPT,T,SL,CYO,CYN,DCDT,E,LIM,ERROR,NUM)
```

```
      WRITE(6,2005) KOUNT,T,A,DA,SL,S,C(1),Y95,X95,NUM
      IF(KOUNT .GE. KLIM) GO TO 300
      IF(A .GE. AMAX) GO TO 300
      GO TO 200
  300 WRITE(6,2004)
      WRITE(6,2001)
  400 CONTINUE
 1000 FORMAT(I5)
 1001 FORMAT(5A10)
 1002 FORMAT(5F10.3,E10.3)
 1003 FORMAT(I10,2F10.5,E10.3)
 2000 FORMAT(1H1)
 2001 FORMAT(1X,106(1H*))
 2003 FORMAT(*   SC    *,F12.1,*    NPT   *,I4/
     1       *   G    * ,F13.1,/
     2       *   GAMMA*,F12.1,*    DT    *,F12.7/
     3       *   V     *,F12.1,*    TICON*,E13.4/
     4       *   PHI   *,F12.1,*    TMCON*,E13.4/
     5       *   JABAR*,F12.1/
     6       *   BBARR*,F12.1,*    ERROR*,1PE13.4/    )
 2004 FORMAT(1X,14X*T*11X*A*10X*DADT*11X*SL*11X*S*9X*C(0)*7X*Y95*7X*X95
     14X*NUM*)
 2005 FORMAT(1X,I5,1PE15.3,0PF10.3,2(1PE14.3),0PF10.3,F12.6,2F10.4,I5)
      STOP
      END


      SUBROUTINE FUNCTS(AA,BB,CC,DD,T,Y,IU,IDUDX)
      COMMON /CMN2/ A,DA,S
      Z1=1.0-Y
      Z2=Z1*Z1
      Z3=Z2*Z1
      Z4=Z3*Z1
      AA=Z4/(S*S)
      B1=A*Z1+S*Y
      BR=(2.0*Z1/B1 + (1.0-A*A*Z2/(B1*B1))*DA)*Z2/S
      CC=0.0
      DD=0.0
      RETURN
      END


      SUBROUTINE RUNKUT(X,Y,Z,H)
      AN = H*F(X,Y,Z)/2.0
      BE = H*(Z + AN/2.0)/2.0
      XX = X + H/2.0
      YY = Y + BE
      ZZ = Z + AN
      BN = H*F(XX,YY,ZZ)/2.0
      ZZ = Z + BN
      CN = H*F(XX,YY,ZZ)/2.0
      DF = H*(Z + CN)
      XX = X + H
      YY = Y + DE
      ZZ = Z + 2.0*CN
      DN = H*F(XX,YY,ZZ)/2.0
      X  = X + H
      Y  = Y+ H*(Z+(AN+BN+CN)/3.0)
      Z  = Z+(AN+2.0*BN+2.0*CN+DN)/3.0
      RETURN
      END
```

```
      FUNCTION F(T,A,DA)
C***  NEWTONIAN FLUID
      COMMON /CMN1/ SC,G,PI,PHI
      T1 = G*(PI - PHI/A)
      T2 = 1.5*DA*DA
      T3 = 4.0*SC*DA/A
      F = (T1-T2-T3)/A
      RETURN
      END


      FUNCTION F(T,A,DA)
C***  POWER LAW LIQUID, EXPONENT PL
      COMMON /CMN1/ SC,G,PI,PHI
      COMMON /POWER/ PL
      T1 = G*(PI - PHI/A)
      T2 = 1.5*DA*DA
      T3 = (12.0**((PL+1.0)/2.0))*SC*(DA/A)**PL/(3.0*PL)
      F  = (T1 - T2 - T3)/A
      RETURN
      END
```

Program P 3

Non-linear least squares regression

```
      SUBROUTINE BAILEY(Y,X,ND,B,TOL,NP,CON,YCAL)
      DIMENSION Y(ND),X(ND),YCAL(ND),TOL(5),CON(5),B(5),Z(5),ZZ(5,5),
     1C(5),DELB(5)
      COMMON /LAWA/ PHI,Z
      COMMON /LAWB/ SSQ,ZZ,C
      IKOUNT = 0
      JKOUNT = 0
      BETA = 0.25
      CALL SUMSQ(Y,X,ND,CON,B)
      SSQA = SSQ
      WRITE(6,2000)
      WRITE(6,2001)
      WRITE(6,2002) IKOUNT,JKOUNT,(B(K), K=1,NP),SSQA
  100 ALPHA = 1.0
      IKOUNT = IKOUNT + 1
      IF(IKOUNT .GE. 20) GO TO 400
      CALL MATZZC(Y,X,ND,CON,B,NP)
      CALL CROUT(DELB,ZZ,C,NP)
      DT = 0.0
      DO 102 K=1,NP
  102 DT = DT + C(K)*DELB(K)
      IF(DT .GE. 0.0) GO TO 104
      DO 103 K=1,NP
  103 DELB(K) = -DELB(K)
      DT = -DT
  104 DO 105 K=1,NP
  105 B(K) = B(K) + DELB(K)
      DO 106 K=1,NP
      IF( ABS(DELB(K)/B(K)) .GT. TOL(K)) GO TO 300
  106 CONTINUE
      DO 107 K=1,ND
      CALL MODEL(K,Y,X,ND,CON,B)
      YCAL(K) = PHI
  107 CONTINUE
      CALL SUMSQ(Y,X,ND,CON,B)
      WRITE(6,2003)
      WRITE(6,2004) (B(K), K=1,NP),SSQ
      GO TO 500
  300 JKOUNT = 1
  301 SSQB = 0.0
      CALL SUMSQ(Y,X,ND,CON,B)
      SSQB = SSQB + SSQ
      WRITE(6,2002) IKOUNT,JKOUNT,(B(K), K=1,NP),SSQB
      IF(SSQA-SSQB-BETA*DT*ALPHA*(2.0-ALPHA) .GE. 0.0) GO TO 303
      ALPHA = ALPHA/2.0
      DO 302 K=1,NP
  302 B(K) = B(K) - ALPHA*DELB(K)
      JKOUNT = JKOUNT + 1
      IF(JKOUNT .GE. 21) GO TO 400
      GO TO 301
  303 SSQA = SSQB
      GO TO 100
  400 WRITE(6,2005)
  500 RETURN
 2000 FORMAT(10X,*LAW AND BAILEY NON-LINEAR REGRESSION*,//)
 2001 FORMAT(10X,*VALUES OF PARAMETERS AND SUM OF SQUARES AT EACH ITERA
     1ION*)
 2002 FORMAT(9X,I3,6(1PE15.4))
 2003 FORMAT(20X,*CONVERGED VALUES OF PARAMETERS AND FINAL SSQ*)
 2004 FORMAT(15X,6(1PE15.4))
 2005 FORMAT(15X,*NO CONVERGENCE AFTER 20 ITERATIONS-CALC STOPPED*)
```

```
      SUBROUTINE SUMSQ(Y,X,ND,CON,B)
      DIMENSION Y(ND),X(ND),CON(5),B(5),Z(5),ZZ(5,5),C(5)
      COMMON /LAWA/ PHI,Z
      COMMON /LAWB/ SSQ,ZZ,C
      SSQ = 0.0
      DO 100 K=1,ND
      CALL MODEL(K,Y,X,ND,CON,B)
  100 SSQ = SSQ + (Y(K) - PHI)**2
      RETURN
      END



      SUBROUTINE MATZZC(Y,X,ND,CON,B,NP)
      DIMENSION Y(ND),X(ND),CON(5),B(5),Z(5),ZZ(5,5),C(5)
      COMMON /LAWA/ PHI,Z
      COMMON /LAWB/ SSQ,ZZ,C
      DO 100 K=1,NP
      C(K) = 0.0
      DO 100 L=1,NP
  100 ZZ(K,L) = 0.0
      DO 101 J=1,ND
      CALL MODEL(J,Y,X,ND,CON,B)
      DO 101 K=1,NP
      C(K) = C(K) + (Y(J) - PHI)*Z(K)
      DO 101 L=1,NP
  101 ZZ(K,L) = ZZ(K,L) + Z(K)*Z(L)
      RETURN
      END
```

```
      SUBROUTINE CROUT(X,AMAT,CMAT,NP)
      DIMENSION X(5),AMAT(5,5),CMAT(5),A(5,6)
      N = NP
      NN= N+1
      DO 600 I=1,N
      A(I,NN) = CMAT(I)
      DO 600 J=1,N
  600 A(I,J) = AMAT(I,J)
      DO 601 JJ=1,N
      J = N+2-JJ
  601 A(1,J) = A(1,J)/A(1,1)
      M = 1
  602 M = M+1
      MM=N+2-M
      J = M
      DO 603 II=2,MM
      I = N+2-II
      KK= J-1
      DO 603 K=1,KK
  603 A(I,J) = A(I,J) - A(I,K)*A(K,J)
      I = M
      MM= MM-1
      DO 605 JJ=1,MM
      J = N+2-JJ
      JTEST = J
      KK = I-1
      DO 604 K=1,KK
  604 A(I,J) = A(I,J) - A(I,K)*A(K,J)
  605 A(I,J) = A(I,J)/A(I,I)
      IF ( JTEST - (N+1)) 602,606,606
  606 X(N) = A(N,NN)
      DO 608 II=2,N
      I = N+1-II
      KK= I+1
      G = 0.
      DO 607 K=KK,N
  607 G = G + A(I,K)*X(K)
  608 X(I) = A(I,NN)-G
      RETURN
      END
```

REFERENCES

ADACHI, K.
YOSHIOKA, N.
YAMAMOTO, K.
On non-newtonian flow past a sphere.
Chem. Eng. Sci., 28, 2033-2043 (1973).

AKGERMAN, A.
GAINER, J.L.
Diffusion of gases in liquids.
Ind. Eng. Chem. Fund., 11, 373-379 (1972).

ASTARITA, G.
Diffusità in liquidi altamente viscosi, newtoniani e non-newtoniani.
Atti Accad. Nazl. Lincei, Rend., Classe. Sci. Fis., Mat. Nat., 36, 836-843 (1964).

ASTARITA, G.
Diffusivity in non-newtonian liquids.
Ind. Eng. Chem. Fund., 4, 236-237 (1965).

BANKOFF, S.G.
Heat conduction of diffusion with change of phase.
Advan. Chem. Eng., 5, 75-150 (1964).

BANKOFF, S.G.
Diffusion controlled bubble growth.
Advan. Chem. Eng., 6, 1-60 (1966).

BIRD, R.B.
STEWART, W.E.
LIGHTFOOT, E.N.
Transport Phenomena.
Wiley, New York (1960).

BLAKE, T.D.
KITCHENER, J.A.
Stability of aqueous films on hydrophobic methylated silica.
J. Chem. Soc. Far. Trans. I, 68, 1435-1442 (1972).

BRINSON, G.
Nucleation of gases from liquids.
J. Aust. Inst. Metals, 11, 227-230 (1966).

BUEHL, W.M.
WESTWATER, J.W.
Bubble growth by dissolution: Influence of contact angle.
A. I. Ch. E. J., 12, 571-576 (1966).

CABLE, M.
The dissolving of a stationary gas bubbles in a liquid.
Chem. Eng. Sci., 22, 1393-1398 (1967).

CABLE, M.
EVANS, D.J.
Spherically symmetrical diffusion controlled growth or dissolution of a sphere.
J. Appl. Phys., 38, 2899-2096 (1967).

CHEH, H.Y.
TOBIAS, C.W.
On the dynamics of hemispherical phase growth in non- uniform concentration fields.
Int. J. Heat Mass Trans., 11, 709-719 (1968).

CLOUGH, S.B.
READ, H.E.
METZNER, A.B.
BEHN, V.C.
Diffusion in slurries and in non-newtonian fluids.
A. I. Ch. E. J., 8, 346-349 (1962).

COLE, R.
SHULMAN, H.L.
Bubble growth at high Jakob numbers.
Int. J. Heat Mass Trans., 9, 1377-1390 (1966).

COULSON, J.M.
RICHARDSON, J.F.
Chemical Engineering, Volume II. p701
Pergamon Press, London (1966).

DAVIDSON, J.F.
CULLEN, E.J.
The determination of diffusion coefficients for sparingly soluble gases in liquids.
Trans. Inst. Chem. Engrs., 35, 51-60 (1957).

DERGARABEDIAN, P.
The rate of growth of vapour bubbles in superheated water.
J. Appl. Mech., 20, 537-545 (1953).

DERGARABEDIAN, P.
Observation of bubble growths in various superheated liquids.
J. Fl. Mech., 9, 39-48 (1960).

EPSTEIN, P.S.
PLESSET, M.S.
The stability of gas bubbles in liquid-gas solutions.
J. Chem. Phys., 18, 1505-1509 (1950).

FLORSCHUETZ, L.W.
CHAO, B.T.
On the mechanisms of vapour bubble collapse.
J. Heat Trans., 87, 209-220 (1965).

FORSTER, H.K.
ZUBER, N.
Growth of a vapour bubble in a superheated liquid.
J. Appl. Phys., 25, 474-478 (1954).

HIMMELBLAU, D.M.
Bubble initiation in supersaturated solutions.
U. S. A. E. C. Report No. ORO-3326-1 (1972).

HOUGHTON, G.
McLEAN, A.M.
RITCHIE, P.D.
Compressibility, fugacity and water solubility of carbon dioxide in the region 0-36 atm and 0-100° C.
Chem. Eng. Sci., 6, 132-137 (1957).

-
International Critical Tables Volume III.
McGraw- Hill, New York (1928).

KAYE, G.W.C.
LABY, T.H.
Tables of physical and chemical constants, 13th edition.
Longmans, London (1966).

KLASSEN, V.I.
MOKROUSOV, V.A.
An Introduction to the Theory of Flotation.
Butterworths, London (1963).

KREYSZIG, E.
Advanced Engineering Mathematics. p151
Wiley, New York (1967).

LAPIDUS, L.
Digital Computation for Chemical Engineers. p247
McGraw- Hill, New York (1962).

LAW, V.J.
BAILEY, R.V.
A method for the determination of approximate system transfer functions.
Chem. Eng. Sci., 18, 189-202 (1963).

LAWRIE, J.W.
Glycerol and the Glycols. p207
Chemical Catalog Co. Inc., New York (1928).

LIEBERMANN, L. Air bubbles in water. J. Appl. Phys., 28, 205-210 (1957).

MANLEY, D.J. Change of size of air bubbles in water containing a small dissolved air content. Brit. J. Appl. Phys., 11, 38-42 (1960).

MARIQUE, L. HOUGHTON, G. Analogue computer solution of the modified Rayleigh equation and parameters affecting cavitation. Can. J. Chem. Eng., 40, 122-126 (1962).

MILLER, I. FREUND, J.E. Probability and Statistics for Engineers. Prentice-Hall, New Jersey (1965).

OSMERS, H.R. METZNER, A.B. Diffusion in dilute polymeric solutions. Ind. Eng. Chem. Fund., 11, 161-168 (1972).

PACKHAM, R.F. RICHARDS, W.N. Water clarification by flotation - 1. Water Res. Assn. TP87 (1972a).

PACKHAM, R.F. RICHARDS, W.N. Water clarification by flotation - 2. Water Res. Assn. TP88 (1972b).

PERRY, J.H. (ed) Chemical Engineer's Handbook, 4th Edition. McGraw-Hill, New York (1963).

PIGNET, T. SCRIVEN, L.E. On the dynamics of phase growth. Chem. Eng. Sci., 27, 1753-1754 (1972).

PLESSET, M.S. The dynamics of cavitation bubbles. J. Appl. Phys., 16, 277-282 (1949).

PLESSET, M.S. ZWICK, S.A. A non-steady heat diffusion problem with spherical symmetry. J. Appl. Phys., 23, 95-98 (1952).

PLESSET, M.S.
ZWICK, S.A.
The growth of vapour bubbles in superheated liquids.
J. Appl. Phys., 25, 493-500 (1954).

PRATT, K.C.
SLATER, D.H.
WAKEHAM, W.A.
A rapid method for the determination of diffusion coefficients of gases in liquids.
Chem. Eng. Sci., 28, 1901-1902 (1973).

QUINN, E.L.
JONES, C.L.
Carbon Dioxide.
Reinhold, New York (1936).

Lord RAYLEIGH
On the pressure developed in a liquid during the collapse of a spherical cavity.
Phil. Mag., 34, 94-98 (1917).

READY, D.W.
COOPER, A.R.
Molecular diffusion with a moving boundary and spherical symmetry.
Chem. Eng. Sci., 21, 917-922 (1966).

REINER, M.
Deformation, Strain and Flow.
H.K. Lewis & Co. Ltd., London (1960).

ROSNER, D.E.
EPSTEIN, M.
Effects of interface kinetics, capillarity and solute diffusion on bubble growth in highly supersaturated liquids.
Chem. Eng. Sci., 27, 69-88 (1972).

SADDY, M.
JAMESON, G.J.
Experiments on the dynamics of phase growth.
Chem. Eng. Sci., 26, 675-684 (1971).

SCRIVEN, L.E.
On the dynamics of phase growth.
Chem. Eng. Sci., 10, 1-13 (1959).

SCRIVEN, L.E.
On the dynamics of phase growth.
Chem. Eng. Sci., 17, 55 (1962).

SEIDELL, A.
Solubilities of Inorganic and Metal-organic Compounds. p232
Van Nostrand, New York (1940).

SISKO, A.W. The flow of lubricating greases. Ind. Eng. Chem., 50, 1789-1792 (1958).

SKELLAND, A.H.P. Non-newtonian flow and heat transfer. Wiley, New York (1967).

SMITH, G.D. Numerical Solution of Partial Differential Equations. p9-54 O. U. P., London (1965).

SUTHERLAND, K.L. WARK, I.W. Principles of Flotation. 2nd Edition. Aust. Inst. Min. Met., Melbourne (1955).

SZEKELY, J. FANG, S. -D. Non-equilibrium effects in the growth of spherical gas bubbles due to solute diffusion - II. Chem. Eng. Sci., 28, 2127-2140 (1973).

SZEKELY, J. MARTINS, G.P. Non-equilibrium effects in the growth of spherical gas bubbles due to solute diffusion. Chem. Eng. Sci., 26, 147-159 (1971).

U.K.A.E.A. Harwell Subroutine Library - a Catalogue of Subroutines (1973). H.M.S.O. / AERE R7477, (1973).

VALENTIN, F.H.H. Absorption in gas-liquid dispersions: some aspects of bubble technology. Spon Ltd., London (1967).

WESTWATER, J.W. Boiling of liquids. Advan. Chem. Eng., 1, 2-78 (1956).

WILKE, C.R. CHANG, P. Correlation of diffusion coefficients in dilute solutions. A. I. Ch. E. J., 1, 264-270 (1955).

LIST OF SYMBOLS

(Excluding other author's nomenclature used in Chapter 2 and in Appendix A.5)

a Dimensionless radial coordinate distance

A Dimensionless bubble radius

a_b Instantaneous area of a bubble

$B = \frac{Ja^2}{G^{\frac{1}{2}}}$ Growth regime characterisation parameter

$\overline{B} = \frac{\overline{Ja}^2}{G^{\frac{1}{2}}}$ Reference value of B

C Concentration of dissolved gas

C_o Concentration in equilibrium with P_o

C_{sat} Concentration in equilibrium with P_∞

$C^* = \frac{C - C_{sat}}{C_o - C_{sat}}$ Dimensionless concentration

$\Delta C = C_o - C_{sat}$

D Diffusivity coefficient

D Total differential

g Acceleration due to gravity

$G = \frac{R_o^2 \Delta P}{D^2 \rho_\ell}$ Inertial characterisation parameter

H Henry's law coefficient

$Ja = \frac{\Delta C}{\rho_g}$ Jakob number

$\overline{Ja} = \left.\frac{\Delta C}{\rho_g}\right|_{P_\infty}$ Reference value of the Jakob number

k Constant in continuity equation 3.2

k_i Mass transfer coefficient

K_ℓ Overall mass transfer coefficient, liquid film

$m = \frac{m'}{\rho_\ell}$ "kinematic vicosity coefficient" for a power law liquid

m' Coeffient in power law

n Power law liquid exponent

N_g Dissolved gas mass transfer flux

P Pressure

P_{rr} Normal stress

P_o Initial pressure, saturated pressurised

P_g Pressure inside bubble

P_∞ Ambient pressure

$\Delta P = P_o - P_\infty$

r Radial coordinate distance

R Bubble radius

R_o Initial bubble radius

$\dot{R}$ Velocity of bubble surface

$\ddot{R}$ Acceleration of bubble surface

Re Reynolds number

s Spacing parameter

S Similarity transformation

$Sc = \frac{\nu}{D}$ Schmidt number, newtonian liquid

$Sc^* = \frac{m\ R_o^{2(1-n)}}{D^{(2-n)}}$ Schmidt number, power law liquid

$Sh = \frac{2\ R\ K_\ell}{D}$ Sherwood number

t Time

$T = (\frac{2}{3} G)^{\frac{1}{2}} \tau$ A dimensionless time

v Velocity

$V = \frac{Sc}{G^{\frac{1}{2}}}$ Viscous/inertia parameter, newtonian

$V^* = \frac{Sc^*}{G^{(1-\frac{n}{2})}}$ as above, power law liquid

x = $a - A$ Dimensionless distance beyond the bubble surface

y = $\frac{x}{s + x}$ Spatial transformation variable

Greek letters

β Dimensionless growth coefficient

γ = $\frac{\Delta C}{C_{sat}}$ Supersaturation driving force

δ Unit tensor

Δ Rate of deformation tensor

Δ_{ii} Component of Δ

ε = $1 - \frac{\rho_g}{\rho_\ell}$

ζ A spatial transformation variable

η Scalar function of power law 'viscosity'

λ_1, λ_2 Parameters in Sisko flow model (Equation 3.53)

μ Viscosity coefficient

ν = $\frac{\mu}{\rho_\ell}$ Kinematic viscosity

π 3.14159....

Π = $\frac{P_g - P_\infty}{P_o - P_\infty}$ Dimensionless pressure

σ Surface tension

τ = $\frac{Dt}{R_o^2}$ Dimensionless time

τ Shear stress tensor

τ_{ij} Component of τ

$\Phi\{\varepsilon,\beta\}$ Driving force parameter for bubble growth

ϕ = $\frac{2\ \sigma}{\Delta P\ R_o}$ Surface tension parameter

ψ_1, ψ_2 Parameters in Ellis flow model (Equation 3.52)

Subscripts and superscripts

g Gas phase

i Interface

ℓ Liquid phase

r In radial direction

R At bubble surface

θ In θ direction

ϕ In ϕ direction

∞ At a distance or ambient

* For a power law liquid (except when used on C when it implies non-dimensionality)

• Differentiation with respect to time